ALMA MATER STUDIORUM – UNIVERSITÀ DI BOLOGNA

SCUOLA DI INGEGNERIA E ARCHITETTURA

Dipartimento di ingegneria civile, chimica, ambientale e dei materiali (DICAM)

CORSO DI LAUREA MAGISTRALE IN INGEGNERIA CHIMICA E DI PROCESSO

TESI DI LAUREA

in

Thermodynamics of Energy and Materials

High-pressure adsorption differential volumetric apparatus (HP-ADVA) for accurate equilibrium measurements

CANDIDATE:

Ilaria Ceteroni

SUPERVISOR:

Prof. Marco Giacinti Baschetti

CO-SUPERVISORS:

Prof. Enzo Mangano

Ing. Riccardo Rea

A.A. 2019/2020

Session III

Abstract

The volumetric system is a commonly used experimental method for gas adsorption measurements. Starting from the conventional volumetric system (single-branched), the development of differential (double-branched) apparatus has been proposed to overcome some criticalities connected to the original design. The following study is focused on the assessment of the high-pressure differential volumetric apparatus (HP-ADVA) built at the University of Edinburgh in order to discover and characterise system peculiarities at different experimental conditions, in terms of temperature and pressure. To do this, an integrated approach is proposed: an initial experimental campaign has been performed to take confidentiality with the apparatus, then, the experimental results were the starting point for the development of a sensitivity and error analysis aimed at describing the effect of each operating parameter into the final result. In this regard, a different analytical approach, compared to the ones commonly proposed in literature, has been proposed to closely reproduce the real system. Beyond having obtained promising results, some criticalities, matching what originally hypothesized from the experimental campaign, have been noted: valve volume effect and temperature control and measurements have been discovered being crucial aspects, and, supposedly, source of errors leading to explain the unexpected results obtained by the experimental campaign. Moreover, the importance of symmetry maintenance among the branches has been repeatedly confirmed in the analysis. Some recommendations aimed at improving the system set-up have been moved regarding the installation of a temperature control system and more accurate temperature measurement devices. Additionally, an accurate assessment and characterisation of pneumatically-actuated valves, as well as of the differential pressure transducer used for pressure measurement, before the installation, could be useful to reduce inaccuracies.

Keywords: Adsorption - Isotherm - Volumetric method - Differential pressure gas adsorption - High pressure adsorption - Sensitivity and error analysis

Table of contents

Introduction

A separation can be defined as a process that transforms a mixture of substances into two or more products that differ from each other in composition. In a process scheme, the separation steps often account for the major operative costs, for this reason the research and development of novel technologies is of interest in many fields. The separation is caused by a mass separating agent which is different depending on the technique considered; for example, in adsorption processes, the separating agent is the solid sorbent while in absorption processes is the liquid solvent (King, 1980; Yang, 2003).

Separation processes can be applied to gas stream: it is a widely used technique in which the objective is the separation of one or more gases from a mixture. It is becoming crucial for several industrial applications such as the treatment of fumes from coal-fired plants aimed at the removal and the storage of CO_2 to reduce the greenhouse effect and environmental issues. Growing interest is also given to separation and purification of commercially important gases such as H_2, CH_4 and O_2 from natural gas. In particular, the rapid growth in greenhouse gas emissions has stimulated worldwide attention to look for green and clean energy resources alternatives to traditional fossil fuels. Hydrogen and methane, as clean and low-carbon energy sources, have shown the increased demands in the energy system and transport sector such as electricity generation, heating, and vehicle fuels (Luo et al., 2018). Oxygen, from air purification, is ranked among the most widely used commodity chemicals in the world because it is used for oxy-fuel combustion process and oxygen-blown gasification to convert coal and natural gas into intermediate synthesis gas (Bose, 2009).

The principal techniques used to perform gas separation are:

- separation by cryogenic distillation
- separation with membrane
- separation with solvents/sorbents

Cryogenic distillation is based on the fact that, in a gas mixture, all components have different boiling points and the separation can be performed by increasing/decreasing the temperature and pressure of the system. The gas mixture is cooled down to low temperature (typically < -50 °C). Once in the liquid state, the components of the mixture can be directed in

a distillation column and through a series of compression, cooling and expansion steps, they can be distributed to different channels, depending on their boiling points (see Fig. 1). It is a widely used technique for streams that already have a high concentration in the desired gas (typically >90%) but it is not very appropriate for diluted gas streams. The main advantage of the cryogenic gas separation is the direct liquefaction, which is useful for transportation. A major disadvantage is connected with the high amount of energy required for refrigeration. Cryogenics would normally only be applied to high concentration and high pressure gases, such as in pre-combustion capture processes or oxygen-fired combustion.
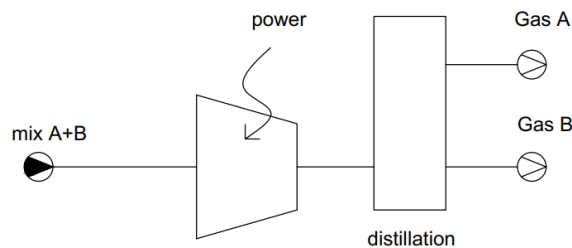
Figure 1 - Separation by cryogenic distillation (basic scheme).

Membrane technologies are among the most developing fields for gas separation: one of the greatest advantages regards the variety of membrane materials leading to high diversification in the potential applications. Operatively, the gas mixture is directed into a vessel and put in contact with the membrane material which is at the interface with another vessel. The mixture is allowed to diffuse into the second vessel under a pressure gradient which promotes the mass transport through the membrane separating the retentate (slower gas) from the permeate (faster gas) (see Fig. 2). The use of membranes for gas separation offers several benefits, probably the most valuable is the high cost-efficiency (both for the mechanical simplicity of the system and for low-energy requirements) in fact, they do not require thermal regeneration, phase change or active moving parts for the operation. On the other hand, the greatest limitation of membranes for gas separation derives from their trade-off relationship between permeability and selectivity: highly permeable membranes generally show low selectivity, requiring several run for a good separation, while, highly selective membranes have low permeability, meaning long operational times. Among the major industrial applications are comprised the H_2 recovery from NH_3-synthetic loop, enhanced oil recovery, N_2/O_2 separation for modified atmospheres production and CH_4 upgrading with CO_2 removal.
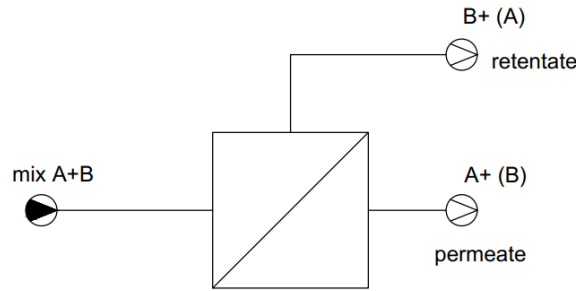
Figure 2 - Separation with membrane (basic scheme).

The use of solvents for gas separation is based on the affinity of the target gas toward a solvent. For instance, amine scrubbing technology was established over 60 years ago in the oil and chemical industries, for removal of H_2S and CO_2 from gas streams and, commercially, it is the most well-established of the techniques available (see example in Fig. 3). Mono-ethanolamine (MEA) is a widely used type of amine for carbon capture. CO_2 recovery rates of 98% and product purity in excess of 99% can be achieved. There are, however, questions about its rate of degradation in oxidising environment and about the amount of energy required for regeneration. Improved solvents could reduce energy requirements, by as much as 40% compared to conventional MEA solvents. For example, there is considerable interest in the use of sterically-hindered amines which are claimed to have good absorption and desorption characteristics.
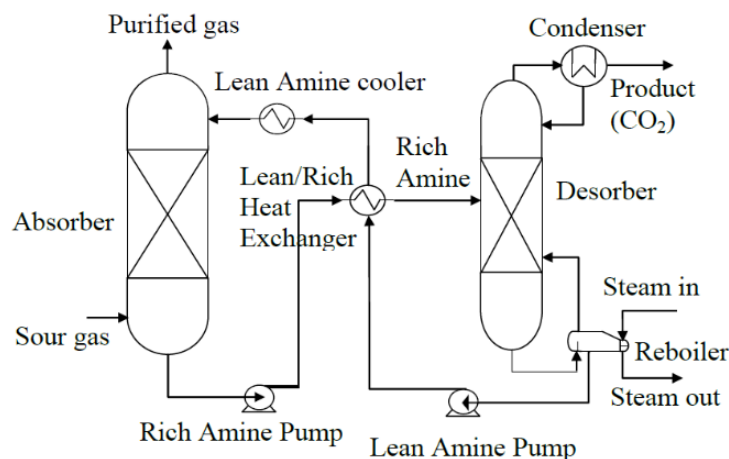
Figure 3 – Example of separation with solvent/absorption (basic scheme) (Aforkoghene Aromada & Øi, 2015).

Finally, gas separation can be performed by using sorbents: the gas mixture is put in contact with a solid support (adsorbent) which acts as separating agent. The invention and development of new sorbents and adsorption process cycles have made adsorption a key separation tool in the chemical, petrochemical and pharmaceutical industries. Some examples of adsorption applications are the energy storage: materials such as metal hybrids and carbon nanotubes are employed to improve the effectiveness of hydrogen storage for fuel cell powered automobiles (Zielinski et al., 2007). Technologies for meeting high standards on air and water purification: trace impurity removal (less than 1% concentration) is of major interest due to the difficulties in applying other separation processes. In this concern, the field of carbon dioxide sequestration captured high attention in last years coupled with dehydration and sweetening of natural gas, desulfurization of hydrocarbon streams and removal of organic pollutants from water which are processes yet implemented in large scale. Some industrial bulk separations are based on adsorption technique too and account of processes like hydrogen production, air separation O_2/N_2, linear/branched by cyclic paraffins, olefin/paraffin and aromatic isomers separation.

The heart of an adsorptive process is the porous solid medium: it should provide a very high surface area or high micropore volume with which high adsorptive capacity can be achieved. The classification of sorbents can be done considering the mean pore size as recommended by IUPAC (Sing et al., 1985) into microporous (d<2 nm), mesoporous (2 nm<d< 50 nm) and macroporous materials (d>50 nm). At commercial level, six types of sorbents can be distinguished: activated carbon, silica gel, activated alumina, zeolites, clays, polymers and resins (Yang, 2003). The success of the process depends on how the solid performs in both equilibria and kinetics: a combination of the two classifies the material as a good adsorbent (Do, 1998). The adsorptive separation is indeed based on one of three existing mechanisms: steric, kinetic or equilibrium.

The steric effect derives from the sieving properties of the sorbent: due to the dimension of the pores of the solid, small molecules can enter the material while large molecules are excluded from entering. Two major applications are drying with 3A zeolite and the normal from iso-paraffins or cyclic hydrocarbons separation using 5A zeolite.

Kinetic separations are nowadays a field of intense research and development for their potentiality when equilibrium separations are not feasible. The mechanism is based on the different rates of diffusion of the species into the pore: controlling the time of exposure, the faster diffusing species is removed by the solid. Air separation by PSA (i.e. pressure-swing-

adsorption) using zeolite to produce O_2 from air is a good example of kinetic separation; separation of methane from CO_2 and upgrading of natural gas by nitrogen removal are large potential applications too.

Last mechanism of adsorption is the equilibrium one and it is based on the type of interactions between the solid and the species. The starting point is the examination of the properties of the targeted molecule such as polarizability, magnetic susceptibility, permanent dipole moment and quadrupole moment. In this case the stronger adsorbing species is preferentially removed by the solid (Do, 1998; Yang, 2003).

A basic schematization is provided in the Fig. 4:
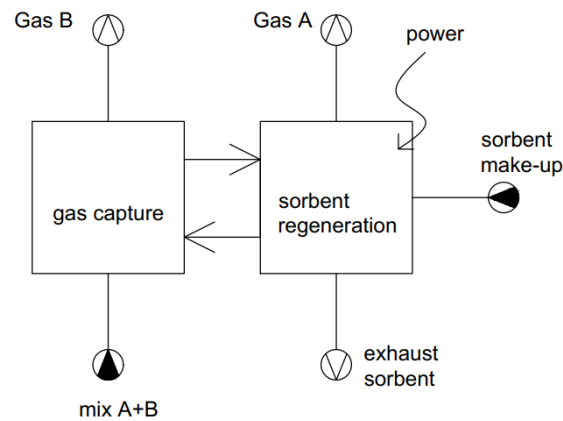
Figure 4 - *Separation with sorbent/adsorption (basic scheme).*

Adsorption equilibria information is the most important piece of information in understanding an adsorption process: it is essential for understanding how much of a component can be accommodated by a solid adsorbent. This information can be used in the study of adsorption kinetics of a single component, adsorption equilibria of multicomponent systems, and then adsorption kinetics of multicomponent systems (Do, 1998).

Commonly, the adsorption isotherms are measured or predicted using molecular simulations. Among them, Monte Carlo simulation is used for adsorption analyses helping visualizing how the adsorption takes place. Experimentally, the majority of adsorption measurements are carried out with three techniques: volumetric, chromatographic/flow and gravimetric. A more detailed discussion of the experimental methods is provided in the *Chapter 1*, because it will be the focus of the thesis.

Attention needs to be paid to the origin of the data collected experimentally: when measuring adsorption of a gas onto a solid sorbent, it is not possible to measure directly the absolute adsorbed amount; the *absolute* adsorbed amount is defined as the ratio among the number of gas moles adsorbed and the volume of adsorbent (or mass). However, what is actually measured, is the difference between two quantities which are the *excess* adsorbed amount, typically measured as the difference between the molecule of interest and a reference (99% of the time Helium is used as reference) and the *net* adsorbed amount, which is the measure relative to the same system without the adsorbent. For microporous solids, the estimation of the absolute adsorbed amount requires the calculation of the solid volume that includes the micropores, in fact, the accumulation inside the pores is higher compared to adsorption on the external surface, which is generally negligible.

Briefly, considering a system having a total volume V_S , comprising the porous and micropore volume; the total number of moles in the system is:

(1) $n_{TOT} = n_A + n_S$

where "A" stands for the adsorbate and the "S" for the solid.

In the *absolute* adsorption evaluation, the solid is removed:

(2) $n^{abs} = n_{TOT} - n_S$

In the *net* adsorbed amount, the moles in a fluid at same temperature and pressure, in equilibrium with the adsorbed phase, that would occupy the system volume is removed:

(3) $n^{net} = n^{abs} - V_S c = n_A - V_S c$

where $c = \dfrac{P}{zRT}$, is the total concentration.

The *excess* adsorbed amount is finally defined through the definition of the so called non-accessible volume (V_{NA}):

(4) $n^{ex} = n^{abs} - (V_S - V_{NA})c = n_A - (V_S - V_{NA})c$

Some difficulties arise in defining and estimating the non-accessible volume, this is the reason why the excess quantity is generally more difficult to be calculated. Once defined the number of moles, relationships for the adsorbed phase concentration can be obtained:

$$(5) \quad q^{abs} = \frac{n_{abs}}{V_S} = \frac{n_A}{V_S}$$

$$(6) \quad q^{net} = \frac{n_{abs}}{V_S} - c = q_{abs} - c$$

$$(7) \quad q^{ex} = \frac{n_{abs}}{V_S} - \frac{V_S - V_{NA}}{V_S} c = q_{abs} - \varepsilon_m c$$

where ε_m is the porosity of the material. An accurate definition of absolute, excess and net adsorbed amount can be found in (Brandani et al., 2016).

The clear definition of these three magnitudes is a core aspect when dealing with adsorption measurements to be consistent and free from errors. Indeed, the absolute amount is the one used for mass balances and modelling. Equilibrium adsorption models are used for fitting the experimental data: along the discussion, reference to different models is done such as the Langmuir model, the Dual-site Langmuir and the Toth model. However, a detailed analysis of the models is not provided because it is not the focus of the thesis; reference to (Ruthven, 1985) manual is advised for a detailed description of all the approaches used.

Aims and objectives

The overall goal of this thesis is to perform an accurate characterisation and final commissioning of the novel high-pressure volumetric differential apparatus (HP-ADVA) for gas adsorption analysis built at the University of Edinburgh (*University of Edinburgh - Fleeming Jenkins Building Lab 1.196D*).

The approach used for the analysis can be divided in three main sections: first of all a literature review has been developed, followed by a brief experimental campaign, which was stopped due to the closure of laboratories for the Covid-19 pandemic situation. This was the reason to propose a third section in which an error and sensitivity analysis has been developed for the system.

In the section dedicated to the experimental campaign, an example of adsorption experiment without adsorbent (blank experiment) is proposed, from which some issues have been pointed out justifying the following experimental steps: firstly, the calibration of the apparatus, performed in a wide pressure range, has been performed to evaluate the effect of the absolute pressure on calibration procedure. Moreover, valve characterisation assessment has been conducted to account for the presence of no-zero volume valves in the system. The development of a protocol for cryogenic experiments has been explored too, to better understand the behaviour of the apparatus in different and extreme experimental conditions.

A said, the experimental campaign was blocked due to the pandemic and it will result incomplete to the reader. Alternatively, the development of a sensitivity and error analysis, for the high-pressure volumetric differential apparatus (HP-ADVA), is proposed, in line with the overall aim of the project to accurately study all the criticalities of the apparatus.

Indeed, a high volume of literature has been produced providing data for accurate experimental procedures and the acquisition of reliable data at low pressure conditions using different experimental apparatus such as gravimetric, volumetric and chromatographic systems. The same work should be done for high-pressure data acquisition systems. The experimental techniques, used for the determination of high-pressure pure gas adsorption isotherms, are not different in their principle from those used in the low-pressure area (Bereznitski et al., 1997; Nakashima et al., 1995; Rouquerol et al., 1999). However, high-pressure adsorption measurements are more difficult to be achieved than low-pressure ones and the number of experimental studies remains too low to provide comparative tests between experimental results obtained for the same systems on different equipment (Belmabkhout et al., 2004).

Consequently, this thesis aims to study and someway assess the reliability of the HP-ADVA apparatus in performing adsorption equilibrium measurements focusing the attention on the analysis of the performances at high pressure conditions. Finding the effective impact of uncertainties introduced in operating/design parameters and, in particular, how and to which extent each uncertainty affects the final isotherm construction is within the objectives of the study. In particular, a comparison among a conventional (single-branched) volumetric apparatus and our differential (double-branched) apparatus is proposed: a consistent lack in the available literature can be noticed also in this case, being the majority of the studies focused on the analysis of the only conventional volumetric system (Belmabkhout et al., 2004; Blach & Gray, 2007; Blackman et al., 2006; Broom & Moretto, 2007; Demirocak et al., 2013; Mohammad et al., 2009; Wang et al., 2020; Webb & Gray, 2014a, 2014b).

An important point to be considered is that the common practices used for the development of sensitivity analysis of volumetric systems appear poorly reproduce the reality; thus, an attempt to propose a new approach to the analysis is provided too.

Chapter 1 - Theoretical focus

Chapter 1 is dedicated to a brief introduction of the experimental techniques that are commonly used for adsorption experiments: the gravimetric and chromatographic/flow systems will be simply mentioned in their principles, while a deeper description of the volumetric system is provided being the subject of the research project. Additionally, a short section regarding the sensitivity and error analysis applied to volumetric systems will be furnished as literature base for the analysis proposed forward.

1.1 Overview of gravimetric apparatus

The gravimetric method consists of exposing a clean adsorbent sample to a pure gas at constant temperature. This experimental method is considered a well-established and quite accurate measurement technique (Belmabkhout et al., 2004). There are several possible configurations in which a micro-balance can be inserted into a system to measure adsorption kinetics. Commercially available systems in common use are electronic microbalances, but other examples such as the McBain balance, that rely on the optical measurement of the extension of a spring connected to the sample, are also used. The sensitivity of an electro-balance is strongly dependent on how and where the system is mounted as the stability of the baseline is affected by any vibration. Ideally the balance should be mounted rigidly and anchored to a basement wall. The first important distinction between electronic micro-balances is whether the system is symmetric or asymmetric. In the symmetric case the two branches of the balance are exposed to the same gas and are thermostated to the same temperature. In the asymmetric case only one branch of the balance is at the same conditions of the sample, while the reference branch is at near to room temperature exposed to the same gas or with an inert purge that is used to protect the electronic part of the balance (Wang et al., 2020).

The measurements are based on the estimation of the force acting on the sample in a configuration schematically shown in Fig. 5. The absorbed amounts are determined by a force balance whose main contributions are the weight, buoyancy and drag. So, the measured force is the resultant of the weight of the sample holder (M_{Bu}), the weight of the solid (M_S) and adsorbate (MW_A) minus the buoyancy acting onto the volume of the solid which includes the micropores (ε_m) and the volume of the sample holder (V_{Bu}) (Brandani et al., 2016).
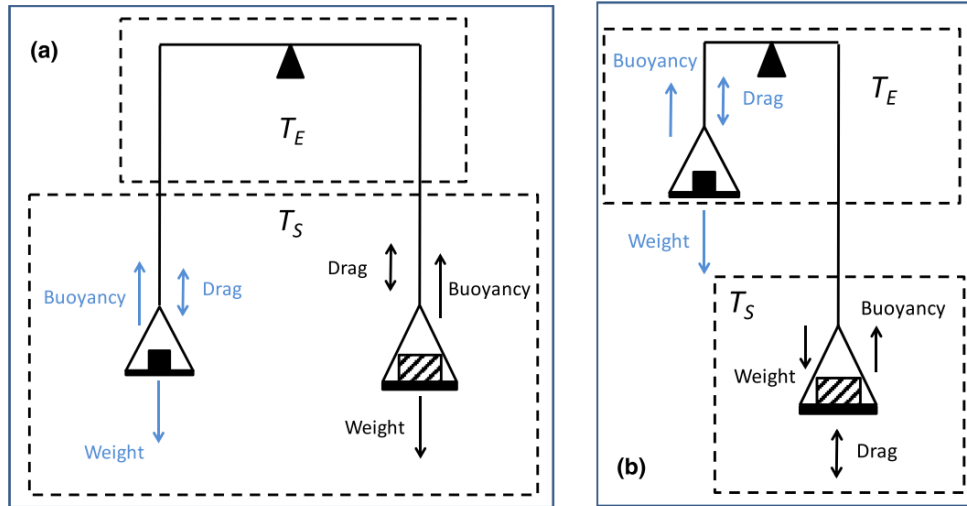
Figure 5 *- Schematic diagram of a (a) symmetric gravimetric system and (b) asymmetric gravimetric system (Wang et al., 2020).*

In particular:

$$(8) \quad \Omega = (M_{Bu} + M_S + n_A MW_A)g - (\varepsilon_m V_S + V_{NA} + V_{Bu})cMW_A g$$

the expression is obtained neglecting the drag force due to the moving system; if $\varepsilon_m V_S + V_{NA} = V_S$ is known, the experimentally determined force can be converted into absolute absorbed amount. If only the mass and the volume of the sample holder are used to correct the reading, the net adsorbed amount is then calculated:

$$(9) \quad \Omega - (M_{Bu} + M_S)g + V_{Bu}cMW_A g = \frac{n_A MW_A}{M_S}g - \frac{V_S}{M_S}cMW_A g = \frac{V_S}{M_S}q^{net}$$

The non-accessible volume (V_{NA}) can be determined through Helium experiments. Refer to (Brandani et al., 2016) for specific definitions.

Clearly, the amount adsorbed is related to the force change (Ω_1, Ω_2) before and after the exposure of the sample to the gas. The pressure and temperature conditions (P_1, P_2, T_1, T_2) are detected using appropriate devices.

The major advantage in using the gravimetric method is the direct measurement of the adsorbed amount adsorption capacity and the little dependence on calculational methods (Lachawiec et al., 2008), on the other hand, the most important source of errors is the determination of the correct system volume ($\varepsilon_m V_S + V_{NA} + V_{Bu}$) (Belmabkhout et al., 2004).

Among design proposals for improvement of the experimental technique, the installation of a gas circulator can be helpful in enhancing adsorption and reducing waiting times for

equilibrium, however, the circulator may cause problems for fine grained sorbent materials like powders or activated carbon fibres which may be removed or simply blown away from the sorbent vessel (Keller & Staudt, 2005).

1.2 Overview of chromatographic/flow apparatus

Chromatographic/flow method for adsorption measurements is schematized in Fig. 6. The gas flows into the system and, at time zero, either a pulse of adsorbate is added to the carrier gas (chromatographic experiment) or the system is perturbed by a step change in concentration (breakthrough experiment).
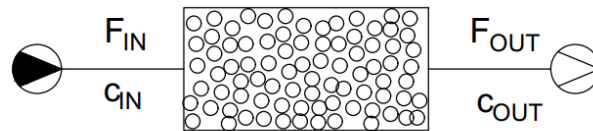
Figure 6 *- Schematic diagram of a chromatographic system.*

The outlet concentrations and volumetric flowrates are measured (Mason et al., 1997), allowing to determine the difference in the amount of gas that enters and exits the system through the following mass balance (Brandani et al., 2016):

$$(10) \quad V_F \frac{d}{dt}\left(\frac{\int c\,dz}{L}\right) + V_S \frac{d}{dt}\left(\frac{\int q\,dz}{L}\right) = (Fc)_{IN} - (Fc)_{OUT}$$

The terms are the accumulation in the fluid and liquid phase and the integrals state for the average gas and solid phase concentration along the length of the column (*L*).

With this experimental method, none of the three magnitudes among absolute, net and excess amount are estimated directly: the *absolute* adsorbed amount can be established by using large molecules, size-excluded by the micropores of the adsorbent at high temperature, to determine the solid volume required for the calculation. On the other hand, the *excess* amount can be evaluated through Helium expansion for the estimation of the non-accessible volume and the *net* amount using empty column with very low pressure drops. Among the drawbacks of the chromatographic method the high values of pressure drops along the column: the development of apparatus like the zero-length column, besides other reasons, is also aimed to minimize this phenomenon (Eic & Ruthven, 1988).

1.3 Volumetric apparatus

The operating principle of a conventional, single-branched, volumetric apparatus is simple: a known amount of gas is added to a calibrated dosing cell, the valve, separating the dosing and uptake section, is then opened letting the gas expand to the uptake cell, which contains the adsorbent, so the gas can adsorb onto the material (Fig. 7). Knowing the dosing and uptake cells volumes (V_d, V_u), the pressures (P_d, P_u) and temperatures (T_d, T_u) of both cells are measured, before and after opening the valve, and a mass balance is applied to determine the amount of gas effectively adsorbed into the sample (V_s).
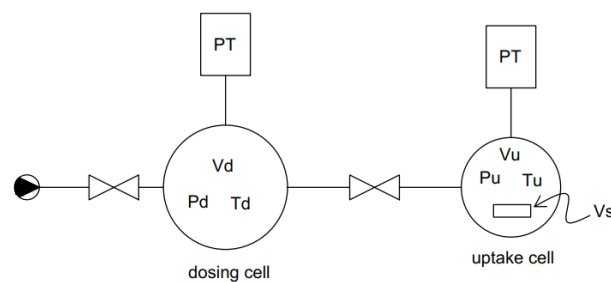

Figure 7 - *Schematic diagram of a conventional volumetric system.*

A considerable amount of literature has been written over years about the conventional volumetric method for adsorption measurement, among them (Ahn et al., 1998; Belmabkhout et al., 2004; Blach & Gray, 2007; Blackburn et al., 2008; Checchetto et al., 2004; Cheng et al., 2007; Giacobbe, 1991; Lachawiec et al., 2008; Lee et al., 2008; Malbrunot et al., 1997; Park et al., 2016; Ramaprabhu et al., 1998; Tibbetts et al., 2001).

As said, the volumetric method is based on an indirect measurement of the amount adsorbed: this is the main drawback related to this experimental approach. Mass balances are applied to obtain the final gas uptake starting from measured experimental data, errors can be then introduced during the experimental campaign and progressively propagate through data analysis. This is one of the reasons why high attention needs to be paid during experimentation; moreover, operational recommendation and improvements of the system design have been proposed developing more reliable system configurations for adsorption measurement.

An important step forward has been done with the development of double-branched systems. A double-branch, differential, apparatus is constituted by two branches, each one similar to a single-branch unit, connected together by a differential pressure transducer. The amount of gas adsorbed into the sorbent is calculated from the differential pressure change among a reference

cell and a sorption cell, containing the sample (see Fig. 8). The experiments are performed in the same way as for a conventional apparatus: the reference and sample dosing cells (V_{dr}, V_{dr}) are charged with a known amount of gas, then, the valves, separating the dosing and uptake cells (V_{ur}, V_{us}), are simultaneously opened, to perform the expansion. After waiting the time for the equilibration, the differential pressure among the two branches is detected and used to determine, through mass balance, the amount of gas effectively adsorbed into the sample (V_s).
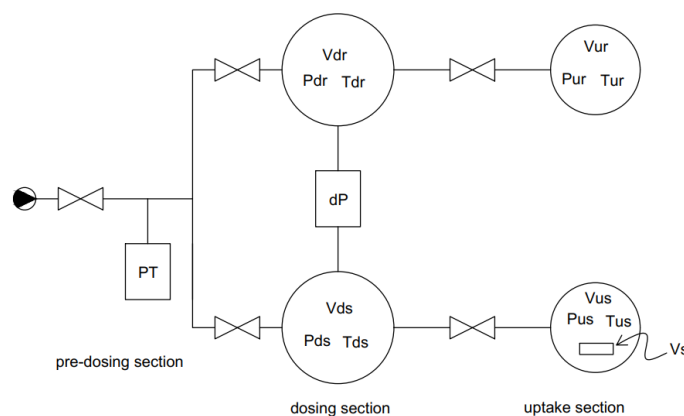

Figure 8 - *Schematic diagram of a differential volumetric system.*

The differential unit has several advantages over the conventional unit. It incorporates a differential pressure transducer (*dP* in the Fig. 8), which has an increased grade of accuracy in a wider pressure range, if compared to absolute pressure readings. What is expected, is to obtain the same system reliability for adsorption at low and high-pressure conditions.

Furthermore, the differential apparatus has been shown reducing artifacts associated with temperature deviations and gas non-idealities, as both branches experience the same effects equally (Blackman et al., 2006; Browning et al., 2002; Zielinski et al., 2007). This last effect can be negligible at low pressure, however, it is particularly relevant for high pressure measurements, returning back to the original goal of the apparatus design.

Besides the differential pressure transducer, at least one absolute pressure transmitter (*PT* in the Fig. 8) is present and generally placed in the pre-dosing section (in the Fig. 8, the pre-dosing section is the one comprised among the inlet gas line and the valves connecting to the dosing cells); this is aimed to the reduction of asymmetries in the adsorption region and to limit the number of transducers used to two, relying to a more cost-effective system. An example is the apparatus proposed by (Sircar et al., 2013). In literature, the reference to other types of configurations can be found, in which, for example, two absolute pressure transducers are

placed in the dosing volumes (Zielinski et al., 2007). The point is that, with one absolute pressure transducer, all the system pressures are determined by mole balance, because the pre-dosing section pressure is the only one directly measured. In these terms, the possibility of error propagation is in a way exacerbated due to the fact that all quantities are calculated referring to a single experimental reading.

In a differential configuration, the symmetricity among the two branches is an important design feature: some differential volumetric apparatus have been developed being not symmetrical, so the two branches have different internal volumes (Zhang et al., 2004). Other systems are instead designed being symmetric, which means having the branches much similar as possible in terms of internal volumes. (Suzuki, 1982; Suzuki et al., 1987) proposed the use of a symmetrical differential apparatus for sub-atmospheric adsorption measurements of solid having low-adsorption capacity; in the paper, the reference to symmetricity in terms of volume and temperature among the branches is detected being crucial for the reliability of the results. Other examples of differential apparatus with two mirror-image single-branch units are proposed by (Blackman et al., 2006; Browning et al., 2002; Qajar et al., 2012; Sircar et al., 2013; Zielinski et al., 2007). Concerning the internal volumes, another consideration can be done related to the difference in the dosing and uptake cell volumes: some systems are built up having the dosing/uptake cells with almost the same volume (Zielinski et al., 2007), but, the majority of the apparatus proposed, show the dosing cell volumes quite bigger than the uptake cell volumes (generally, the dosing volume is the double of the uptake cell) (Blackman et al., 2006; Qajar et al., 2012; Sircar et al., 2013).

The HP-ADVA apparatus is a symmetric system having the dosing/uptake cell volumes almost equal. The design details and specifications, the experimental procedures and analytical methods for the determination of the gas adsorbed are described in the *Chapter 2* and *Chapter 3* of the thesis.

1.3.1 Volumetric apparatus: sensitivity analysis

The volumetric method is considered an advantageous way to measure adsorption isotherms as it is easy to develop even for high-pressure measurements, it is relatively cheap, physically robust and reasonably reliable. The accuracy of conventional (Belmabkhout et al., 2004; Blach & Gray, 2007; Broom & Moretto, 2007; Demirocak et al., 2013; Mohammad et al., 2009; Webb & Gray, 2014a, 2014b) and differential (Blackman et al., 2006; Browning et al., 2002; Qajar et

al., 2012; Sircar et al., 2013) units have been addressed, and the inter-laboratory tests indicate error is common in this kind of practice. As previously mentioned, the disadvantage of this method are the errors due to the indirect determination of the adsorbed quantities.

Using a higher sample size has been sufficiently proven to increase the accuracy of the volumetric measurement, however this is often not possible with novel adsorbent materials, for which quantities are often limited. Another point is the confirmation that using small cell volumes led to more accurate results. (Demirocak et al., 2013) concludes that, if, for some material, a sample in gram quantities cannot be prepared, selecting the smallest reservoir volumes can alleviate the accuracy problem. One point to remember is that, even if the sensitivity can be optimized by minimizing the cell volumes, in practice some distance is required between the valve and the sample to allow regeneration and preconditioning of the sample. Moreover, most commercial systems are designed for cryogenic measurements (using Liquid Nitrogen), so room for placing the dewars is needed. This means that generally the volume ratio among dosing/uptake cell volume is maintained among 0.5 and 1 (Wang et al., 2020). These two aspects will not be analysed having been largely assessed and confirmed.

A series of other pitfalls need to be accounted such as uncertainties in the volume calibration, tied to the accuracy of the pressure transducer used; uncertainties in correcting for the volume occupied by the sample by errors introduced due to low accuracy of the instrument used for the measurement such as laboratory balance used to weight the sample mass; temperature effects and gradients and treatment of gas compressibility. All these effects accumulate together when calculating the final gas uptake; moreover, many of these features are exacerbated at high pressures, which are the conditions of major focus in our discussion. Overall, the effects of the following parameters have been considered in the mentioned literature:

- deviations in calibrated volumes (dosing/uptake volume) (Belmabkhout et al., 2004; Qajar et al., 2012; Sircar et al., 2013; Webb & Gray, 2014b)
- valve internal volumes calibration (Sircar et al., 2013)
- pressure measurement accuracy (absolute/differential pressure transducer accuracy) (Belmabkhout et al., 2004; Broom & Moretto, 2007; Qajar et al., 2012; Sircar et al., 2013; Webb & Gray, 2014a)
- temperature measurement accuracy and temperature gradient for differential apparatus (Belmabkhout et al., 2004; Broom & Moretto, 2007; Qajar et al., 2012; Sircar et al., 2013)

- accuracy in the sample mass weighing (Belmabkhout et al., 2004; Qajar et al., 2012)
- amount of sample used for the measurement (Demirocak et al., 2013; Sircar et al., 2013; Webb & Gray, 2014a)
- free volume after sample loading (Blackman et al., 2006; Broom & Moretto, 2007; Demirocak et al., 2013; Webb & Gray, 2014a)
- cumulative error and system volume ratio (Qajar et al., 2012; Sircar et al., 2013)

The precision of a volumetric method can be also significantly improved by proper choice of the operating equation to process the data, as assessed by (Sircar et al., 2013). Indeed, the majority of the approaches in literature propose the use of simplified forms of the mass balances, through which the gas adsorbed is calculated. However, the completeness of the mass balance used in data analysis seems affecting the final results. A deeper reflection about this aspect is provided in *Chapter 3*, *Section 3.2*. Moreover, an appropriate equation of state for the treatment of gas non-idealities can lead to the reduction of errors in the gas uptake calculated.

In performing the sensitivity analysis, different approaches are then used in terms of analytical approach: standard analytical method has been used in most cases (Demirocak et al., 2013; Mohammad et al., 2009; Qajar et al., 2012; Sircar et al., 2013; Webb & Gray, 2014a, 2014b); however, computational approach (e.g. Monte Carlo simulation) can be used as alternative procedure: (Mohammad et al., 2009) proposes both approaches confirming the obtainment of similar results.

The parameters studied, the specific approach and the analytical method used are presented in detail in the *Chapter 5* of this thesis, while the results and discussion of the sensitivity analysis is presented in the *Chapter 6*.

Chapter 2 - Experimental methods and materials

In *Chapter 2,* the materials and methods used in the experimental campaign are accurately described: starting from the description of the apparatus set-up, all the procedures to perform the experiments are reported. In particular, equilibrium experiments at ambient temperature are carried out as base analysis for finding potential issues. Subsequently, equilibrium experiments at cryogenic conditions are proposed: carrying on experiments in extreme conditions is a good way to discover and underline other criticalities of the system, which may not occur at ambient conditions.

2.1 System set-up: real laboratory apparatus

The HP – ADVA apparatus is a high-pressure volumetric differential apparatus used for adsorption analysis (Mangano, Wang , & Brandani, 2019). A detailed system schematization is provided:
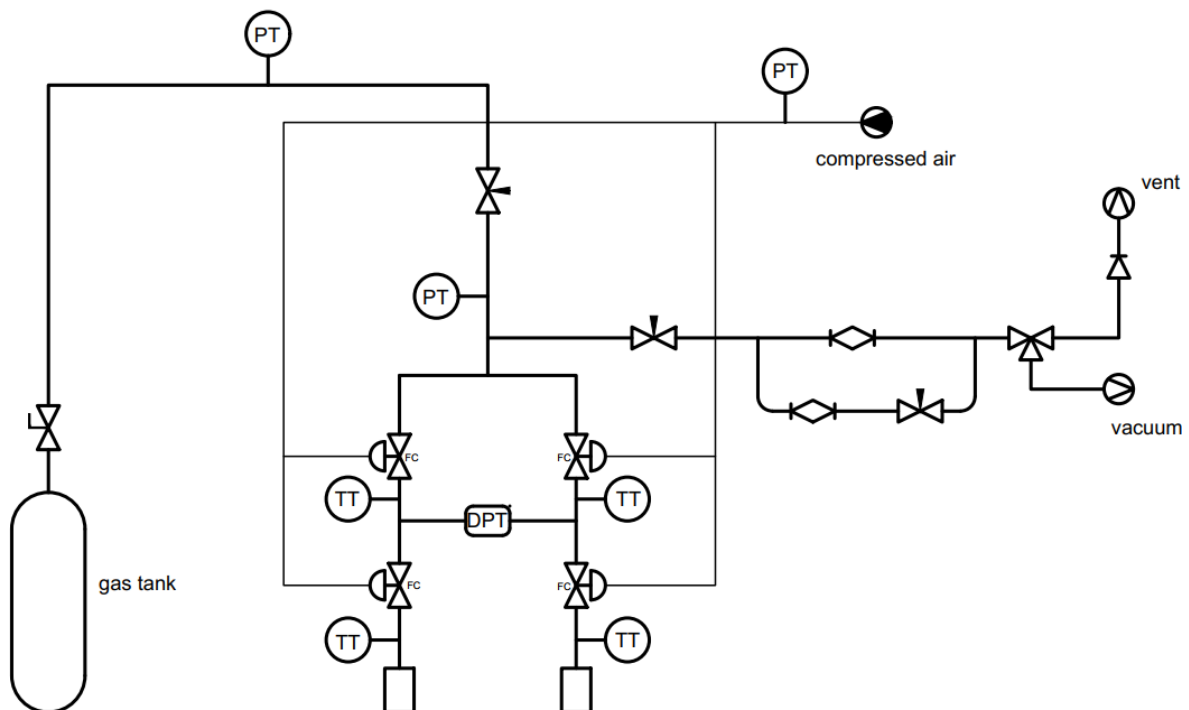

Figure 9 - *HP-ADVA scheme (UNICHIM P&ID standards).*

A simplified schematisation is then used along the discussion for simplicity sake:
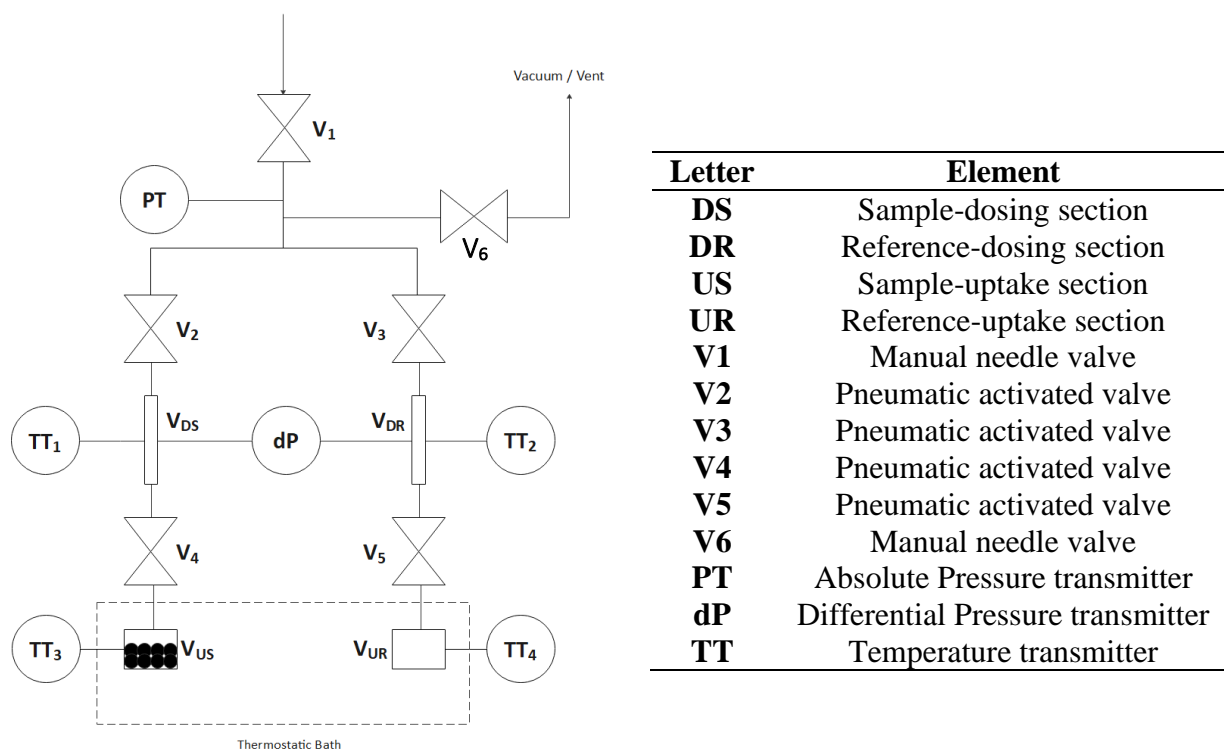
Figure 10 - *HP-ADVA simplified schematics (left), legend of the schematics (right).*

The apparatus is formed by two symmetrical branches: the sample-branch in which the adsorbent material is loaded during experiments and the reference-branch, without the adsorbent material. The amount of gas adsorbed in the material is based on the differential pressure change between the reference cell and the cell containing the sample. Further details will be given later in the discussion (*Chapter 2* and *3*).

All system components are made of $1/4''$ stainless steel tubing. Pneumatic remotely-controlled high-pressure bellow valves (*Swagelok High-Pressure, Pneumatically Actuated Bellows-Sealed Valves SS-HBV51-C*) are used to reduce the user error during the valve opening/closing. The system is connected to gas lines provided with safety connections: the gas streams available are Helium (*BOC- Helium Ultra High Purity Grade Compressed, 99.999% (Grade 5)),* Carbon Dioxide, Nitrogen, Methane. The specifications of the other gas lines, different from the Helium, are not reported because not directly used during the experimental campaign.

Leak tests are periodically performed to confirm the system remains leak free; in particular, Helium expansions are performed and absolute/differential pressure transducers signal is

recorded over time to see the trend and to detect potential leaks. If a leak is suspected, an electronic gas leak detector is generally used to localize and adjust the leak.

Three sections can be distinguished in the apparatus:

- Pre-dosing section: volume comprised between valves V1,V6,V2,V3, it is the connection among the dosing cells, the inlet gas pipeline and the lines of the vent and the vacuum pump (*Pfeiffer HiCube, model TC110*). The gas inlet flow rate is regulated via manual valves, in the same way the vacuum and vent lines which are provided by flow restrictors too. In particular, the vent/vacuum line presents a three-way plug valve, and the vent line is equipped with an excess flow activated diaphragm valve. Through Helium expansion at low pressure, this section has been evaluated having a volume $V_{Pre} \approx 16$ cc.

  In the pre-dosing section, the absolute pressure transducer (*Rosemount-In-line Pressure Transmitter, model 3051TA4A2A21BI1Q4D4*) is used to directly measure the pressure in the system. Placing it in the pre-dosing section avoids the introduction of asymmetries among the dosing and uptake sections, crucial for adsorption evaluation. Once valves V2,V3 are closed, knowing that value, and by means of moles balance, is then possible to characterize all the pressures in the system by reading at the differential measurements, dP. Further details provided in *Chapter 3*.

- Dosing section: divided from the pre-dosing section by pneumatic valves V2 and V3, and from the uptake section by valves V4 and V5. It is provided with the differential pressure transmitter (*Rosemount-Coplanar Pressure Transmitter, model 3051CD2A22A1BI1Q4D4*) for accurate pressure measurements. The temperatures, on both branches, are measured through thermocouples (TT1,TT2) (*K-type thermocouples*).

- Uptake section: last section of the apparatus, in the sample-side the adsorbent is loaded during the adsorption experiments. The uptake cells are generally maintained at constant temperature using a liquid bath with a service fluid (water/ethylene glycol, 50%v/v) and the temperature is measured through the installation of thermocouples (TT3, TT4).

The other components of the apparatus are exposed to room temperature so not provided with a system for temperature maintenance. The absence of external temperature control led to system temperatures variation with room temperature: typically the variations are below 1°C.

The four thermocouples TT1, TT2, TT3, TT4 allows a continuous monitoring of the gas temperature in each section of the apparatus.

As mentioned in *Chapter 1,* a key feature of the apparatus is the symmetry of the two sides: the dosing and uptake sections are created much symmetrical as possible to obtain reliable results in the measurements. The symmetry between the branches is provided by:

- The volumes of the dosing/uptake sections fall between $\approx$11-12 cc, with a volume ratio $\Gamma_V = \frac{V_{DS}}{V_{US}} \approx \frac{V_{DR}}{V_{UR}} \approx 1.16$. These volumes are calibrated using the pressure expansion method: a more detailed analysis about volume calibration will be provided in the *Sections 2.2.2 and 4.3.*

  The apparatus has been designed with internal volumes much lower than other examples of similar apparatus (Sircar et al., 2013; Zielinski et al., 2007) and maintaining the ratio among dosing/uptake cells close to 1. These choices are aimed to obtain more reliable results.

- The use of a single bath with the recirculation of the service fluid to maintain "temperature symmetry" during the isotherm analysis (Zielinski et al., 2007). Generally, during experiments, the uptake cells need to be maintained at a constant temperature and this is done by using a single dewar, made by insulated steel, connected to a liquid circulator and temperature controller *(Julabo CORIO® CD - Bath circulator)*, through thermally isolated pipelines, which allows to maintain the same liquid level in both sides.

  However, for measurements at cryogenic conditions (77 K, Liquid Nitrogen), the bath circulator cannot be employed. Moreover, two separate cryogenic dewars were required introducing potential temperature asymmetries during experiments. As better explained in *Section 2.3*, this aspect has been challenging to face.

- The use of the same valve type separating the dosing and the uptake sections on both branches: the four valves are connected, through apposite pipes of the same length, to compressed air, which pressure has been set before each experiment for the best operation conditions, as provided by manufacturer; moreover, the valves are remotely controlled in order to open/close them perfectly at the same time. The use of no-zero volume valves is tied to the unavailability in the market of high-pressure models, from here the need of an accurate characterisation of the valve, which is proposed in *Section 2.2.2.1.*

The absolute and differential pressure transmitter readings, as well as the thermocouples measurements are computer-recorded using the National Instruments™ LabView software; moreover, the software allows the collection of the experimental data and the contemporaneous creation of Microsoft ™ Excel sheets, that can be used repeatedly for future experiments and analysis.

Pictures of HP-ADVA system are provided:
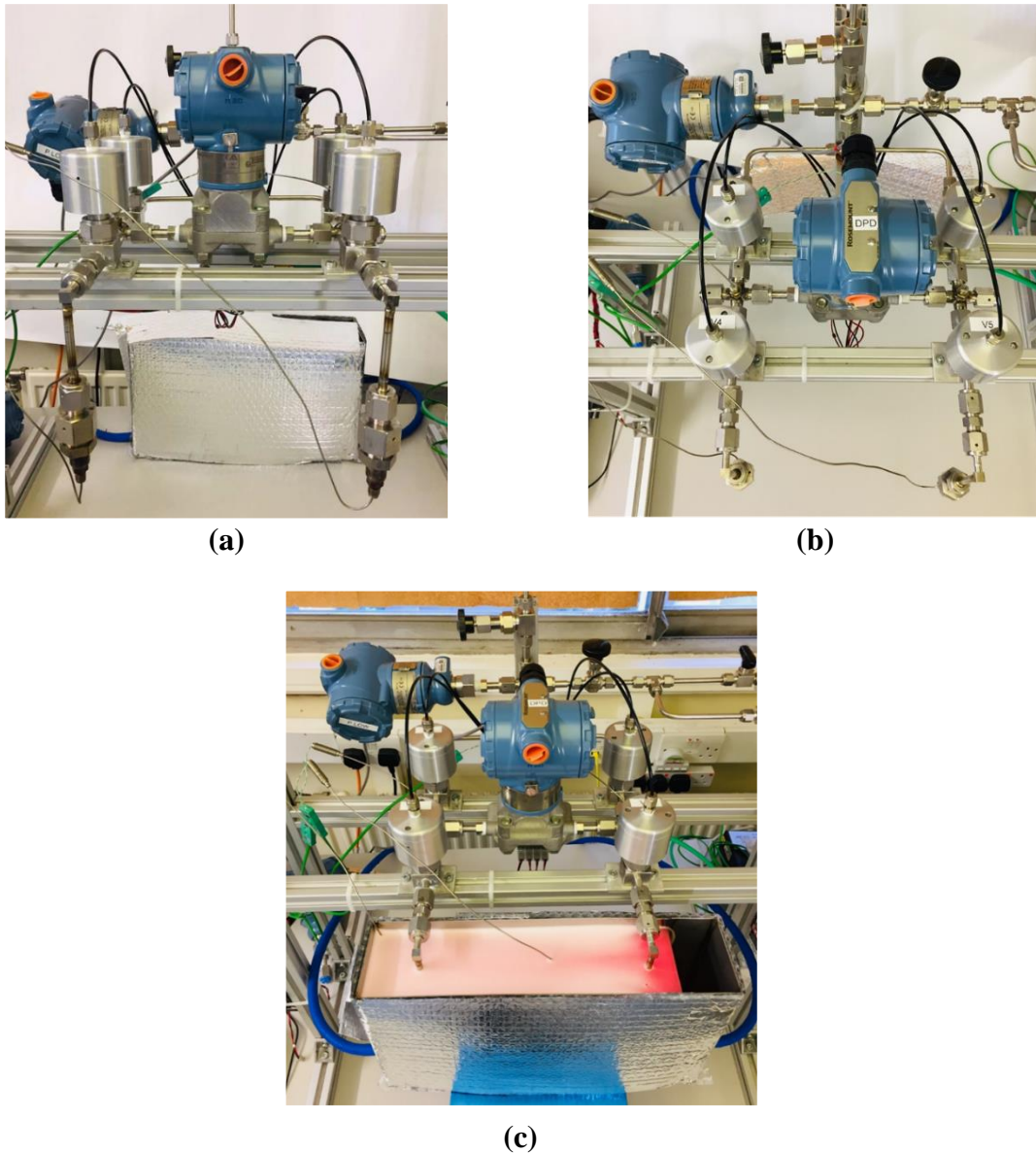

(a)

(b)

(c)

*Figure 11 – Laboratory apparatus pictures (**University of Edinburgh - Fleeming Jenkins Building Lab 1.196D**): (a) front view, (b) top view and (c) thermostatic bath (ethylene glycol/water mixture 50%v/v).*

2.2 Experimental procedure at ambient temperature

2.2.1 Procedure for equilibrium measurements: isotherm construction

To carry out an adsorption experiment, the sample is prepared and loaded in the uptake-sample cell with a weighed and counted number of stainless-steel beads: this is done to reduce the void volume, to enhance the heat transfer rate achieving near isothermal conditions and to put sample particles away from each other (Wang et al., 2020). In the uptake-reference cell, an equal number of the same stainless-steel beads are loaded to maintain, as much as possible, symmetric conditions between the branches. The entire system is then outgassed by the vacuum pump for a proper amount of time (15-30 minutes).

Depending on the adsorbent, a regeneration procedure is required before each experiment ensuring the solid is free from traces of moisture and gases adsorbed. It can be performed on-line, so without opening the system using an external electric furnace built for the apparatus: it is constituted by an insulated cage inside which the uptake-sample cell is enclosed and the temperature for the regeneration is controlled remotely through an electrical device.

As a first, one needs to exactly evaluate the volume available for the gas inside the uptake cell (sample-branch), once the adsorbent has been filled in the system. This can be easily estimated by carrying out a Helium expansion at low pressure, between 1 and 2 bar, and room temperature, ranging from 20 and 25 °C, from dosing to uptake. Assuming that in these conditions the adsorption of Helium is negligible, it is possible to retrieve the value required. After having connected the desired gas stream to the inlet line, the vacuum is again applied to remove traces of Helium.

The uptake cells are isolated closing the valves V4, V5 and immersed into the liquid bath, for the required temperature conditions. The valves V2, V3 are closed too and, after the time required for the stabilisation of the temperature (remote control by LabView software), the experiment is started. In these vacuum initial conditions, data of the absolute, differential pressure and temperature is logged to establish, for the pressure transducers, the offset point for the measurements.

The pre-dosing section is pressurised until the desired value, opening manually the valve connecting the inlet gas stream pipeline and data is collected. Valves V2, V3 are then opened to perform the first expansion from pre-dosing to dosing volumes: the valves V2, V3 are newly

closed and, after waiting a time for pressure stabilisation, the values of pressure and temperature are logged.

The last step is to perform the expansion from the dosing to the uptake cells by opening the valves V4, V5. The time for the equilibration is now a key aspect: since the absolute pressure transducer, at this point, remains isolated from the experiment (V2 and V3 closed) the operator relies only on the differential pressure signal to establish when the equilibrium is reached. For multistep isotherms, the pressurisation procedure is repeated as explained before, without reducing the uptake cells pressure, for the entire pressure range under investigation.

The same procedure is done for "blank measurements". Blank experiments are performed without the adsorbent loaded in the uptake-sample cell and using Helium. The analysis is aimed to check the correct calibration of the system and the response of the apparatus, particularly at high pressure, so in condition of saturation. Indeed, blank measurements are not directly tied to the effective estimation of the *absolute* adsorbed amount, but they are required to estimate the *net* adsorbed amount (see *Introduction*).

In particular, the blank experiments have been carried out in a pressure range between 0 – 100 bar and at two different temperature conditions: ambient temperature (25 °C) and cryogenic conditions (T_{LN}). For more details see *Section 4.1*.

2.2.2 Procedure for apparatus calibration

The calibration of the apparatus, consisting in the estimation of the pre-dosing/dosing/uptake cells internal volume is a key aspect to obtain reliable results from experimental data analysis.

The gas used for the calibration is Helium and the measurements are performed at fixed temperature: generally, the uptake cells are maintained at 25 °C using the ethylene glycol solution bath, while the dosing cells are exposed to room temperature (around 20-25 °C). Helium is selected as gas to be used because, at this conditions, the adsorption is considered negligible avoiding interferences with the analysis.

Operatively, the calibration is performed through alternate gas expansions in the system: the sample and reference branch are calibrated singularly by isolating one branch from the other, closing alternatively the valves V2, V3. Moreover, the expansions are carried out with the

empty system and then loading inside the uptake cells, of both sample and reference branches, a weighted and counted number of stainless-steel beads. The stainless-steel beads are used as non-adsorbent material to add a known volume in the mole balance for the internal volumes' calculation.

For each branch, two series of expansions are performed: from dosing to uptake section and from uptake to dosing section to collect an appropriate number of experimental data.

As a general rule for operating, after any operation involving the opening of the system, the apparatus is washed with Helium three times to eliminate any trace of air from the line and, before each experiment, the vacuum is created to collect the offset point for the calculations.

The accuracy in performing the apparatus calibration, in this type of apparatus, becomes significantly relevant due to the presence of the absolute pressure transducer outside the dosing cells: as mentioned in the *Section 2.1*, the transmitter is placed in the pre-dosing section, so no direct measurement of the dosing/uptake internal pressure is possible. All the volumes are then effectively calculated and, to avoid the introduction and the consequent propagation of error in the analysis, very accurate calibration needs to be met in both the experimental and analytical aspects.

In the experimental campaign, the calibration of the apparatus has been completed in a pressure range of 0-100 bar to check unexpected behaviour at high pressure. A detailed analysis is proposed in the *Section 4.3*.

2.2.2.1 Procedure for apparatus calibration: valve characterisation

The characterization of the pneumatic actuated valves (*Swagelok, SS-HBV51-C*), separating the pre-dosing to the dosing section and the dosing to the uptake section, consists in the estimation of their effective internal volume. Hypotheses have been moved towards the potential influence of the valves volume in the total internal volume: unexpected results, obtained during the experimental campaign (*Section 4.1 and 4.3*), can be linked to the valve internal volume which may be negligible at low pressure (below 50 bar), but could be relevant and to be considered at high pressure (between 50 – 100 bar).

The estimation of the internal volumes is aimed to better understand the internal configuration of the valve: an inlet and an outlet section are evident from the manufacturer's

datasheet sketch (Fig. 12) and the effective volumes can be estimated to check the symmetricity/asymmetricity of the valve. Moreover, an estimation of the valve volume can be useful in the perspective of taking account, explicitly, of the valve volumes in the mole balances used for data analysis (*Chapter 3*).
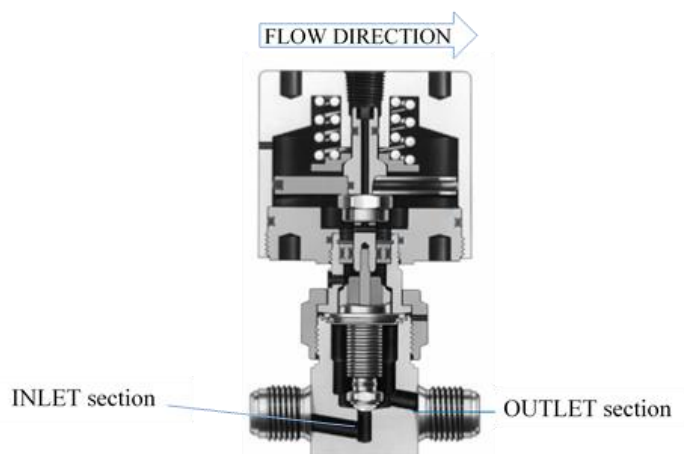

Figure 12 – Pneumatic actuated valve (Swagelok, SS-HBV51-C) sketch taken from manufacturer's datasheet. The "flow direction" arrow shows the direction of the gas expanding from pre-dosing to dosing and from dosing to uptake sections.

Experimentally, the estimation of the volume of the valves has been done performing alternate Helium expansions, separately in the two branches, with the system originally under vacuum and at room temperature (20-25 °C). The hypothesis of asymmetricity of the valves led to perform two consecutive series of expansion:

- for the "inlet" section volume: expansion from dosing section to uptake section (valves V2, V3 closed): the valves V4, V5 are opened for the gas expansion and then closed to detect the pressure variation
- for the "outlet" section volume: expansion from dosing + uptake section (valves V4, V5 opened) to pre-dosing section: the valves V2, V2 are opened for the gas expansion and then closed to detect the pressure variation

The pressure variation is related to gas mole displacement due to the valve internal volume. These kinds of expansions have been selected based on the position of the pressure transmitter in the system: the uptake cells pressure cannot be measured directly but only through mass balance.

2.3 Experimental procedure at cryogenic conditions

Adsorption equilibrium analysis at different temperatures with respect to ambient conditions (around 25 °C) is required for applicative, industrial purposes or to have a wider spectrum of the gas-adsorbent behaviour. Operatively, the experiments are carried out in the same way as explained in the *Section 2.2.1*, so the procedure will not be explained newly. However, some peculiarities need to be assessed in performing cryogenic experiments.

Overall, the HP-AVDA apparatus is not provided with a device for temperature maintenance and control: the uptake cells can be maintained at a constant required temperature through the immersion in the recirculating bath (see *Section 2.1*). When performing measurements at uptake cells temperature consistently different from room temperature, such as for cryogenic conditions, the estimation of the precise portion of uptake cells effectively immersed in the bath and the portion remaining outside is required. This because inconsistencies may arise if not taking account of the effective volume immersed: this is negligible in the cases of no high differences of temperature, but it is exacerbated when the immersed and not immersed portions are at considerably different temperature conditions.

For simplicity sake, the nomenclature "hot volume" will be referred to the immersed portion of uptake cells while the portion remaining outside, will be denominated as "cold volume" (Fig. 13). The choice could appear counter intuitive, anyway this definition is not only specific for cryogenic experiments, but to experiments in which the temperature of the bath will be considerably higher than the room temperature too.

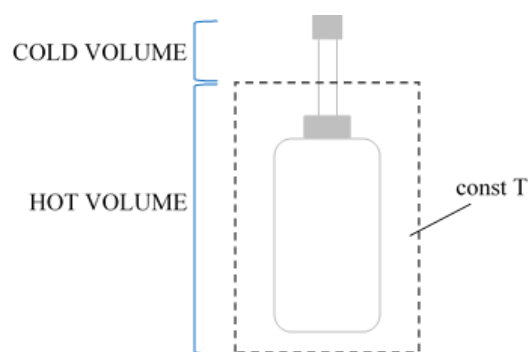*Figure 13 - Uptake cell schematisation: distinction between "hot" and "cold" volume. The dotted line represents the recirculating bath borders.*

Operatively, cryogenic measurements and the estimation of the hot/cold volume require the development of a protocol to obtain reliable results. Experimental issues are mainly related to the handling of Liquid Nitrogen which has a high evaporation rate, if exposed to atmospheric

conditions and the use of two separated dewars, one for the sample-branch and one for the reference-branch, instead of a unique one. This is due to the unavailability, among the laboratory facilities, of a device for the recirculation of Liquid Nitrogen.

As mentioned, the experiment, for blank construction, is carried out in the same way as the operation at ambient temperature, (*Section 2.2.1*); differently, for the estimation of the hot/cold volume portions Helium expansion are carried out with the unbalanced system: 110 stainless-steel beads are loaded in the reference – branch, while the sample – branch uptake cell is maintained empty. This choice is related to exaggerating the asymmetricity among branches detecting higher differential pressure variations, leading to more accurate calibration of the internal volumes.

During the experimental campaign, four protocols have been tested to check the operational feasibility and the quality of the results. In general, the dewars, containing the Liquid Nitrogen, are placed above two separated laboratory elevators as medium to control the effective level in both branches: practically, the amount of nitrogen evaporating during experiments is not equal in both branches.

- *Protocol 1*: the initial level of Liquid Nitrogen in the dewars reaches the end of the nut of the uptake cells (both sample and reference branches) to maintain the symmetry. The nut has been selected as a physical element to have a benchmark between the sides. During experimentation, the symmetry is maintained by moving up and down the two elevators.

- *Protocol 2*: the initial level of the Liquid Nitrogen reaches the end of the nut of the uptake cells, but, in this case, filling completely the dewars with Liquid Nitrogen. A way to potentially control the level of the nitrogen inside the separated dewars and to maintain, as much as possible, the symmetry among the branches, is to fully fill the dewars, in this way the level of LN, which evaporates during experiment, is controlled by refilling the entire volume of the dewars and no more moving up and down the elevators.

Figure 14 - *Uptake cells immersed in Liquid Nitrogen bath*[1] *(protocol 2).*

- *Protocol 3*: operation done as in Protocol 2, but adding an equal number of isolating floating balls onto the surface of the LN in order to decrease the surface effectively exposed to the atmosphere, trying to reduce the evaporation rate. This protocol has been demonstrated being difficult to carry out.

- *Protocol 4*: once selected an equal level for both branches, a plastic transparent cover (specially built for the apparatus) is used on top of the dewars to reduce the Liquid Nitrogen evaporation rate. An issue faced in this last configuration, is the limitation in moving the dewars by means of the laboratory elevators, due to the presence of the covers.
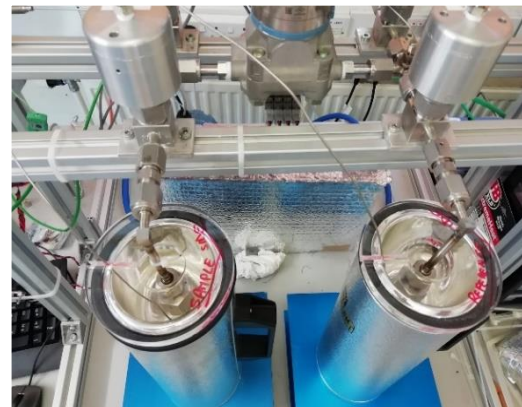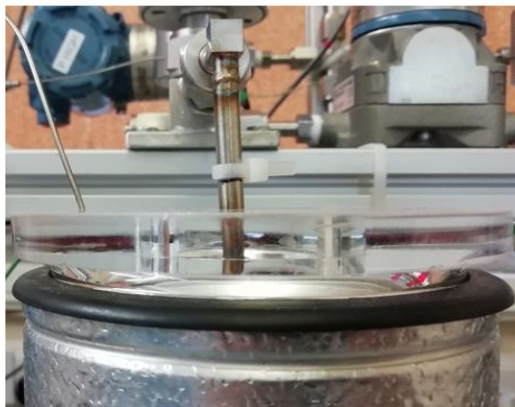
Figure 15 - *Uptake cells immersed in Liquid Nitrogen bath (protocol 4).*

---

[1] In recent development of the experimental set-up, the tubes have been provided with an isolating cover to limit condensations/solidification phenomena like happening in the picture proposed (Fig. 14)

From the experience, *Protocol 4* appeared the best procedure with the laboratory facilities available, because the signal of the pressure readings appeared more stable: data analysis confirmed the experimental scenario too (see *Section 4.1.2*).

Chapter 3 - Analytical methods

Chapter 3 is a resume and schematisation of the analytical sources: the governing equations used for data analysis and for the sensitivity analysis are presented, considering both single-branch and differential systems. Precisely, very general forms of the equations are listed to justify the approach, but the analytical details are reserved to the research group.

The analyses are performed using PTC Mathcad® 15.0 simulator: spreadsheets have been specifically implemented starting from material already available.

3.1 Single-branch system mass balance

The adsorption analysis, performed using a conventional volumetric system, is based on the measure of the absolute pressure before and after the gas expansion: the difference among the initial and final conditions, knowing the internal volumes of the apparatus, will represent the amount of gas adsorbed into the sample (see *Section 1.3*).

A scheme of a single-branch apparatus, in line with the differential schematisation described in the *Section 2.1*, is reported for simplicity sake:
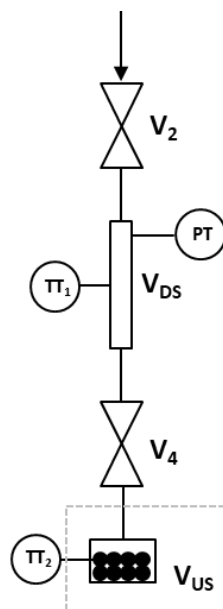

Figure 16 – Single-branch volumetric apparatus simplified schematic.

In the equations presented, the same notation is maintained among single-branch and differential apparatus: "S" refers to sample-side and "R" to reference-side (see *Section 2.1*).

In general, for a single gas, the number of moles in a closed volume V, at a temperature T and pressure P is given by the equation:

$$(11) \quad N = \frac{PV}{zRT}$$

where $z(T, P)$ is the compressibility factor of the gas at T and P, R is the ideal gas constant. Along the discussion, the compressibility factor is determined by the GERG-2008 Equation of State (Kunz & Wagner, 2012) for all the cases studied.

In case of single-branch volumetric system, writing the moles balance equation at each data point, leads to the following relationship:

$$(12) \quad \frac{P_{DS_{i-1}} V_{DS_c}}{z_{DS_{i-1}} R \, T_{DS_{i-1}}} + \frac{P_{US_{i-1}} V_{US_c}}{z_{US_{i-1}} RT_{US_{i-1}}} = \frac{P_{S_i} V_{DS_c}}{z_{DS_i} RT_{DS_i}} + \frac{P_{S_i} V_{US_c}}{z_{US_i} RT_{US_i}} + \Delta n_i$$

where the notation "i" stands for the ith adsorption data point: "i-1" before the gas expansion, "i" after gas equilibration. Δn_i are the moles of gas adsorbed in the material at i[th] adsorption step.

The terms V_{DSc}, V_{USc} account for the free space of the dosing and uptake cells available for the gas. The subscript "c" refers to the fact that these terms are not coincident to the entire cell volumes, but they are corrected by considering the effective space available for the gas after the sample and beads loading (see *Chapter 2*). As said in the *Section 2.1.1*, once the adsorbent and the beads are loaded inside the cell, an Helium expansion is performed to estimate the effective void volume available inside the cell (negligible adsorption of Helium inside the sample).

The internal valve volume needs to be considered too, because no-zero volume valves are used. In this concern, the presence of pneumatic actuated valves, separating the dosing and uptake sections is accounted through the term α:

$$(13) \quad \alpha = \frac{V_{valve,inlet}}{V_{valve,inlet} + V_{valve,outlet}} = \frac{V_{valve,inlet}}{V_{valve}}$$

for α = 1 all the valve internal volume is in the inlet section, for α = 0 all the valve internal volume is in the outlet section (see *Section 2.2.3*). In the general form of the mass balance (Eq. (12)), this factor is accounted in the correction of the volumes (V_{DSc}, V_{USc}).

The terms P_{DS}, P_{US} and P_S are the pressure of the dosing cell, the uptake cell and the equilibrium pressure in the sample-branch, after the opening of the valve V4 (see Fig. 16), so

the one connecting the dosing and uptake cells. In addition, T_{DS} and T_{US} are the temperature of the dosing and uptake cells before and after the expansion. The compressibility factors are calculated at each Temperature and Pressure condition.

The adsorption isotherm represents the quantity of gas adsorbed by the material over pressure (or fugacity). The construction of experimental isotherm is done by summing up the moles Δn_i adsorbed at each consecutive step until the last one, corresponding to the final operating pressure. Operatively, the isotherms are performed as multistep adsorption of the gas into the material without restoring the initial conditions.

3.2 Differential system mass balance

The differential volumetric apparatus for adsorption measurement can be considered as two independent traditional volumetric sorption units, so the mole balance consists in a differential mole balance between the two branches (see Fig. 10).

From an analytical point of view, the key aspect of the procedure is to take account of the differential pressures between the two branches instead of considering the absolute pressure: the differential pressure transducer is consistently more accurate than the absolute one, allowing to obtain more precise results.

The mole balances for the sample and reference branches of the differential apparatus at the ith adsorption step can be written as:

$$(14) \quad \frac{P_{DS_{i-1}} V_{DS_c}}{z_{DS_{i-1}} R\, T_{DS_{i-1}}} + \frac{P_{US_{i-1}} V_{US_c}}{z_{US_{i-1}} RT_{US_{i-1}}} = \frac{P_{S_i} V_{DS_c}}{z_{DS_i} RT_{DS_i}} + \frac{P_{S_i} V_{US_c}}{z_{US_i} RT_{US_i}} + \Delta n_{S_i}$$

$$(15) \quad \frac{P_{DR_{i-1}} V_{DR_c}}{z_{DR_{i-1}} R\, T_{DR_{i-1}}} + \frac{P_{UR_{i-1}} V_{UR_c}}{z_{UR_{i-1}} RT_{UR_{i-1}}} = \frac{P_{R_i} V_{DR_c}}{z_{DR_i} RT_{DR_i}} + \frac{P_{R_i} V_{UR_c}}{z_{UR_i} RT_{UR_i}} + \Delta n_{R_i}$$

The subscript "i" stands for the ith adsorption step: "i-1" before the expansion, "i" after the gas equilibration. Δn_{Si} and Δn_{Ri} are the amount of gas moles adsorbed into the material in the sample and reference branch, respectively.

The terms V_{DSc}, V_{USc}, V_{DRc} and V_{URc} account for the free space in the dosing and uptake cells, for both sample and reference sides, available for the gas.

As for the single-branch system, these terms are not coincident to the entire cell volumes, but they are corrected by considering the effective space available for the gas after the sample and beads are loaded (see *Chapter 2*). Experimentally, the estimation of the effective void volume available inside the cell is performed through Helium expansion (*Section 2.1.1*). The same parameter α, described by the equation (3) is used to account for the pneumatically-actuated valve volume. In the same way, α = 1 for the entire valve volume placed in the inlet section and α = 0 placed in the outlet section. Also in this case the α parameter is accounted in the volume corrections (V_{DSc}, V_{USc}, V_{DRc} and V_{URc}).

The terms P_{DS}. P_{US}, P_{DR}. P_{UR} are the pressure of the dosing and the uptake cells before gas expansion, for sample and reference branch, respectively. While P_S and P_R are the pressure in the sample-branch and in the reference-branch after the opening of the valves V4, V5 (see Fig. 10), so the ones connecting the dosing and uptake sections. In addition, T_{DS}, T_{US}, T_{DR} and T_{UR} are the temperature of the dosing-sample, uptake-sample, dosing-reference and uptake-reference cells before and after the expansion. The compressibility factors $z(T,P)$ are calculated at each relative condition (Kunz & Wagner, 2012).

Defining the pre-expansion dosing differential pressure (ΔPD_{i-1}) and the post-expansion system differential pressure (ΔP_i) as:

(16) $\Delta PD_{i-1} = P_{DR_{i-1}} - P_{DS_{i-1}}$

(17) $\Delta P_i = P_{R_i} - P_{S_i}$

the effective number of moles adsorbed is obtained by the difference among the moles adsorbed in the two branches (Eq. (4), (5)):

(18) $\Delta n_{ads_i} = \Delta n_{S_i} - \Delta n_{R_i}$

being the adsorbent sample only loaded in the sample-branch, so $\Delta n_{R_i} \cong 0$.

The construction of experimental isotherm is done by summing up the moles Δn_i adsorbed at each consecutive step until the last one, corresponding to the final operating pressure. As said, the isotherms are performed as multistep adsorption of the gas into the material without restoring the initial conditions.

For cryogenic experiments, the Eq. (18), resulting from the combination of the Eq. (14) and (15), is used by modifying the equation dividing the uptake cell volume in two terms referred to the "hot volume" and the "cold volume". Each section, calibrated experimentally by the procedure in the *Section 2.2.2*, will be assessed with the corresponding pressure and temperature conditions.

Comparing with known literature examples, in the expression used for the data analysis no particular simplifications are considered: for example, (Zielinski et al., 2007) assumes that the temperatures of the sample and reference branches are equal, i.e. $T = T_S = T_R$, leading to the consideration of equal compressibility factors prior and post-expansion among the two branches; moreover, the effect of the valve volumes is not considered, even if the same type of no-zero volume valves are used in the apparatus. (Sircar et al., 2013) considers a quite comprehensive form of the governing equation, but introducing some approximations, such as the neglection of the valve volume, which is considered negligible for hydrogen adsorption analyses: for other gases, the effect of the valve volume has been discovered being not negligible, particularly at high pressure conditions. Moreover, the consideration of perfect symmetricity among the two branches of the apparatus is proposed, which is quite unrealistic for a real system design. Another important feature is the new approach proposed in terms of hot/cold volume: when the equilibrium measurements are performed at temperature conditions consistently different from ambient temperature, additive details need to be estimated experimentally.

In the approach used, the only simplifying assumption is the instantaneous closing/opening of the pneumatic actuated valves separating the dosing and the uptake cells. In this concern, a deeper understanding of the valve behaviour is necessary and aimed at the modification of the mass balance considering the influence of the valve opening/closing. In fact, the procedure could be influenced by the operating pressure: at high pressure (above 50-60 bar) the valve should take more time for opening/closing, causing a different distribution of the gas moles in the volumes with respect to the instantaneous closure.

3.3 System calibration

The analytical procedure for system calibration is not reported in detail: it hinges on the mass balances presented above (Eq. (14), (15)) and, specifically, on the calculation of volume ratios

(Γ_V, see *Section 2.1* for the definition), considering the empty system and the system uptake cells loaded with a known amount of stainless-steel beads (see *Section 2.2.2* for the experimental procedure details). As mentioned, this procedure becomes crucial due to the fact that all the system volumes are calculated analytically since no direct measurement of the internal pressure is possible.

The introduction of errors in the calibration could lead to consistently high errors in the final result, as it will be assessed and studied thoroughly in the sensitivity analysis (*Chapter 6*).

In line with the overall path, the analytical approach for valve characterisation, performed as described in the *Section 2.2.2.1*, is based on the mass balances and on the pressure readings detecting the internal pressure variations before and after the closure of the valve.

Chapter 4 - Results and discussion of experimental campaign

In *Chapter 4*, the results of the experimental campaign are shown underlying the issues detected. Firstly, the results of blank experiments at ambient temperature and cryogenic are reported being the starting point for the following studies.

4.1 Equilibrium measurement: blank response

4.1.1 Blank response at ambient temperature

Equilibrium measurements are performed through the procedure explained in *Section 2.2.1*: the procedure is done without the adsorbent loaded in the uptake-sample cell and using Helium, assuming that the adsorption of the gas is negligible. As said before, the analysis is aimed to check the correct calibration of the system and the operativity of the apparatus in the pressure range among 0-100 bar.

The operative conditions at which the blank isotherm has been performed are summarized in the Table 1, while the results are plotted in Fig. 17:

V_{DS} (cc)	12.7826
V_{US} (cc)	11.1551
V_{DR} (cc)	12.8558
V_{UR} (cc)	11.2289
T_{DS} (°C)	room temperature (22-23)
T_{US} (°C)	25
T_{DR} (°C)	room temperature (22-23)
T_{UR} (°C)	25
$m_{beads,sample}$ (g)	14.4785
$m_{beads,reference}$ (g)	14.4831
ρ_{beads} (g/cc)	7.817

Table 1 – Operative conditions set in the apparatus during equilibrium experiment (Helium expansion at T = 25°C, Pressure 0-100 bar$_a$).

A sample mass of 518.2 mg is considered for the aim of the calculations, even if a null sample volume is then used. This is because a value different from zero needs to be specified in the calculation sheet to avoid numerical errors dividing by zero. The amount is the one used in the inter-laboratory analysis proposed by (Nguyen et al., 2020), aimed to give a unique and commonly recognized reference isotherm for different adsorbate-adsorbent systems.
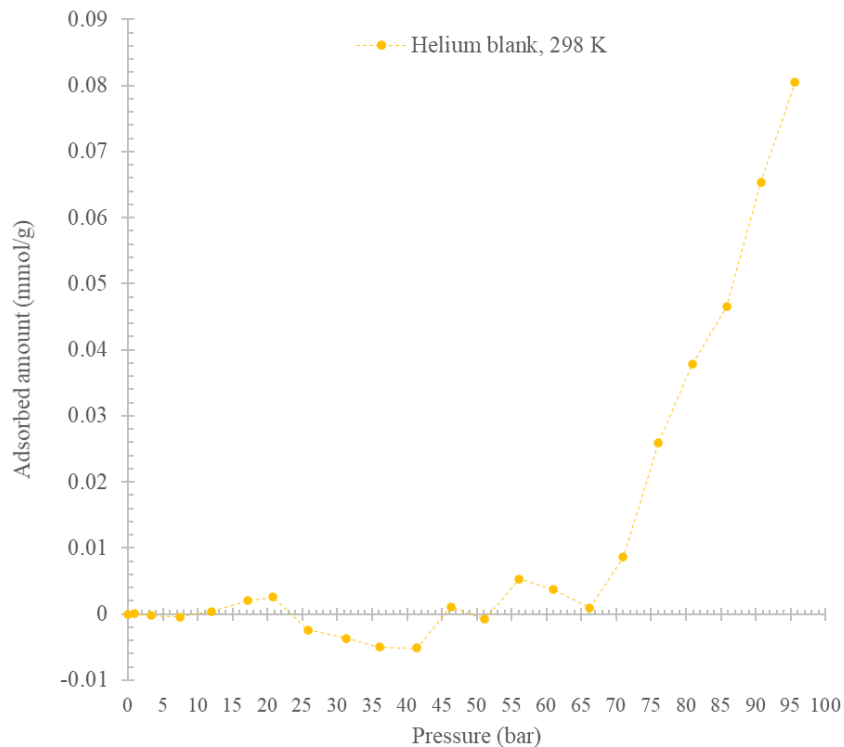

Figure 17 - *Blank isotherm with Helium at Temperature = 25°C, Pressure = 0-100 bar$_a$.*

The final isotherm should be constituted by a series of data points oscillating around the zero value: no adsorption conditions. However, if at low pressure and until reaching 60-65 bar the results appear quite appropriate, for higher pressure (P > 65 bar), the data points start increasing detaching from the zero value. So issues are evidenced at saturation conditions.

Some hypotheses are moved to explain the increasing trend: firstly, the influence of the absolute pressure onto the differential pressure reading, then the effect of absolute pressure in volume calibration procedure are studied.

The effect of valve volume can be suggested being negligible at low pressure, but relevant at higher pressure conditions, this is the reason why an accurate valve characterisation is then proposed.

A more recent discovery pointed out the presence of a gradient among the two branches in the readings of the thermocouples: so a different offset point should be considered (see *Chapter 6*, *Section 6.5*).

4.1.2 Blank response at cryogenic conditions

The operative conditions at which the blank isotherm has been performed are summarized in Table 2; these consider the estimated immersed volume V_{Uhot}, which is considered equal in the procedure following protocol 1,2, and 3:

V_{DS} (cc)	12.7826
V_{US} (cc)	12.8558
V_{DR} (cc)	11.1551
V_{UR} (cc)	11.2289
V_{Uhot} (cc)	6.2978
V_{Ucold} (cc)	4.8573 (sample) - 4.9311 (reference)
T_{DS} (°C)	room temperature (22-23)
T_{US} (°C)	-196
T_{DR} (°C)	room temperature (22-23)
T_{UR} (°C)	-196
$m_{beads,sample}$ (g)	14.4794
$m_{beads,reference}$ (g)	14.4832
ρ_{beads} (g/cc)	7.817

Table 2 – *Operative conditions set in the apparatus during equilibrium experiment (Helium expansion at T = -196°C, Pressure 0-100 bar$_a$) for protocols 1,2 and 3.*

For protocol 4, a smaller portion of uptake volume is effectively immersed in the liquid nitrogen, so V_{Uhot} = 5.9066 cc. An approximation is to consider an equal "hot volume" for both branches, while the resulting "cold volumes" are estimated by considering the exact uptake cell volumes calibrated.

The same reference sample mass of 518.2 mg is considered for the calculations and a null sample volume is then used. Refers to *Section 4.1.1* for details.
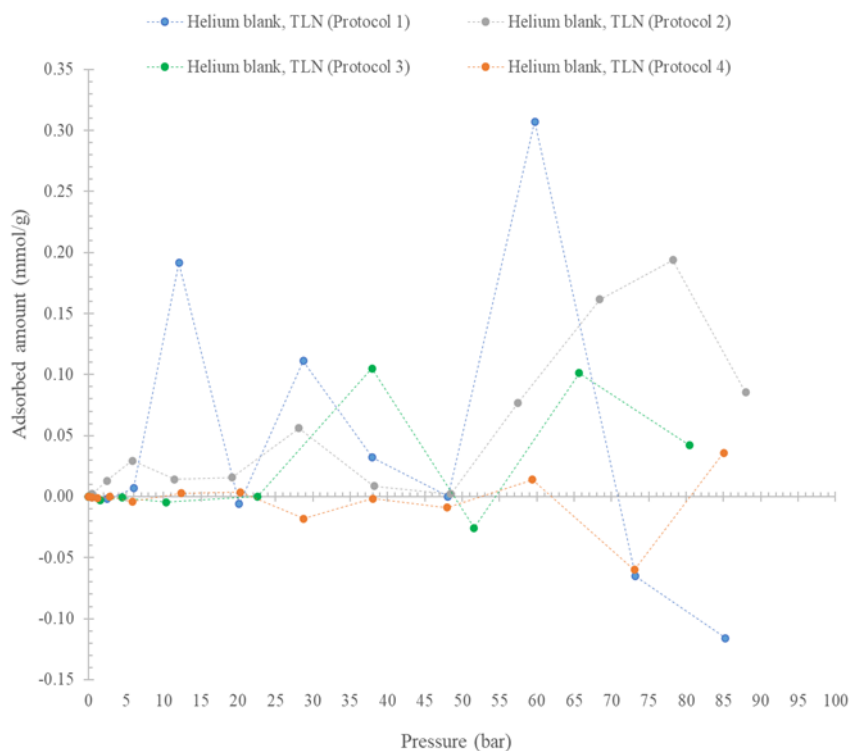
Figure 18 - *Blank isotherm with Helium at Liquid Nitrogen Temperature, Pressure = 0-100 bar$_a$.*

In Fig. 18, a comparison of the blank trends obtained with the four protocols described in *Section 2.3* is provided. In this case, the blank responses appear less stable if compared to the blank at 25 °C, confirming the difficulty in handling the experiments. Also in this case the situation worsens at high pressure.

The result obtained with protocol 4 seems to be the best one, leading to consider the experimental procedure more reliable; this is because the corrective factors used in data analysis are the lowest one. In the *APPENDIX A1* (Table 19)*,* the values of the factors used are reported. No further details will be furnished about this point but, in a very general way: higher the correction, lower the reliability of the experimental procedure.

The experimental campaign in cryogenic was early interrupted, so only preliminary conclusions can be moved; however, even if incomplete, the campaign was very interesting for evidencing some peculiarities. For example, both the evaporation rate and the use of different baths led to the creation of asymmetries during measurements, which is one of the main aspects related to accumulation of errors and uncertainties in adsorption measurements performed with differential volumetric apparatus (see *Chapter 6*). Small volume unbalances creation, in terms of "hot volume" and "cold volume" need to be then accurately assessed. Another point is that, with a single thermostatic bath covering the uptake cells (as it is in the operation at ambient

temperature), it is not possible to evidence the relevance of the liquid level maintenance among the branches. Contrarily, this is evident when handling Liquid Nitrogen in two different dewars, with a different evaporation rate (difficult to be controlled and monitored), leading to the creation of system asymmetries. For future developments, a way to measure the exact level of Liquid Nitrogen needs to be implemented.

As last consideration, the formation of a "third region" having a temperature between the bath and the room temperature has been suggested. The hypothesis of formation of a gradient of temperature along the system could be reasonable, and to be taken in consideration in further analysis. A rough analysis in this way has been done obtaining the results in Fig. 19. By means of an external thermocouple, the temperature at different heights (h) is measured; L is the length of the uptake section equal to 6 cm.
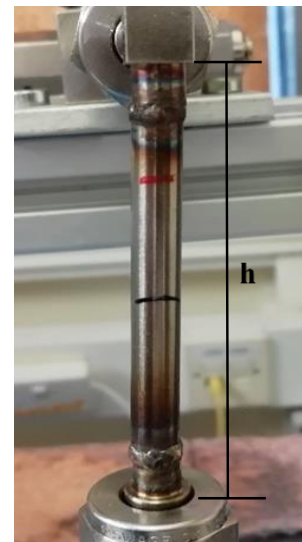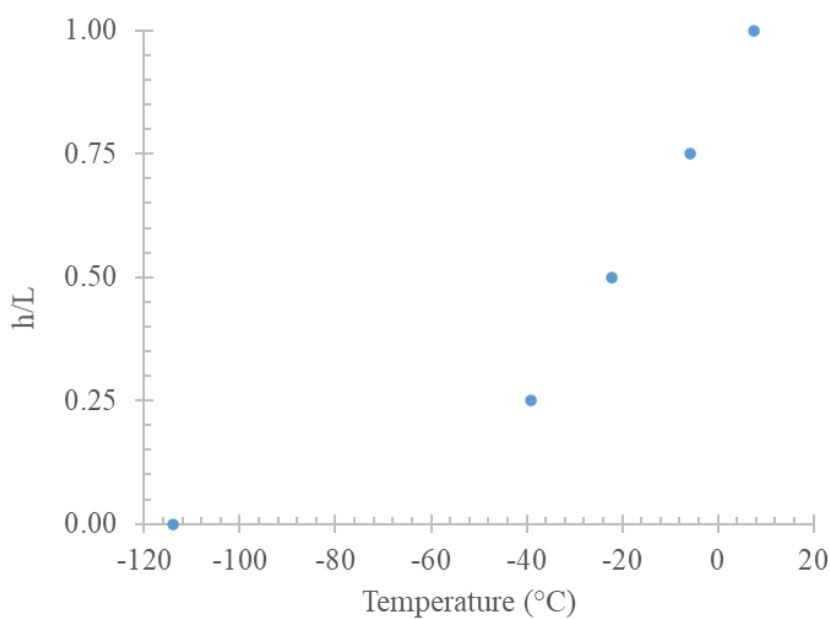

Figure 19 – Temperature gradient along the uptake cell when dealing with cryogenic experiments (right plot), picture of the uptake cell section (left picture).

47

4.2 Differential pressure transducer: offset point

The estimation of the offset point of the differential pressure transmitter is aimed to check the influence of the operating pressure on the "zero" of the instrument. The hypothesis is that a possible variation of the offset, at increasing pressure, is due to a deformation affecting the internal diaphragm of the transmitter.

Further studies could be focused on a more accurate analysis in this direction. In particular, the possibility that the operating pressure could affect consistently the differential pressure measurements should be considered in the data analyses.

The evaluation is performed with all the pneumatic actuated valves (V2,V3,V4,V5) opened and setting the system under vacuum; the signal of the differential pressure transmitter at different absolute pressure is then loaded.

The experimental results show a slight variation of the offset point varying the absolute pressure of the system. A linear dependence between the absolute pressure and the "zero" of the differential pressure transducer has been found:

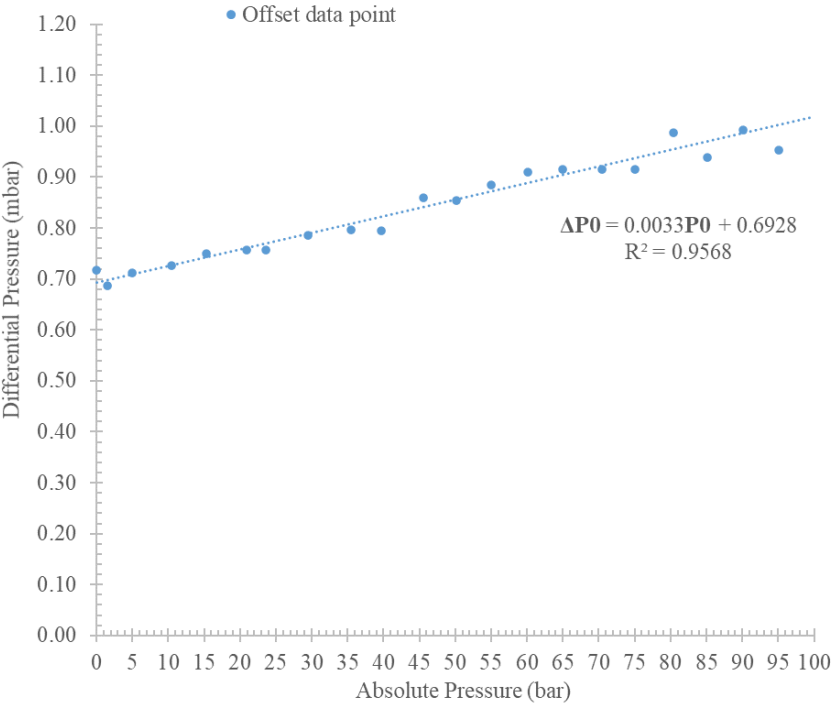$$\Delta P0 = 0.0033 P0 + 0.6928$$
$$R^2 = 0.9568$$

Figure 20 - Offset of differential pressure transducer over absolute pressure.

The slope of the fitting line is then considered in the data analysis to take account of the phenomenon. A very tiny effect can be noticed, at ambient temperature, in reproducing the blank isotherm considering the differential pressure readings dependence and a comparative chart can be found in the *APPENDIX A2* (Table 20).

4.3 Calibration procedure

4.3.1 Volume ratios

The calibration of the system has been performed in a pressure range among 2-100 bar: generally, the estimation of internal volume is done at low pressure. However, the influence of the internal operating pressure in the calibration wants to be analysed.

According to the pneumatic actuated valve datasheet, all the experiments are carried out by setting the correct value of the compressed air pressure for the opening/closure operations (*Section 2.1* and *2.2.2.1*): details are summarized in the *APPENDIX A3*.

The operative conditions at which the experiment has been carried out are resumed in the Table 3:

T_{DS} (°C)	room temperature (22-23)
T_{US} (°C)	25
T_{DR} (°C)	room temperature (22-23)
T_{UR} (°C)	25
$m_{beads,sample}$ (g)	14.47773
$m_{beads,reference}$ (g)	14.48299
ρ_{beads} (g/cc)	7.817

Table 3 - Operative conditions set for system calibration procedure at pressure among 2-100 bar (Helium expansion at T = 25°C).

The calibration has been performed as explained in *Section 2.2.2*; two series of expansion are performed: the subscript "1" refers to the expansion from dosing to uptake volume, while the subscript "2" to the expansion from uptake to dosing volume: Fig. 21 is reported for simplicity sake.
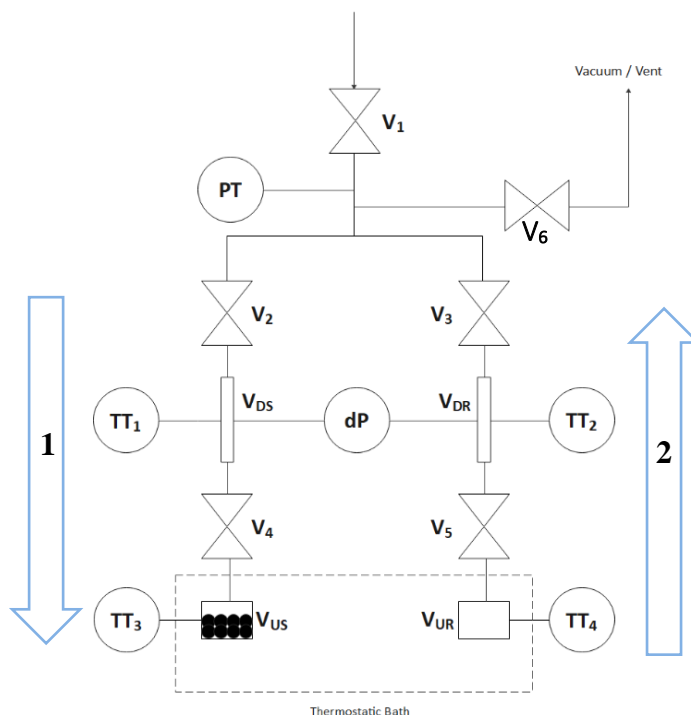
Figure 21 - *HP - ADVA apparatus simplified schematic showing the expansion series performed during calibration procedure.*

The volume ratios are firstly calculated as mentioned in *Section 3.3*. The numbers are summarized in Tables 4 and Table 5, referring to the system loaded with the beads and the empty system, respectively.

Pressure (bar)	Γ_{SC1}	Γ_{SC2}	*%dev*	Γ_{RC1}	Γ_{RC2}	*%dev*
100	1.6694	1.8860	*12.19%*	1.6288	1.6835	*3.31%*
55	1.4261	1.6789	*16.28%*	1.4715	1.6835	*13.43%*
30	1.4260	1.5272	*6.85%*	1.4043	1.4795	*5.22%*
5	1.3779	1.3848	*0.50%*	1.3705	1.3834	*0.94%*
2	1.3717	1.3755	*0.28%*	1.3682	1.3695	*0.10%*

Table 4 - *Volume ratios obtained during calibration procedure with beads loaded in the uptake cells (Helium expansion at T = 25°C).*

Pressure (bar)	Γ_{SC1}	Γ_{SC2}	*%dev*	Γ_{RC1}	Γ_{RC2}	*%dev*
100	1.2860	1.4922	*14.85%*	1.1895	1.4416	*19.16%*
55	1.2438	1.2322	*0.94%*	1.1306	1.3823	*20.03%*
30	1.1907	1.2462	*4.55%*	1.1897	1.2349	*3.37%*
5	1.1491	1.1602	*0.96%*	1.1429	1.1478	*0.43%*
2	1.1412	1.1449	*0.32%*	1.1354	1.1367	*0.11%*

Table 5 - *Volume ratios obtained during calibration procedure with empty system (Helium expansion at T = 25°C).*

The percentage of deviation (*%dev*) is calculated between the two series of expansion: the aim is to minimize this deviation obtaining the ratios more similar as possible.

To visualise the behaviour, charts of the volume ratios over absolute pressure (operating pressure) are drawn:
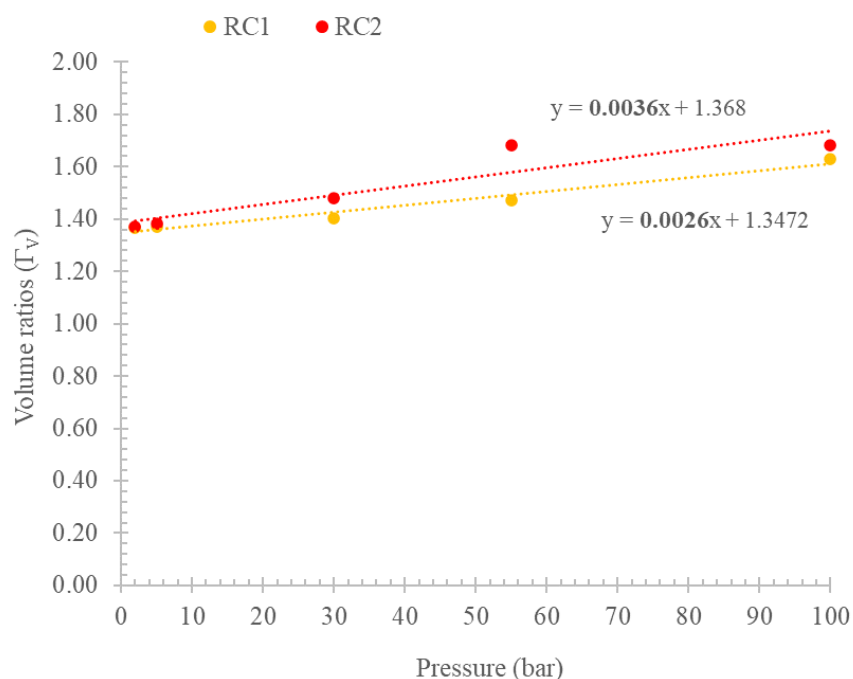

Figure 22 *- Volume ratios trend over system operating pressure for the reference – branch with beads loaded in the uptake cells (Helium expansion at T = 25°C).*
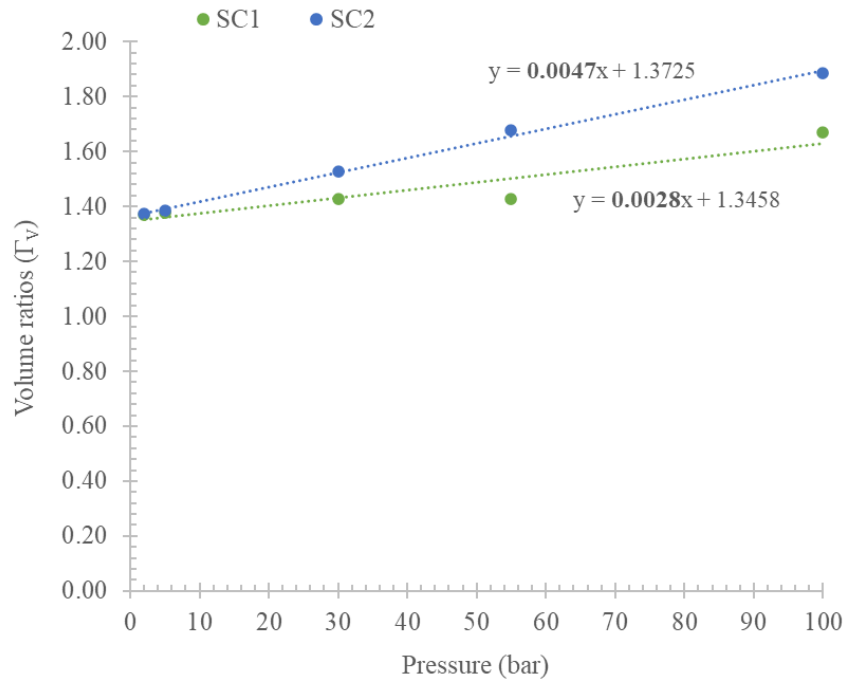
Figure 23 - *Volume ratios trend over system operating pressure for the sample – branch with beads loaded in the uptake cells (Helium expansion at T = 25°C).*
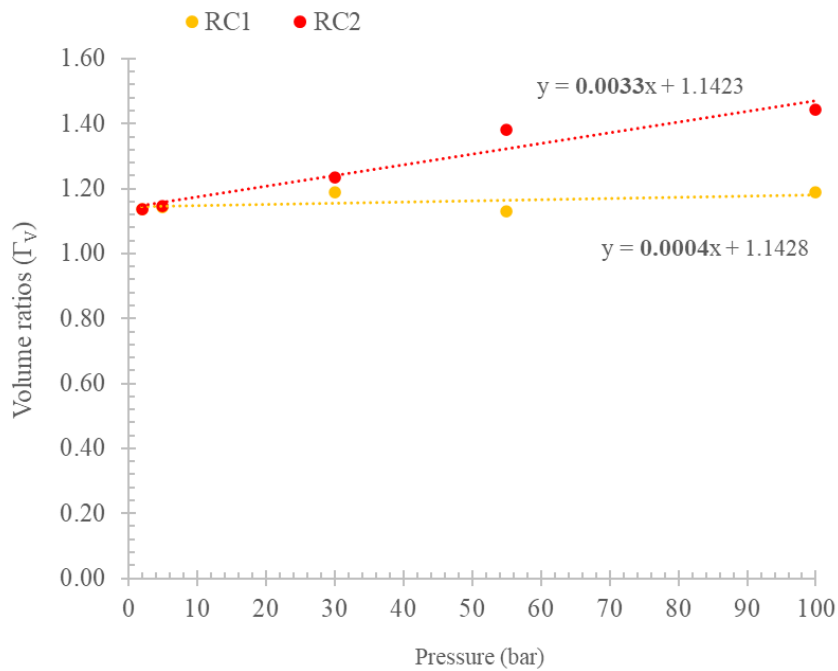

Figure 24 *- Volume ratios trend over system operating pressure for the reference – branch with empty system (Helium expansion at T = 25°C).*
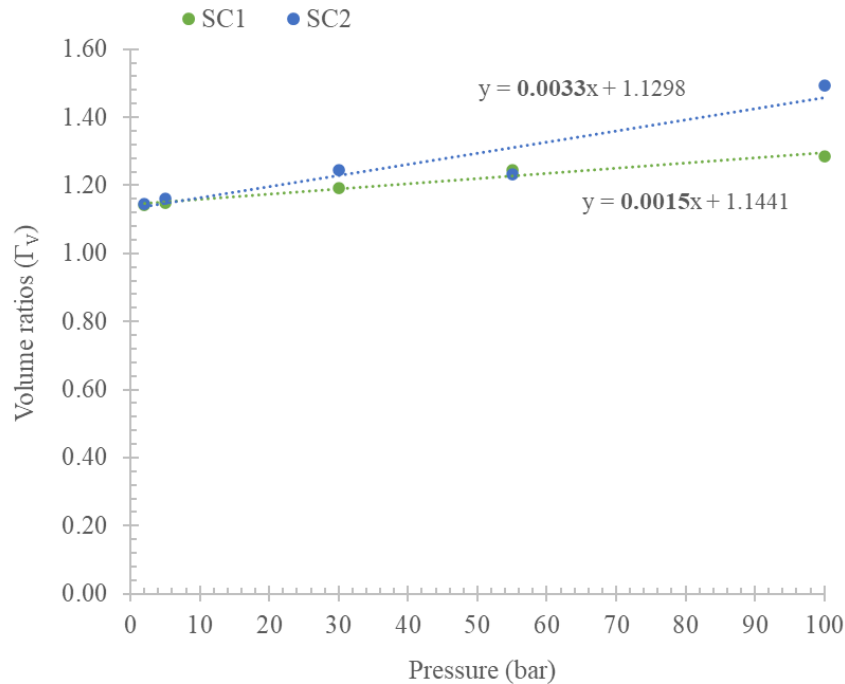
Figure 25 *- Volume ratios trend over system operating pressure for the sample – branch with empty system (Helium expansion at T = 25°C).*

From an overall view, the plots illustrate a slightly increasing trend of the ratios over the absolute pressure. In all the cases, the trend of the data point has been fitted with a linear trend and the resulting slopes are rather small with an order of magnitude of 10^{-3}. A higher deviation has been pointed out in the data collected through type "2" expansion, such as from uptake to dosing volume. The type "1" expansion (from dosing to uptake volume) data points seem to have negligible deviations.

4.3.2 Volume absolute values

Once obtained the values for the volume ratios, the evaluation of the effective cells volumes is possible. For each set of data, corresponding to the same operative pressure and the same modality of expansion, the absolute values have been calculated.

The subscript "1" refers to the expansion from dosing to uptake volume, while the subscript "2" to the expansion from uptake to dosing volume (see the Fig. 21, *Section 4.3.1*).

Pressure (bar)	V_{DS1} (cc)	V_{DS2} (cc)	V_{US1} (cc)	V_{US2} (cc)
1.5	12.7826	12.7826	11.1551 (11.0017^2)	11.1551 (11.0017^2)
2	12.5788	12.6501	11.0224	11.0491
5	12.8159	13.2459	11.1530	11.4169
30	11.6008	12.5434	11.2253	10.0653
100	10.3702	13.2346	8.0639	8.8692

Table 6 – *Sample-branch dosing and uptake volumes calculated from calibration procedure.*

Pressure (bar)	V_{DR1} (cc)	V_{DR2} (cc)	V_{UR1} (cc)	V_{UR2} (cc)
1.5	12.8558	12.8558	11.2289 (11.0433^2)	11.2289 (11.0433^2)
2	12.3656	12.3912	10.8910	10.9011
5	12.7530	12.4868	11.1584	10.8789
30	13.6814	13.8376	12.1252	11.2055
100	8.1719	18.5880	6.8700	12.8940

Table 7 - *Reference-branch dosing and uptake volumes calculated from calibration procedure.*

---

[2] The values in brackets are referred to volumes, calibrated at low pressure, when the uptake cells were connected using thinner metallic gaskets: 1 mm thickness instead of 1.5 mm.

https://simplybearings.co.uk/shop/p300319/High-Quality-Annealed-Copper-Sealing-Washer_10x20x1mm/product_info.html

https://simplybearings.co.uk/shop/p300320/High-Quality-Annealed-Copper-Sealing-Washer-10x20x1.5mm/product_info.html

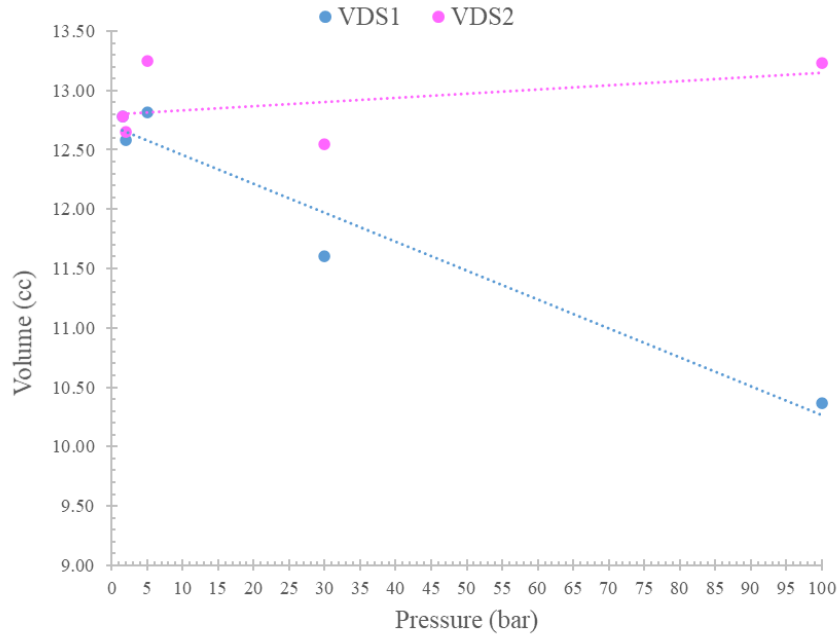Charts of the calculated volumes over absolute pressure (operating pressure) are provided:

Figure 26 - *Dosing-sample volume trend over system operating pressure.*
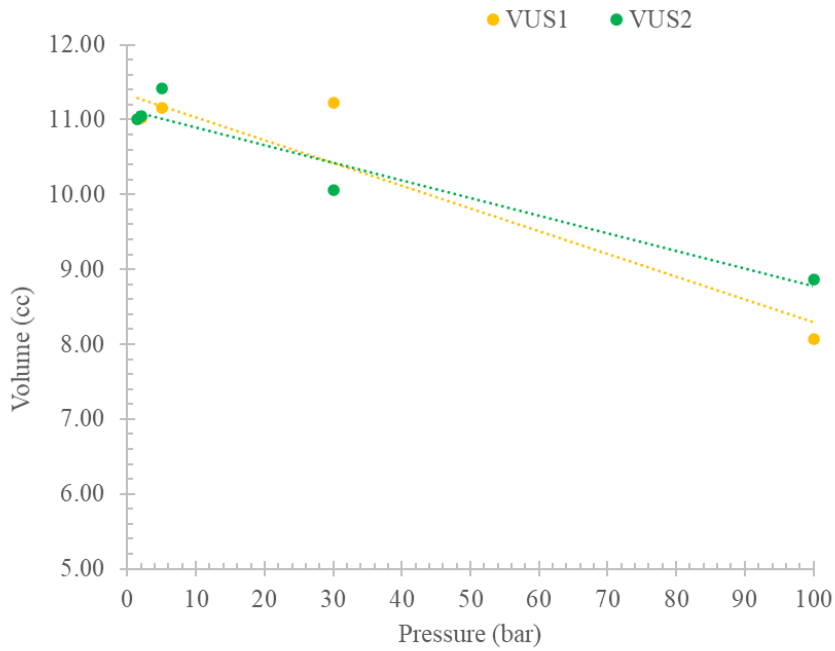

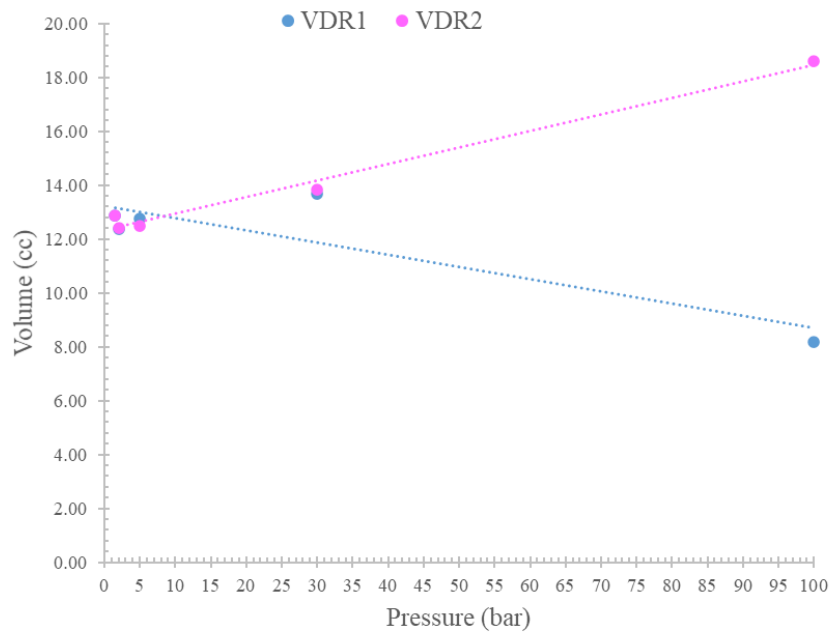*Figure 27* - *Uptake-sample volume trend over system operating pressure.*

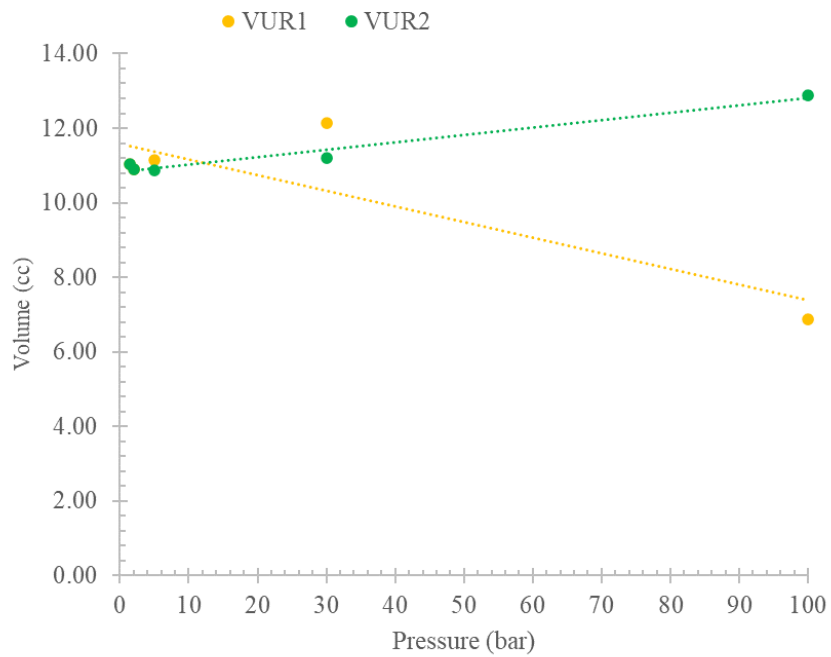***Figure 28*** *- Dosing-reference volume trend over system operating pressure.*

Figure 29 *- Uptake-reference volume trend over system operating pressure.*

Clearly, the same volume ratios and cells internal volume should be obtained in the entire pressure range. The unexpected trends suggest some phenomenon occurring in the system which can be probably neglected at low pressure, but it becomes relevant for high pressure measurements.

The effect of valve opening/closure becomes gradually more relevant at higher pressures. It would be reasonably possible that the instantaneous closing behaviour of the valves is not retained anymore or, better, that the closure slows down allowing part of the moles to flow from one side to another to partially compensate the pressure. This effect has to be further verified experimentally.

Another point is to advocate the change in the calibrated volumes over pressure to the deformation of the internal diaphragm of the differential pressure transmitter: this is clearly not certain, but it is reasonable to think that being a membrane it would deform; however, this effect only depends on the differential pressure, not the total pressure and should result in a slightly higher dosing volume.

The error analysis proposed in the *Chapter 5* and *Chapter 6* is aimed at the characterisation of the sensitivity of the system by each operating parameter: for example, how much an error in the volume calibration can affect the final isotherm.

The values for the sample/reference dosing and uptake volumes taken as reference in the discussion are the one obtained for an operative pressure = 1.5 bar. Clearly, the volumes converge to the one measured at the lowest pressure, so it is reasonable to think that it is also the most accurate estimate (no leaks, ideal gas, not thermal effect of the expansion etc…). Considering the results obtained by the experimental campaign, excluding the calibration at P = 100 bar, which shows too different results, in the other cases a ±1 cc (±10% V) variation is the maximum reached (Table 8).

Pressure (bar)	V_{DS1} (cc)	V_{DS2} (cc)	V_{US1} (cc)	V_{US2} (cc)
1.5	ref.	ref.	ref.	ref.
2	+0.20	+0.13	-0.02	-0.05
5	-0.03	-0.46	-0.15	-0.42
30	+1.18	+0.24	-0.22	+0.94

Pressure (bar)	V_{DR1} (cc)	V_{DR2} (cc)	V_{UR1} (cc)	V_{UR2} (cc)
1.5	ref.	ref.	ref.	ref.
2	+0.49	+0.46	+0.15	+0.14
5	+0.10	+0.37	-0.12	+0.16
30	-0.83	-0.98	-1.08	-0.16

Table 8 – *Deviations of the calibrated volumes estimated with respect to the volume calibrated at P = 1.5 bar taken as reference.*

A ±10%V is a quite high uncertainty which is generally not obtained in the calibration procedure. In the sensitivity analysis the results of the experimental campaign are considered to see the extent of the impact of a wrong calibration in the results.

4.3.3 Valve characterisation

The valve characterisation, described in *Section 2.2.2.1 and Section 3.3*, has been performed at increasing pressure to check the occurrence of unexpected behaviour. The numbers for the inlet and outlet section valve volume are reported in Table 9.

Pressure (bar)	$V2_{out}$ (cc)	$V4_{in}$ (cc)	$V_{valve,sample}$ (cc)	$V3_{out}$ (cc)	$V5_{in}$ (cc)	$V_{valve,reference}$ (cc)
1.2	-	0.01462	-	-	0.01360	-
2	0.01172	0.01186	0.02358	0.01054	0.01156	0.02100
55	0.01590	0.01008	0.02167	0.01052	0.00994	0.02046
100	0.01035	0.00905	0.01941	0.00999	0.00913	0.01901
Average	-	-	*0.02155*	-	-	*0.02052*

Table 9 – *Valve internal volumes calculated for differential system operating pressure.*

The subscripts "2", "3", "4" and "5" refers to the valve (see Fig. 10, *Section 2.1*), while "in", "out" refers to the inlet and outlet section volume, respectively (see Fig. 12, *Section 2.2.2.1*).

From the results obtained considering the pressure change by valves' opening/closure, the valves seem to be symmetric. Moreover, the absolute values slightly decrease with increasing absolute pressure even if they are almost equal in the entire pressure range. The deviation between sample and reference branches seems to tend to zero at higher pressures. For P = 1.2 bar, the expansion from dosing + uptake volume to pre-dosing section has not been performed.

A mean value for the valve volume is considered along the discussion V_{valve} = 0.02104 cc. A maximum uncertainty in valve volume estimation around $\pm 5\% V_{valve}$ has been pointed out, which is taken into account in the sensitivity analysis. However, this is the estimate from which we have the lowest confidence. A more accurate procedure to characterise the valves should include a smaller-range differential pressure transducer, and two low-pressure absolute transmitter inside the dosing cells. This procedure should allow the characterisation of the response time of the valves, too.

In this direction, the choice to develop a sensitivity and error analysis over the system comparing the single-branch and the differential apparatus, to detect the operating parameters which affect the most the final isotherm construction. The aim is to use the results of the sensitivity analysis for eventual modifications and improvements of the system design, the analytical methods used for data analysis or of the way in which the experiments are performed in laboratory to work on the unexpected results of the experimental campaign.

Chapter 5 - Sensitivity analysis: methods and materials

In *Chapter 5*, the methods and materials used for the development of the sensitivity and error analysis are described in detail. The same analysis can be extended to other gases and adsorbent materials, as well as other types of approach for the analysis can be adopted.

5.1 Analytical method

Different approach can be used for the development of sensitivity and error analysis: the analytical method is an example and it can be used for the estimation of the individual errors raised in the gas uptake, due to the introduction of uncertainties in the operating parameter (see previous examples in literature *Chapter 1*, *Section 1.3.1*).

For the analysis, an initial distinction needs to be made among systematic errors and random errors: a systematic error affects the measurements by the same amount or by the same proportion, provided that a reading is taken in the same way each time. This is the case of wrong calibrated volumes or errors in the sample/beads mass weight. The effect of these errors is studied by the implementation of a calculation sheet which allows the construction of adsorption isotherms by varying, arbitrarily, all the system parameters. In particular, the Eq. (12) for the single-branch system and the Eq. (18) for the differential apparatus, have been manipulated to obtain final expressions with all the parameters written explicitly, to allow the variation of the single parameter and recalculate the gas uptake.

On the other hand, random errors are the ones associated with unpredictable changes during experiments: generally, this is considered for the pressure and temperature readings. In this case, the calculation of the partial derivatives of the moles of gas adsorbed (q_i) (Eq. (12) for single-branch system and Eq. (18) for differential system) is required, at each ith adsorption step, with respect to the variables. This is because random errors can be considered as errors introduced step by step in the measurements or can accumulate, in different ways, along the isotherm construction.

For example, in case of single-branch system, it is possible to calculate the error in the final isotherm raised due to inaccuracy of the absolute pressure transducer readings, in dosing phase, by using the following equation:

(19) $\delta q_i = \left|\dfrac{\partial q_i}{\partial P_{DS}}\right| \delta P_{DS}$

where:

(20) $\dfrac{\partial q_i}{\partial P_{DS}} = \dfrac{1}{M_A}\dfrac{\partial n_i}{\partial P_{DS}} - \dfrac{n_i}{M_A^2}\dfrac{\partial M_A}{\partial P_{DS}}$

(21) $\dfrac{\partial n_i}{\partial P_{DS_{i-1}}} = \dfrac{(V_{DS}-\alpha V_{valve})}{RT_{DS_{i-1}}}\left(\dfrac{z_{i-1}\left(T_{DS_{i-1}}.P_{DS_{i-1}}\right) - P_{DS_{i-1}}\dfrac{\partial\left(z_{i-1}\left(T_{DS_{i-1}}.P_{DS_{i-1}}\right)\right)}{\partial P_{DS_{i-1}}}}{z_{i-1}\left(T_{DS_{i-1}}.P_{DS_{i-1}}\right)^2}\right)$

The same approach is applied to the other input parameters and the partial derivatives are calculated and listed in *APPENDIX A4*. In particular, in *APPENDIX* all the partial derivatives referring to single-branch and differential systems are displayed.

In general, the step contribution in terms of uncertainty raised in the gas uptake due to random individual parameter, can be schematized as follows:

(22) $\delta q_i = \left|\dfrac{\partial q_i}{\partial x_k}\right| \delta_{x_k}$

Then the combined effect of all the random individual uncertainties is accounted estimating the cumulative error in the gas uptake by applying the error propagation law:

(23) $\delta q_{i,cumulative}^2 = \left|\dfrac{\partial q_i}{\partial P_{charge_i}}\right|^2 \delta P_{charge_i}^2 + \left|\dfrac{\partial q_i}{\partial P_{equilibrium_i}}\right|^2 \delta P_{equilibrium_i}^2 +$

$\left|\dfrac{\partial q_i}{\partial T_{dosing}}\right|^2 \delta T_{dosing}^2 + \left|\dfrac{\partial q_i}{\partial T_{uptake}}\right|^2 \delta T_{uptake}^2$

summarizing:

(24) $\delta_{q_{i,cumulative}} = \sqrt{\sum_{k=1}^{n}\left(\dfrac{\partial q_i}{\partial x_k}\delta_{x_k}\right)^2}$

where *n* is the number of parameters accounted in the study, q_i is the dependent variable, and x_k are the independent measurement variables (Qajar et al., 2012; Sircar et al., 2013). The

equation (23) is a generic form to write the random cumulative error, the formula needs to be then specifically applied and modified for the system analysed.

A further factor to be taken into account is that the adsorption measurements, done using volumetric systems, are performed as multistep procedure, so the uncertainty in the gas uptake increases each step since the total uncertainty at each step is the accumulation of the uncertainties from all the previous steps as well as the uncertainty in the step of interest (Webb & Gray, 2014a). In other words, the generated uncertainty in the uptake in a single pressure step, calculated through the equation (22), can be considered for single point measurements but, when dealing with isotherm construction, a further step needs to be done, by considering the effect of random error accumulation. The issue is to rely on a conservative but quite realistic analytical approach to reproduce the experimental procedure.

By an accurate literature review (Qajar et al., 2012; Webb & Gray, 2014a, 2014b), the total uncertainty raised in each adsorption step, accounting for the random error accumulation phenomenon can be estimated as sum of the variances and hence the final uncertainty is the square root of the sum of the squares of the two uncertainties:

$$(25) \quad \delta q_{i,TOT} = \sqrt{\delta q_{i-1}^2 + \delta q_i^2}$$

the terms under root are calculated with equation (22).

For the random cumulative error the same approach is then used:

$$(26) \quad \delta q_{i,cumulativeTOT} = \sqrt{\delta q_{i-1,cum}^2 + \delta q_{i,cum}^2}$$

the terms under root are calculated with equation (24).

A confirmation of the consistency of the approach has been done by analysing the accumulation of the random error in the uptake considering that, at each adsorption step, the combined effect of positive/negative contributions can be summed step by step, generating a matrix of errors displaying all the possible combinations of uncertainties in the resulting gas uptake. The check has been done through the implementation of a MathWorks MATLAB® sheet: the procedure has proved to be quite time-consuming, reason why the procedure described above has been then selected as the main method for the analysis.

Along the discussion, the absolute and relative errors are displayed to visualize the error trend over pressure:

(27) absolute error $= |\delta q_i|$

(28) relative error (%) $= \dfrac{|\delta q_i|}{q_i} \times 100$

5.2 Hypothetical isotherm

The sensitivity analysis is performed starting from isotherm taken from literature: equilibrium pressure and adsorbed moles values are considered and assumed to be the correct experimental results of the apparatus analysed. Then the pre-expansion pressures in the dosing-section are retrieved, at each adsorption step, based on the system parameters. Finally, the isotherm construction introducing the uncertainties in the parameters is processed (see *Section 5.3*).

Nitrogen has been chosen as the gas for the analysis: in general, the N_2 shows intermediate behaviour as adsorbate, among a low-adsorbing gas such as H_2 and highly adsorbing gas like CO_2. Data for the Nitrogen reference isotherm is taken from (Gibson et al., 2016). The dual-site Langmuir is selected as the fitting model for the data (Ruthven, 1985). The hypothetical material is considered behaving as 13X zeolite having the saturation capacities shown in the inset table in Fig. 30. Data refers to a temperature of 298 K.

The same analysis for other gases can be then proposed for completeness: the majority of literature mentioned in *Chapter 1*, *Section 1.3.1*, has been written considering Hydrogen (H_2) adsorption.

A $\pm$ 5% absolute error (see *Section 5.1*) in the final isotherm will be considered acceptable for the aim of the sensitivity analysis (Nguyen et al., 2018, 2020). The dashed lines in Fig. 30 represent the accepted detachment from the reference isotherm.
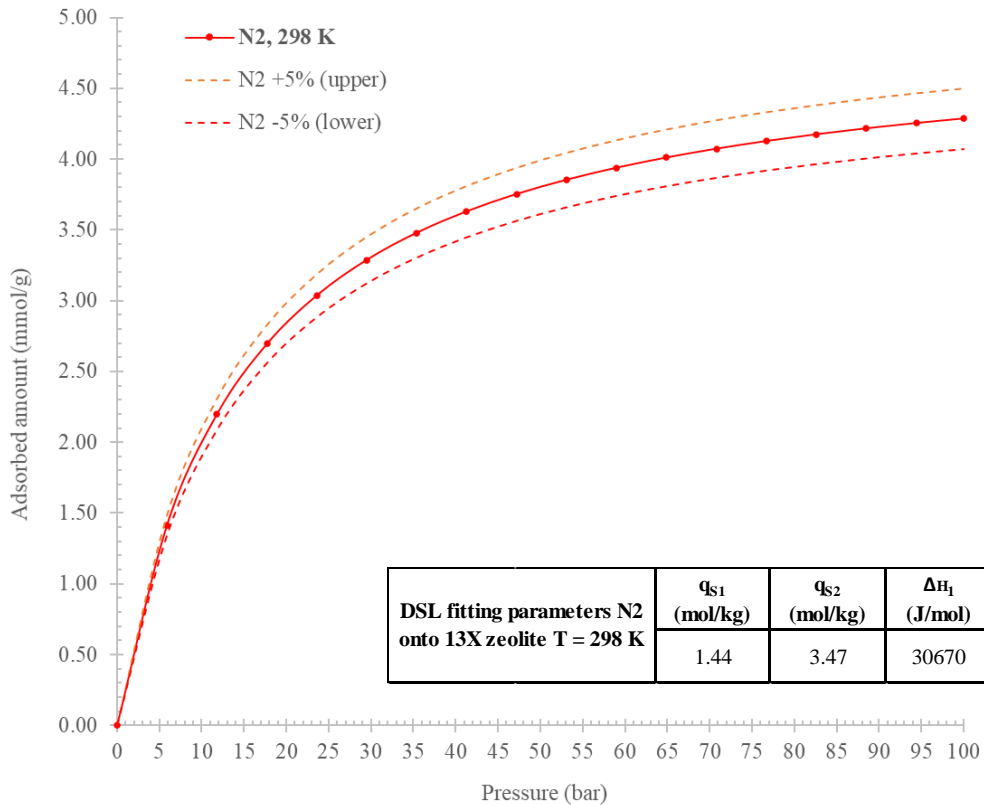
Figure 30 – *Hypothetical isotherm for Nitrogen (N₂) on 13X zeolite at 298 K (0-100 bar) (red solid line), relative error ±5% (red dashed line). Inset: table displaying Dual-site Langmuir fitting parameters.*

5.3 System parameters and individual uncertainties

The sensitivity analysis is performed for single-branched and differential systems: the single-branch configuration comprises the same dosing/uptake volumes of the differential apparatus (considering the sample side) and the same absolute pressure transducer.

Adsorption pressure, moles adsorbed and volume ratios are kept constant between the scenarios and the system pressures are calculated by mole balance. The pressure range considered for the analysis is ranged between 0-100 bar to see the effect of the uncertainties in the operating parameters at low- and high-pressure conditions.

The PTC Mathcad® simulator has been used for the implementation of the spreadsheets required for the retrieval of the hypothetical initial conditions and to build-up the final adsorption isotherms.

5.2.1 Single-branch system

To retrieve the initial conditions, the knowledge of the dosing and uptake cell volumes, the valve volume, a guess amount of adsorbent sample used, the temperature conditions and the compressibility factor of gas is necessary. The values used are real-system quantities and they have been estimated through apparatus calibration and valve characterization procedures, as explained in *Chapter 2* and *3*:

- A sample of 100 mg of adsorbent having a density of 2.50 g/cc[3] is used (Sircar et al., 2013).

- The compressibility factors at different conditions of temperature and pressure z $= f$ (T, P) are estimated using the Wagner equation of state (Kunz & Wagner, 2012).

- The temperature conditions are assumed as constant: the dosing section at room temperature (around 22 – 23 °C) and the uptake cell immersed in a bath at 25 °C during all the hypothetical experiments.

- The volumes considered are the real ones, obtained by the calibration procedure at low pressure: V_{DS} = 12.7826 cc and V_{US} = 11.0017 cc. The system volumes ratio is equal to Γ_V = 1.162.

- The valve volume (assuming all valves equal) is estimated equal to V_{valve} = 0.02104 cc. The valves' volume can be then schematized as entirely concentrated in the inlet/outlet section, through the factor α (see Eq. (13)).

- The mass of the stainless-steel beads selected as m_{beads} = 14.47853 g having a density of ρ_{beads} = 7.817 g/cc.

The additional information needed relates to the initial pressures in the uptake cell of the system at the beginning of the sequence. The vacuum conditions are considered ($P_{US_0} \cong 0$ bar). Moreover, the effect of the opening/closing of the valve is not considered in the pressure conditions inside the uptake cell: the $P_{US_{i+1}} = P_{S_i}$ (see Eq. (12)). So, the initial pressure in the uptake cell is considered equal to the final equilibrium pressure of the sequence before.

---

[3] The skeletal density has been considered because referring to the ref. (Sircar et al., 2013), however, a total density, including micropores, of 1.60 g/cc should be considered for a real 13X zeolite even if not impacting the final results.

V_{DS} (cc)	12.7826
V_{US} (cc)	11.0017
Γ_V	1.162
V_{valve} (cc)	0.02104
m_{beads} (g)	14.478
ρ_{beads} (g/cc)	8.718
m_{sample} (mg)	100
ρ_{sample} (g/cc)	2.50
T_{dosing} (°C)	22-23
T_{uptake} (°C)	25

Table 10 - Summary of the single-branch system specifications.

As mentioned in *Section 1.3.1*, the effect of sample amount and cell volumes are not considered in the analysis being largely confirmed in previous works. In the analysis, the focus will be given to the effect of that parameters less analysed in literature, among them the valve volumes effect will be extensively discussed in terms of wrong characterisation of the valve (through the procedure described in the *Section 2.2.2.1* and *3.3*) and how the valve is considered in the mass balance (see Eq. (13)). Moreover, the aim is to reproduce a real laboratory experiment accounting for the accuracy of the facilities really used during measurements. The values of beads density, estimated experimentally using a water pycnometer, has been assumed as correct, as well as, the density of the adsorbent material.

Individual uncertainties accounted are listed below:

- Calibrated volumes (δV_{DS}, δV_{US})
- Valve internal volume (δV_{valve}), studied in the cases for $\alpha = 1$ and $\alpha = 0$ (see Eq. (13))
- Laboratory balance sensitivity (δm_{beads}, δm_{sample})
- Absolute pressure measurement (δP_A)
- Temperature measurement (δT_{DS}, δT_{US})

Then the cumulative error is evaluated by considering the overall effect of all parameters together.

5.2.2 Differential system

The system specifications are summarized in Table 11: the reference-side additional information is needed.

V_{DS} (cc)	12.7826
V_{DR} (cc)	12.8558
V_{US} (cc)	11.0017
V_{UR} (cc)	11.0433
Γ_{VS}	1.162
Γ_{VR}	1.164
V_{valve} (cc)	0.02104
$m_{beads,sample}$ (g)	14.478
$m_{beads,reference}$ (g)	14.483
ρ_{beads} (g/cc)	8.718
m_{sample} (mg)	100
ρ_{sample} (g/cc)	2.50
T_{dosing} (°C)	22-23
T_{uptake} (°C)	25

Table 11 - Summary of the differential system specifications.

The mass balance used for the differential system is the one described by the equation (18). Assumption made of the opening/closure of the valve not affecting the internal pressure of the system. So, $P_{US_{i+1}} = P_{S_i}$ and $P_{UR_{i+1}} = P_{R_i}$. In line with this assumption, the ΔPD_i is assumed always equal to zero because no effect of the valve opening/closure and no internal deformation of the differential pressure transmitter diaphragm. The vacuum conditions are considered ($P_{US_0} = P_{UR_0} \cong 0$ bar).

As for the single-branch, the sample amount and cell volume will not be discussed, but the same type of analysis will be performed reproducing a real laboratory experiment. However, for the differential apparatus, the effect of system asymmetries in terms of volumes and temperature will be discussed, for lack of literature data.

Individual uncertainties are applied to the parameters listed below:

- Calibrated volumes (δV_{DS}, δV_{US}, δV_{DR}, δV_{UR})
- Valve internal volume (δV_{valve}), studied in the cases for $\alpha = 1$ and $\alpha = 0$ (see Eq. (13))
- Laboratory balance sensitivity (δm_{beads}, δm_{sample})
- Absolute pressure measurement (δP_A)
- Differential pressure measurement ($\delta \Delta P_D$)
- Temperature measurement (δT_{DS}, δT_{US})

Lastly, the cumulative error is evaluated by considering the overall effect of all parameters together.

Chapter 6 - Results and discussion of sensitivity analysis

This chapter is dedicated to the illustration and discussion of the results of the sensitivity analysis: only the most relevant outcomes are presented and described in detail, while supplementary results are reported in the *APPENDIX A5*.

6.1 Calibrated volume

The first analysis is done by considering wrong cell volume calibration: this is a key aspect in volumetric systems and, particularly, for the double-branch (HP-ADVA) apparatus in which the gas uptake is obtained referring to calculated and not measured pressures (see *Chapter 2* and *Chapter 3*). The analysis is performed for both single-branch and differential systems by considering different possible error configurations.

In Fig. 31 and 32, the trend of absolute and relative error in the gas uptake for single-branch and differential volumetric system are reported: the charts a) refer to the deviation in the absolute adsorbed amount over equilibrium pressure (Eq. (27)), while the charts b) report the relative error raised in the gas uptake (Eq. (28)). Specifically, Fig. 31 displays the effect of wrong calibration of dosing volume, while Fig. 32 of the uptake cell volume.

Same results are obtained if comparing the effect of dosing/uptake volumes' error. Interesting different results are instead obtained if comparing the single-branch and differential apparatus: in the case of conventional system, an increasing and linear trend of the relative error over pressure is obtained, so the error is exacerbated when performing high-pressure measurements. Differently, for the differential apparatus, maxima and minima peaks appear. To be noticed the significant difference in the extent of errors raised: deviations of $\pm 0.1\% \, V$ introduced in the single-branch system gives an error higher than $\pm 5\%$, so overcoming the limit of acceptance selected, while, for the double-branch apparatus, the error is completely negligible. In case of single-branch apparatus, a maximum error equal to $\pm 0.06\% \, V_{dosing}$ and $\pm 0.05\% \, V_{uptake}$ is admissible to fall within the limit established, in the entire pressure range. The slight difference is due to the fact that, in the real system design, the uptake volume is a bit smaller than the dosing one. For the differential apparatus, a $\pm 10\% \, V$ error in the volume leads to a maximum error of $\pm 6.5\%$, in case of the dosing volume and $\pm 5.47\%$ for the uptake volume. Such big errors in volume calibration have been studied in line with the results of the experimental campaign (see *Chapter 4*, *Section 4.3.2*); however, they are quite unrealistic if dealing with a correctly set-up system.
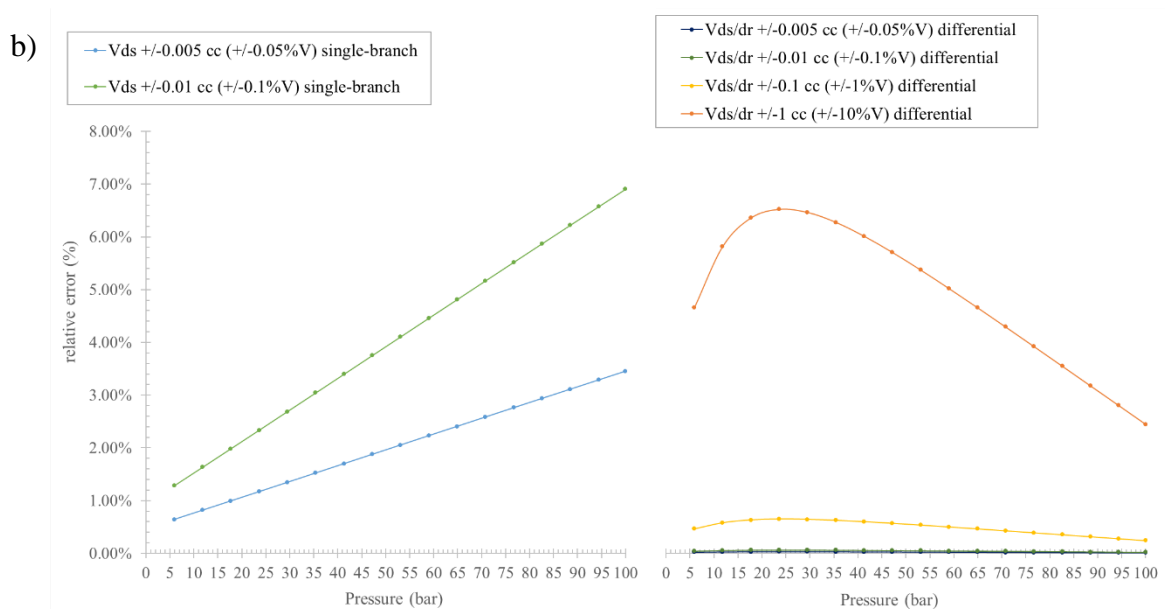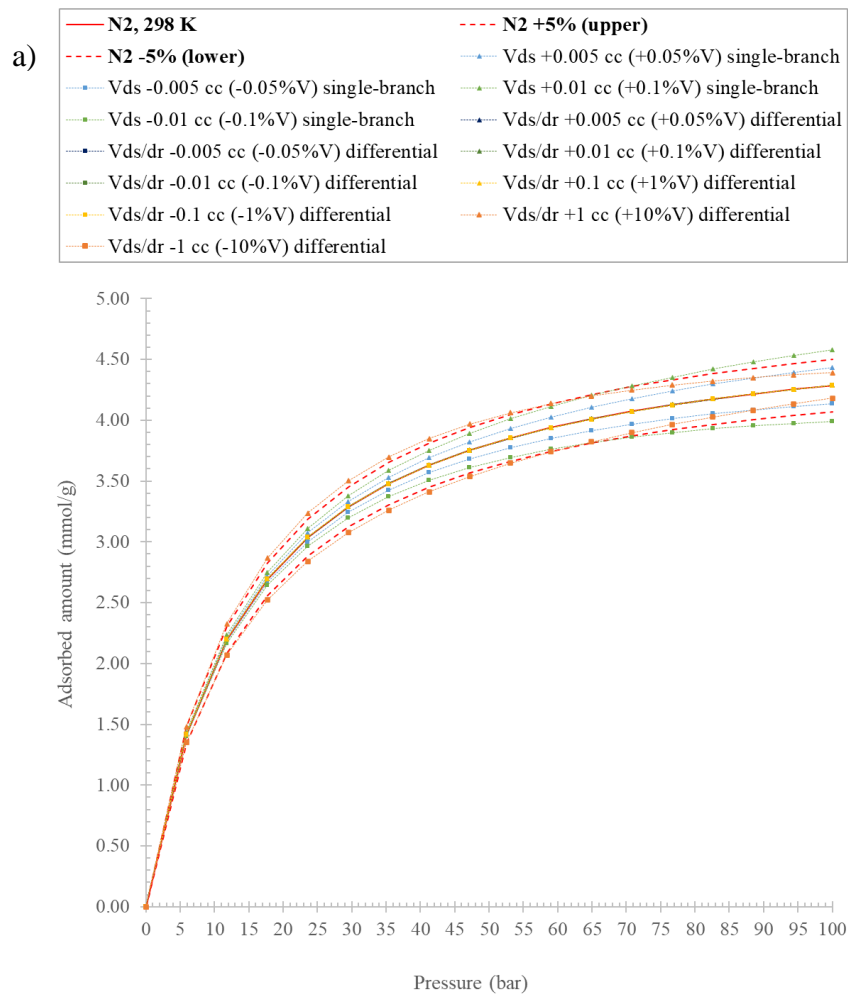
Figure 31 *– Comparison of the effect of errors in dosing volume calibration for N_2 adsorbed onto 100 mg 13X (Gibson et al., 2016) at 298 K, measured by single-branch and differential method: a) absolute errors trend, expected isotherm (red solid line), percentual error ±5% (red dashed lines), b) relative error (%) over pressure for single-branch (left) and differential (right) system.*
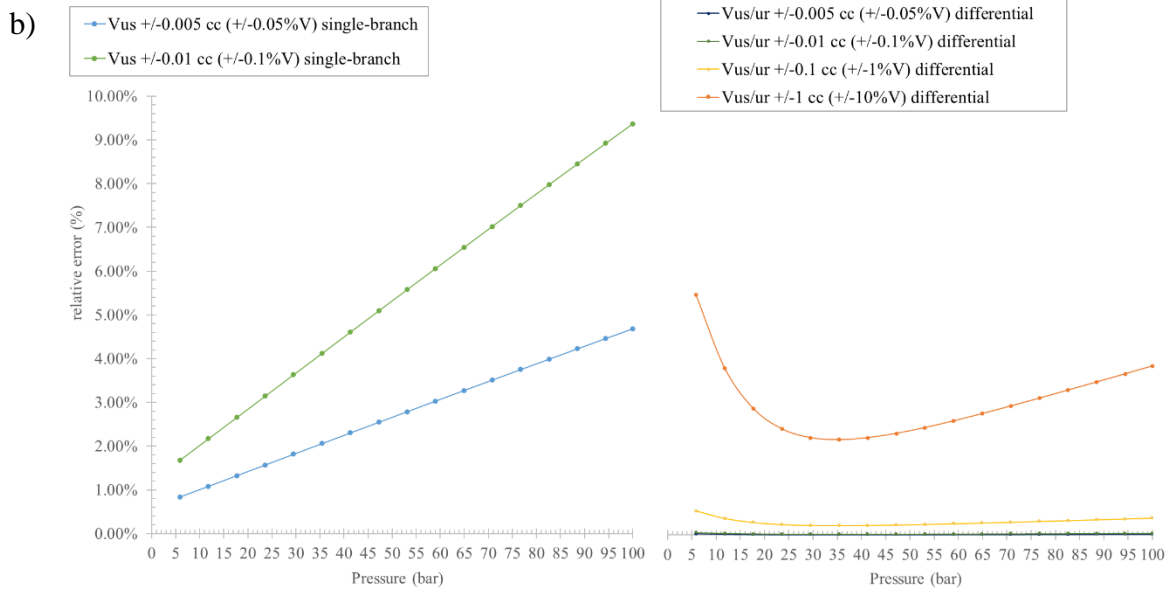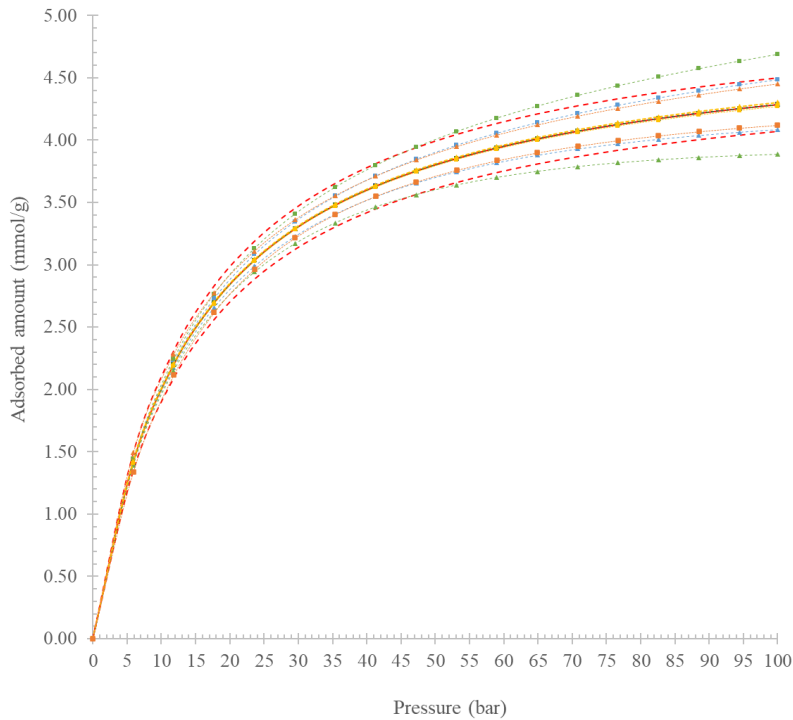
Figure 32 *– Comparison of the effect of errors in uptake volume calibration for N_2 adsorbed onto 100 mg 13X (Gibson et al., 2016) at 298 K, measured by single-branch and differential method: a) absolute errors trend, expected isotherm (red solid line), percentual error ±5% (red dashed lines), b) relative error (%) over pressure for single-branch (left) and differential (right) system.*
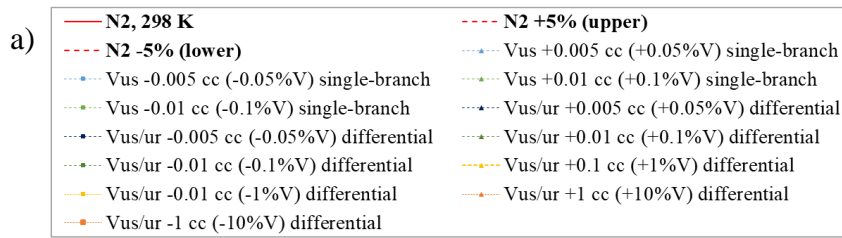
The results allow to say that the differential apparatus is less sensitive to wrong calibration of the volumes: assuming the error is either positive or negative in both sides, i.e. it leads to a symmetric system, an effect of cancellation shows up due to the symmetricity of the system.

Analytically, the results are sustained by the form of the equations used for isotherm construction and data analysis (see Eq. (29) for single-branch and Eq. (30) for differential system, below): in case of single-branch system, the absolute values of the calibrated volumes are multiplied by the absolute pressure, which increases along isotherm construction (blues brackets). So, even the introduction of a small error in one volume leads to significant errors in the uptake, because multiplied by high quantities.

On the other hand, for the differential system, the absolute pressures are multiplied by terms containing the difference among dosing-sample/dosing-reference and uptake-sample/uptake-reference volumes (grey brackets). The absolute values of the calibrated volumes are instead multiplied by the differential pressure, which quantities are significantly smaller compared to the absolute pressure (blues brackets). This point justifies that, if an equal systematic error is introduced in the dosing and/or uptake volumes for both branches, a slight effect in final results will be obtained because the volume differences keep the same, while the terms multiplied by the differential pressures change.

$$(29) \quad \Delta n_{ads_i} = \boxed{\frac{P_{DS_{i-1}} V_{DS_c}}{z\left(T_{DS_{i-1}}.P_{DS_{i-1}}\right)R\,T_{DS_{i-1}}}} + \boxed{\frac{P_{US_{i-1}} V_{US_c}}{z\left(T_{US_{i-1}}.P_{US_{i-1}}\right)RT_{US_{i-1}}}} - P_{S_i}\boxed{\left[\frac{V_{DS_c}}{z\left(T_{DS_i}.P_{S_i}\right)RT_{DS_i}} + \frac{V_{US_c}}{z\left(T_{US_i}.P_{S_i}\right)RT_{US_i}}\right]}$$

$$(30) \quad \Delta n_{ads_i} = P_{DR_{i-1}}\left[\frac{V_{DS_c}}{z\left(T_{DS_{i-1}}.P_{DS_{i-1}}\right)R\,T_{DS_{i-1}}} - \frac{V_{DR_c}}{z\left(T_{DR_{i-1}}.P_{DR_{i-1}}\right)R\,T_{DR_{i-1}}}\right] - \Delta PD_{i-1}\boxed{\frac{V_{DS_c}}{z\left(T_{DS_{i-1}}.P_{DS_{i-1}}\right)R\,T_{DS_{i-1}}}}$$

$$+ P_{UR_{i-1}}\left[\frac{V_{US_c}}{z\left(T_{US_{i-1}}.P_{US_{i-1}}\right)RT_{US_{i-1}}} - \frac{V_{UR_c}}{z\left(T_{UR_{i-1}}.P_{UR_{i-1}}\right)RT_{UR_{i-1}}}\right] - \Delta PU_{i-1}\boxed{\frac{V_{US_c}}{z\left(T_{US_{i-1}}.P_{US_{i-1}}\right)R\,T_{US_{i-1}}}}$$

$$- P_{R_i}\left[\frac{V_{DS_c}}{z\left(T_{DS_i}.P_{S_i}\right)RT_{DS_i}} - \frac{V_{DR_c}}{z\left(T_{DR_i}.P_{R_i}\right)RT_{DR_i}} + \frac{V_{US_c}}{z\left(T_{US_i}.P_{S_i}\right)RT_{US_i}} - \frac{V_{UR_c}}{z\left(T_{UR_i}.P_{R_i}\right)RT_{UR_i}}\right]$$

$$+ \Delta P_i\boxed{\left[\frac{V_{DS_c}}{z\left(T_{DS_i}.P_{S_i}\right)RT_{DS_i}} + \frac{V_{US_c}}{z\left(T_{US_i}.P_{S_i}\right)RT_{US_i}}\right]}$$

For all the symbology used in the mass balances refer to *Chapter 3* of the thesis.

An important point to underline is that, due to how the calibration is performed and the volumes calculated, among dosing and uptake volumes, errors with the same sign are expected. Indeed, the calculations are based on volume ratios so a positive deviation in dosing volume calculation will lead to a positive deviation in the uptake volume too (see *Chapter 3*, *Section 3.3)*. Consequently, Fig. 33 is representative of the most probable error configuration: a systematic error equal to $\pm1\%\,V$ is considered comparing the single-branch and the differential systems. For the single-branch, the same trend as before and very high errors are obtained; the differential system confirms the stability to error introduction being the error in the gas uptake almost constant in the entire pressure range and well below the $\pm2\%$.

In Fig. 46 and 47 of the *APPENDIX A5*, the effect of introducing systematic errors in volume calibration having opposite signs, among dosing and uptake cells is reported. This can be possible in case of wrong procedure, mistakes done during data analysis or problems in the system set-up.
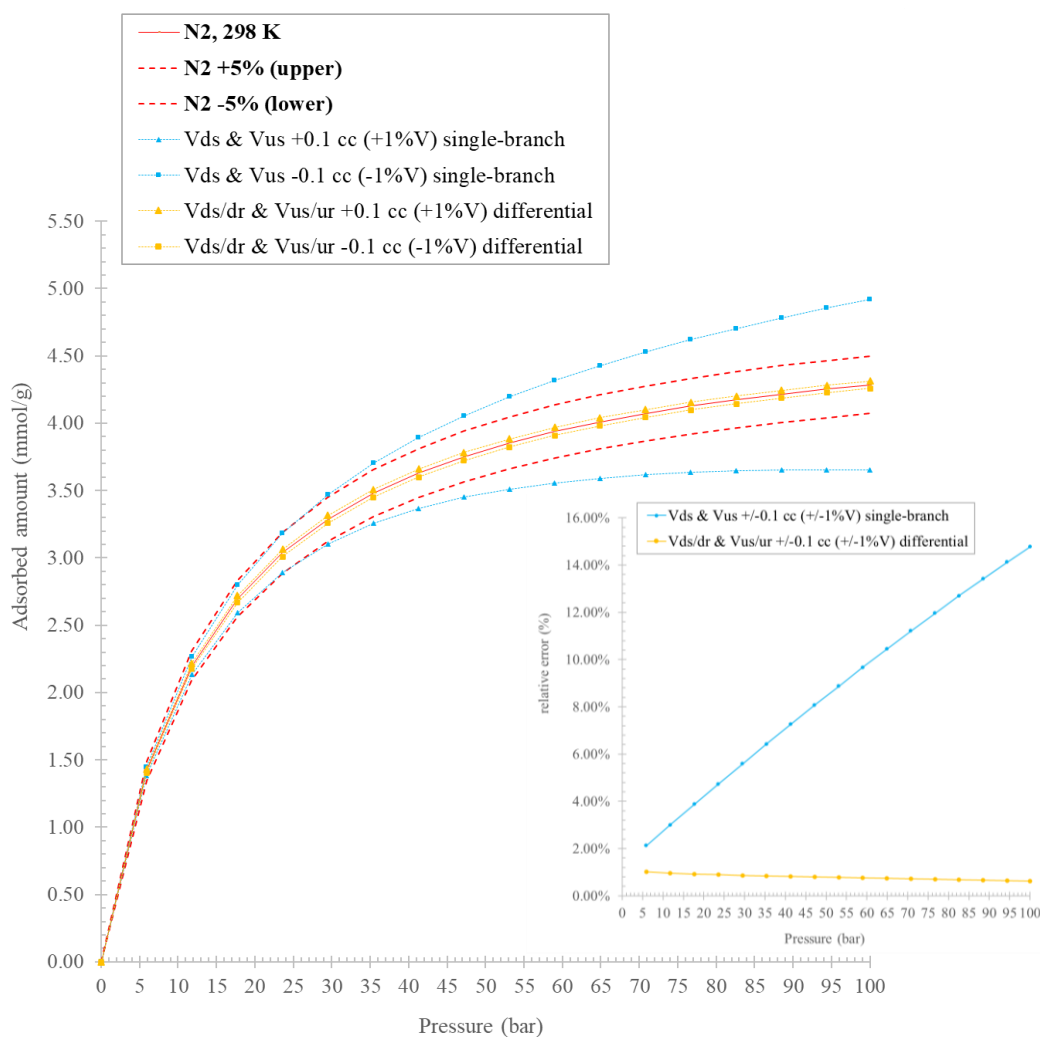
***Figure 33** – Comparison of the effect of errors in volume calibration for N_2 adsorbed onto 100 mg 13X (Gibson et al., 2016) at 298 K, measured by single-branch and differential method. Main plot: absolute errors trend, expected isotherm (red solid line), percentual error ±5% (red dashed lines); Inset plot: relative error (%) over pressure. Configuration 1*

Contrarily, issues raise up when introducing different systematic errors among the two branches, leading to a deviation from the symmetric configuration. Different error configurations have been analysed and some of them are reported in Fig. 48 of the *APPENDIX A5*. Fig. 34 is reported to confirm that the creation of asymmetries among the branches worsen consistently the reliability of the measurements. An error of ±0.1%V, introduced with opposite sign in the branches, gives errors up to ±3.02% (P = 100 bar). Introducing ±1%V leads to completely misleading results with errors in the gas uptake highly above ±20%.
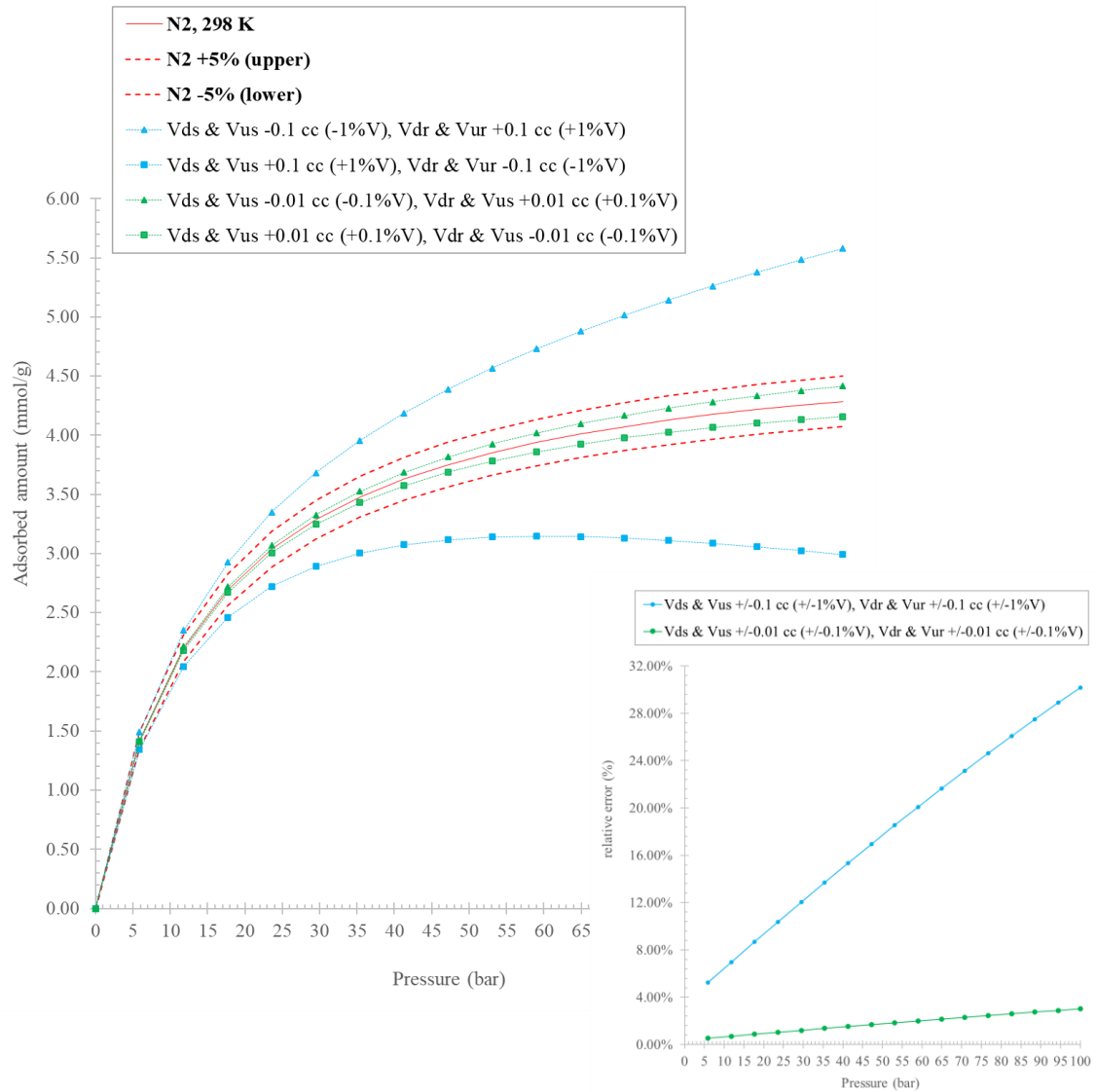
74

Figure 34 – *Effect of asymmetric errors in volume calibration for N_2 adsorbed onto 100 mg 13X (Gibson et al., 2016) at 298 K, measured by differential method. Main plot: absolute errors trend, expected isotherm (red solid line), percentual error ±5% (red dashed lines); Inset plot: relative error (%) over pressure. Configuration 1*

These results endorse the relevance of maintaining the symmetricity among the branches during experiments and give also high significance to the experimental campaign at cryogenics, aimed to find a reliable protocol to maintain as much as possible the symmetry among the two branches. Moreover, the analysis confirms the improved reliability of the double-branch system with respect to the conventional one, being significantly less susceptible to error in volume calibration.

6.2 Valve volume

The approach to the examination of the valve volume in the analysis is quite new: the aim is to point out if, effectively, the wrong estimation of valve internal volume can have an effect in the final isotherm trying also to advocate to this effect some issues revealed during the experimental campaign.

As it is possible to see from Fig. 35 and 36, the effect of valve volume is not negligible at high pressure. The behaviour of the error raised due to the consideration of a systematic error in the valve volume calibration is very similar to the volume one. This can be explained by considering that, in the mass balance, the valve volume contributes in the same manner but with a different extent, to the gas uptake calculation, so does explaining the similar trends.

In the single-branch apparatus (see Fig. 35), an error of $\pm1\%\,V_{valve}$ ($\sim \pm0.0002$ cc) gives rise to a maximum error of $\pm1.95\%$ (P = 100 bar) in the gas uptake: if, for example, we consider the results reported in Fig. 31, a variation of $\pm0.1\%\,V$ ($\sim \pm0.01$ cc) of the dosing volume leads to around $\pm8\%$ error. So, the valve volume seems to consistently affect the final results even to a higher extent with respect to the cell volume. This can be explained by the fact that, when dealing with wrong valve volume calibration, both dosing and uptake sections of the system are affected and in a different manner, depending on the mass balance used.

For differential apparatus, in the same conditions, negligible effect of the error in valve volume calibration can be noticed due to symmetricity of the system (see Fig. 49, *APPENDIX A5*). Indeed, by the governing equation, introducing the same deviation for the valve volume in both branches, will lead to a cancellation effect as in the case of calibrated volume (see *Section 6.1*). Analysing the effect of asymmetries, so introducing a different deviation among sample/reference branches, the increase of the error in gas uptake is evident. This is in line with what happened in the volume analysis too. Particularly, an error of $\pm1\%\,V_{valve}$ gives a maximum error equal to $\pm3.91\%$ however, $\pm5\%\,V_{valve}$ leads to $\pm19.54\%$ in the gas uptake which is a significantly high error (Fig. 36). The $\pm5\%\,V_{valve}$ has been analysed in line with the results of the experimental campaign (see *Chapter 4*, *Section 4.3.3*).

These results underline the importance of ensuring symmetricity of the system during experiments as well as data analysis. Following this reflection, the analytical method chosen for system calibration is aimed to avoid the occurrence of asymmetries by connecting the calculation of one element to the other one. More details will be given in *Section 6.4*.

Another point is that the effect of considering the configuration with α = 1 or α = 0 seems to be negligible for both single-branch and differential apparatus. This is in line with the initial hypothesis of valve symmetricity: the inlet/outlet sections of the valve seem to have almost equal volume (see *Chapter 4*, *Section 4.3.3*). In the caption, "*Vv*" refers to the valve volume.
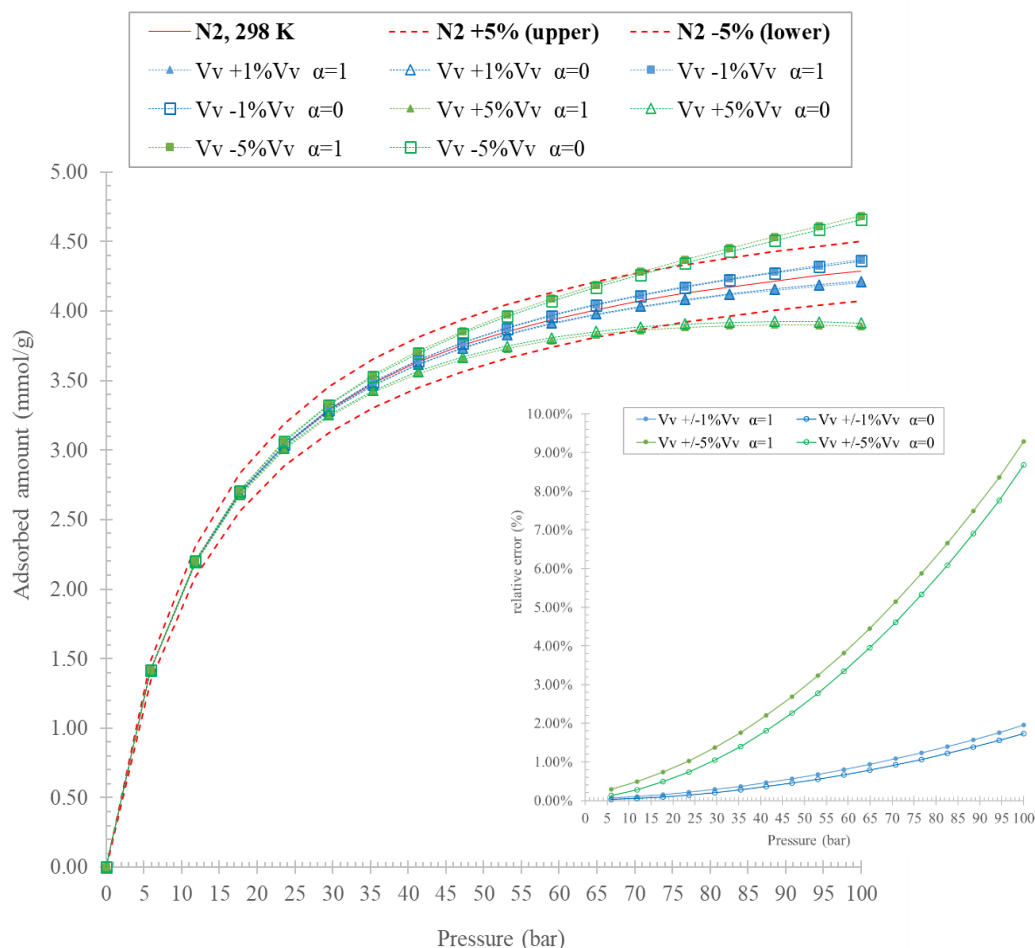

Figure 35 – Effect of the errors in valve volume calibration for N$_2$ adsorbed onto 100 mg 13X (Gibson et al., 2016) at 298 K, measured by single-branch method. Main plot: absolute errors trend, expected isotherm (red solid line), percentual error ±5% (red dashed lines); Inset plot: relative error (%) over pressure.

Figure 36 *– Effect of the errors in valve volume calibration for N₂ adsorbed onto 100 mg 13X (Gibson et al., 2016) at 298 K, measured by differential method. Main plot: absolute errors trend, expected isotherm (red solid line), percentual error ±5% (red dashed lines); Inset plot: relative error (%) over pressure. Configuration 1*
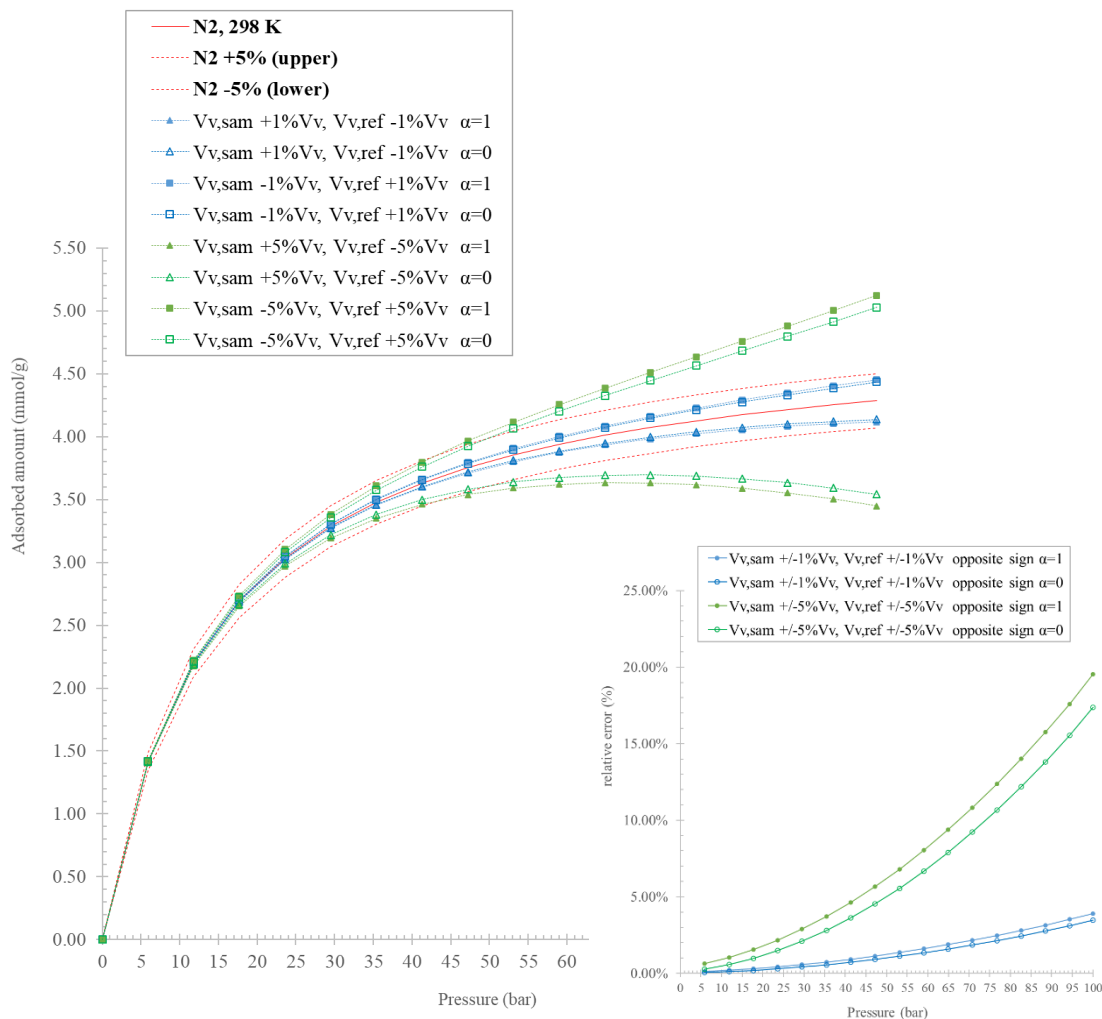
The sensitivity analysis evidenced some criticalities connected to the valve volume consideration: in literature the effect has been always neglected, no volume change was always assumed, so the valve volume is not included in the mass balance.

Another interesting aspect to be considered is that the majority of examples in literature are referred to adsorbate with low adsorption potential (e.g. H_2). However, when dealing with other gases (e.g. N_2, CO_2) and performing high-pressure measurements, the presence of no-zero volume valves has an effect that cannot be neglected. Indeed, in a counter intuitive way the differential system performs better with weak adsorbents. Strong adsorbents (e.g. CO_2) tend to push the system towards higher pressure differences between the reference and the sample side, making the system effectively less symmetric.

Further studies can be aimed at a deeper understanding of valve effect by incorporating experimental tests; moreover, a more error effective method for valve characterization can be developed.

6.3 Laboratory balance accuracy

As mentioned, the effect of the amount of adsorbent loaded is not considered in the analysis being sufficiently assessed in previous works: higher the quantity of sample mass lower the potential errors introduced, so more reliable the measurements. Issues come when dealing with a limited amount of sample or in the space available for placing the sample inside the uptake cell.

The proposed analysis aims to quantify the errors raised in the final results due to unavoidable effects such as the laboratory balance accuracy, used for weighing all the samples and beads used in the experimental campaign. As said in *Chapter 5*, the densities of samples and stainless-steel beads are considered free from errors. For the sample density, the major problem is the variability of the conditions depending on the specific material so general conclusions cannot be done. Regarding the stainless-steel beads, the density has been estimated by using mercury porosimeter intrusion method, which is considered precise and reliable.

The balance (*Mettler Toledo XSR205 Dual Rage Analytical Balance*) used for the weighing has a range of repeatability of ±0.02 mg (from the datasheet, PDF available in the *REFERENCES*), which has been considered for the analysis.

In Fig. 37, a comparison of the effect of sample mass weight among single-branch and differential systems is proposed by highlighting that no differences can be noticed. This is an expected result being the mass sample term independent from the type of apparatus used for the analysis. However, an interesting point to evidence is the pressure dependence: in general the error in the gas uptake, due to incorrect sample mass, should be constant over pressure; but, in the used governing equations, the sample mass is not only accounted in the calculation of the effective adsorbed amount, through the equation:

(31) $\quad q_i = \dfrac{n_i}{M_A}$

where M_A is the sample mass, but also to calculate the sample volume V_A for the estimation of the effective void volume available for the gas after adsorbent loading in the uptake cell (see *Chapter 3*). So the combined effect of errors in the sample mass for the calculation of the

adsorbed amount and the void volume leads to a slightly decreasing trend over pressure; in reality, the values of the error are quite small as well as the deviation over pressure, and overall negligible.
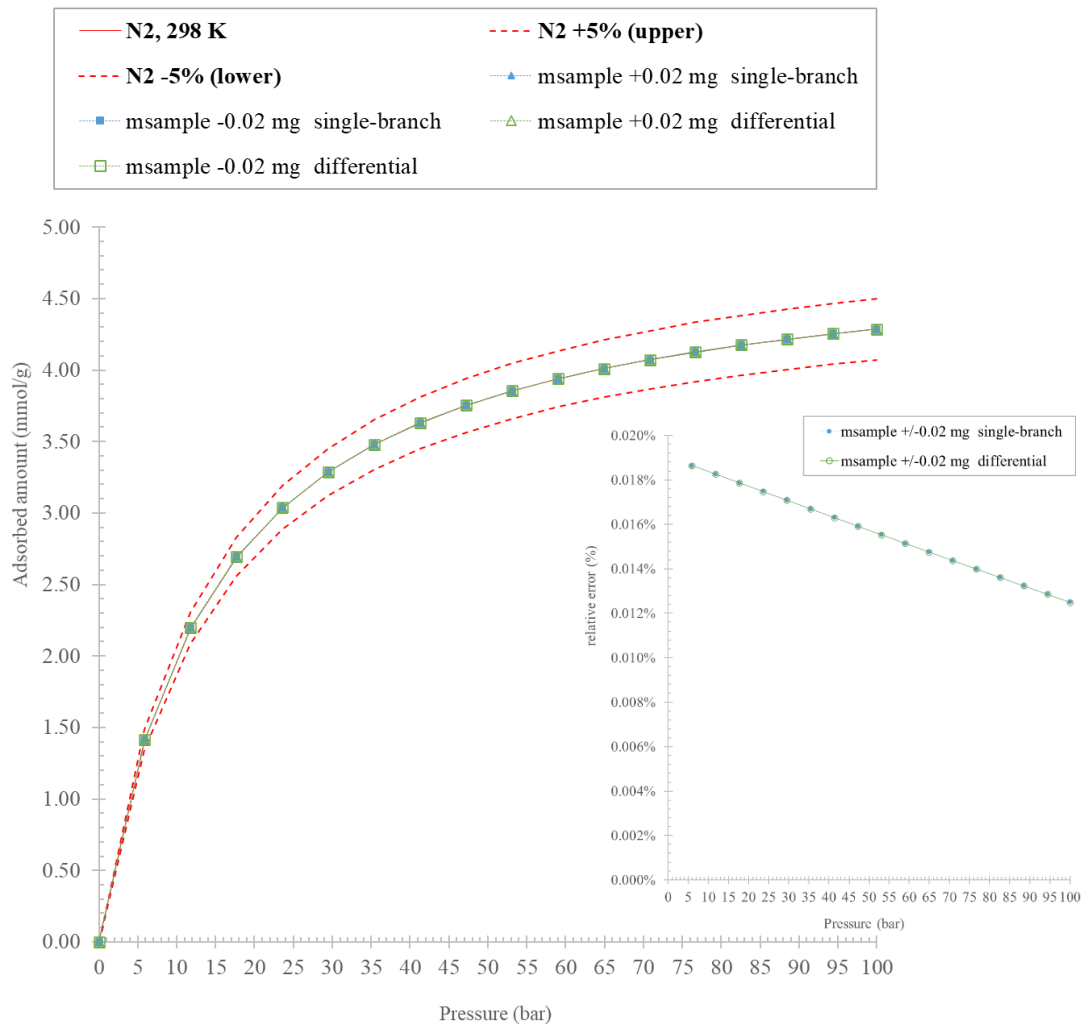

Figure 37 – Comparison of the effect of errors in sample mass weight for N_2 adsorbed onto 100 mg 13X (Gibson et al., 2016) at 298 K, measured by single-branch and differential method. Main plot: absolute errors trend, expected isotherm (red solid line), percentual error ±5% (red dashed lines); Inset plot: relative error (%) over pressure. Configuration 1

Regarding the beads mass (Fig. 38), the same increasing trend over equilibrium pressure is obtained being the stainless-steel beads accounted as a volume in the governing equations: for differential system, if the errors are introduced symmetrically in both branches, the resulting deviations are almost equal to zero in the entire pressure range. The relevance of symmetricity is evidenced in this case too.
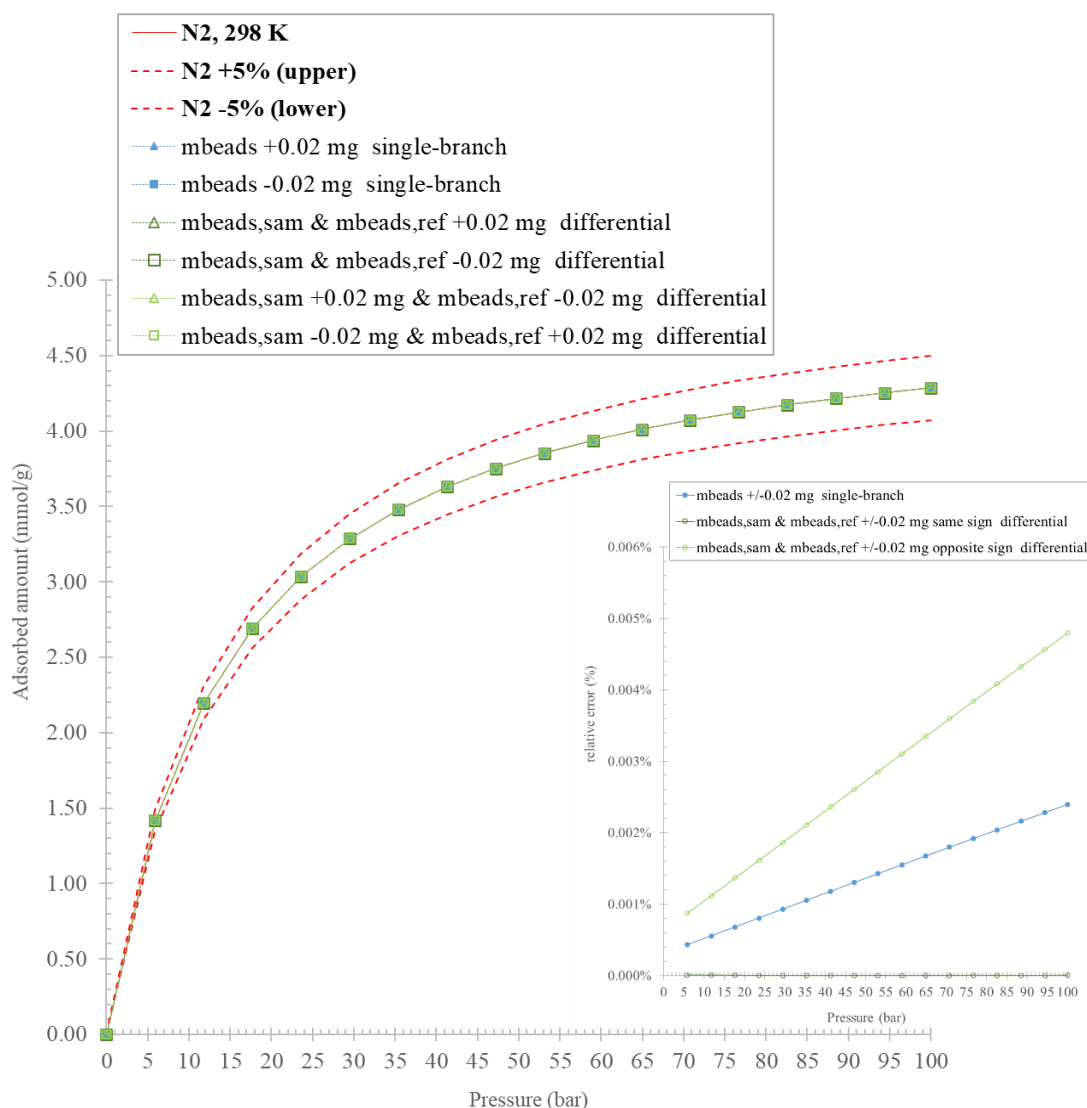
Figure 38 *– Comparison of the effect of errors in beads mass weight for N$_2$ adsorbed onto 100 mg 13X (Gibson et al., 2016) at 298 K, measured by single-branch and differential method. Main plot: absolute errors trend, expected isotherm (red solid line), percentual error ±5% (red dashed lines); Inset plot: relative error (%) over pressure.*

Overall, the systematic uncertainties that can be tied to balance accuracy can be considered negligible for both single-branch and differential apparatus.

Different conclusions could be obtained if, for example, the beads used occupy a big volume having a very low weight: in that case, even considering the density free from errors, the balance accuracy will lead to a consistent change in the beads volume calculation exacerbating the errors in the final results. This to say that the beads are generally used to facilitate the experiments (see *Chapter 2, Section 2.2.1*), but the material needs to be carefully selected to avoid the introduction of criticalities when performing data analysis.

6.4 Pressure readings

The analysis of the effect of pressure readings is among the main objectives of the study: the accuracy of system calibration is directly connected to the accuracy of pressure measurements. So, demonstrating that in the HP-ADVA system the error accumulation due to pressure measurements is somehow minimized, let indirectly demonstrate the reliability of the whole method.

In literature, the pressure has been demonstrated as the most affecting parameter for adsorption analysis performed with a volumetric system: this is not weird since all the calculations are based on pressure measurements. Commonly, the approach to the analysis is the consideration of the pressure readings as a random error introduced at each pressure step and accumulating for multistep isotherm construction; the extent of error is then related to the accuracy of the pressure transmitter used in the apparatus.

The point that the accuracy of the results are highly dependent on the accuracy of the instruments used for data collection is clearly true; the problem arises when dealing with how to consider the error introduction. Indeed, considering that a random error is introduced each time and it is equal to the instrument inaccuracy is quite unrealistic: this is what happens in case of single-shot pressure measurement. In our apparatus, the pressures collected during experiments are the results of an average, done by the instrument, over a big quantity of pressure readings. This is to say that, starting from the accuracy revealed by manufacturer's, the real inaccuracy will be consistently reduced, due to the huge quantities of pressure values taken each time.

Additionally, a consideration can be done in terms of randomization of the error: if the pressure values result from the average of a lot of measurements, the randomization can somehow be neglected considering that the value given by the apparatus is the correct one, or very close to it. In line with this, the possibility to consider the error in pressure readings no more as a random error accumulating over pressure steps, but as a systematic error such for the calibrated volume, due to, for example, the use of an incorrectly calibrated instrument.

In the proposed analysis, the pressure readings as random error and as systematic error (see *Section 5.1*) are presented to highlight the differences in the approach.

For the pressure transducer, the accuracy has been estimated by averaging the values reported in the calibration datasheet of the real instrument:

$\boldsymbol{\delta P_A}$	$\pm 0.0031\%$ FS (± 0.0085 bar)
$\boldsymbol{\delta P_D}$	$\pm 0.0149\%$ FS (± 0.185 mbar)

***Table 12** – Absolute and differential pressure transducer manufacturer's full scale (FS) accuracy.*

Then the analysis has been performed considering an arbitrarily chosen number of measurements, performed each time by the transmitter, by which the random standard error is then calculated:

selected number of pressure measurements (*N*) for each pressure point = *100*[4]

The standard error σ:

(32) $\quad \sigma = \dfrac{\text{std(single measurement)}}{\sqrt{N}}$

where, in the numerator, the standard deviation is calculated for each pressure load.

Fig. 39 shows the relative errors in gas uptake for each pressure step ("step contribution") and the accumulation over pressure ("total"): this last has been estimated by means of the procedure explained before (*Chapter 5*, *Section 5.1*, Eq. (25)). In particular, the plots of the left refer to single-branch, while, on the right, to the differential apparatus. The comparison is made between the error originated considering the given accuracy of the transducer and the standard error accounting 100 measurements for each pressure point.

The charts in Fig. 39 are obtained by considering the whole effect of pressure contributions: in case of single-branch apparatus, the absolute pressure readings in dosing and equilibrium phases; for the differential, the absolute pressure measured at dosing phase then differential pressure readings for dosing and equilibrium steps. Intermediate analysis has been done to see the individual effect of each pressure contribution (see Fig. 50 and 51, *APPENDIX A5*).

---

[4] The quantity selected is highly conservative: an higher number of measurements are collected by the sensor for each pressure point (100-300 measurements) every second; moreover, these values are already averages of a higher number of measurements.
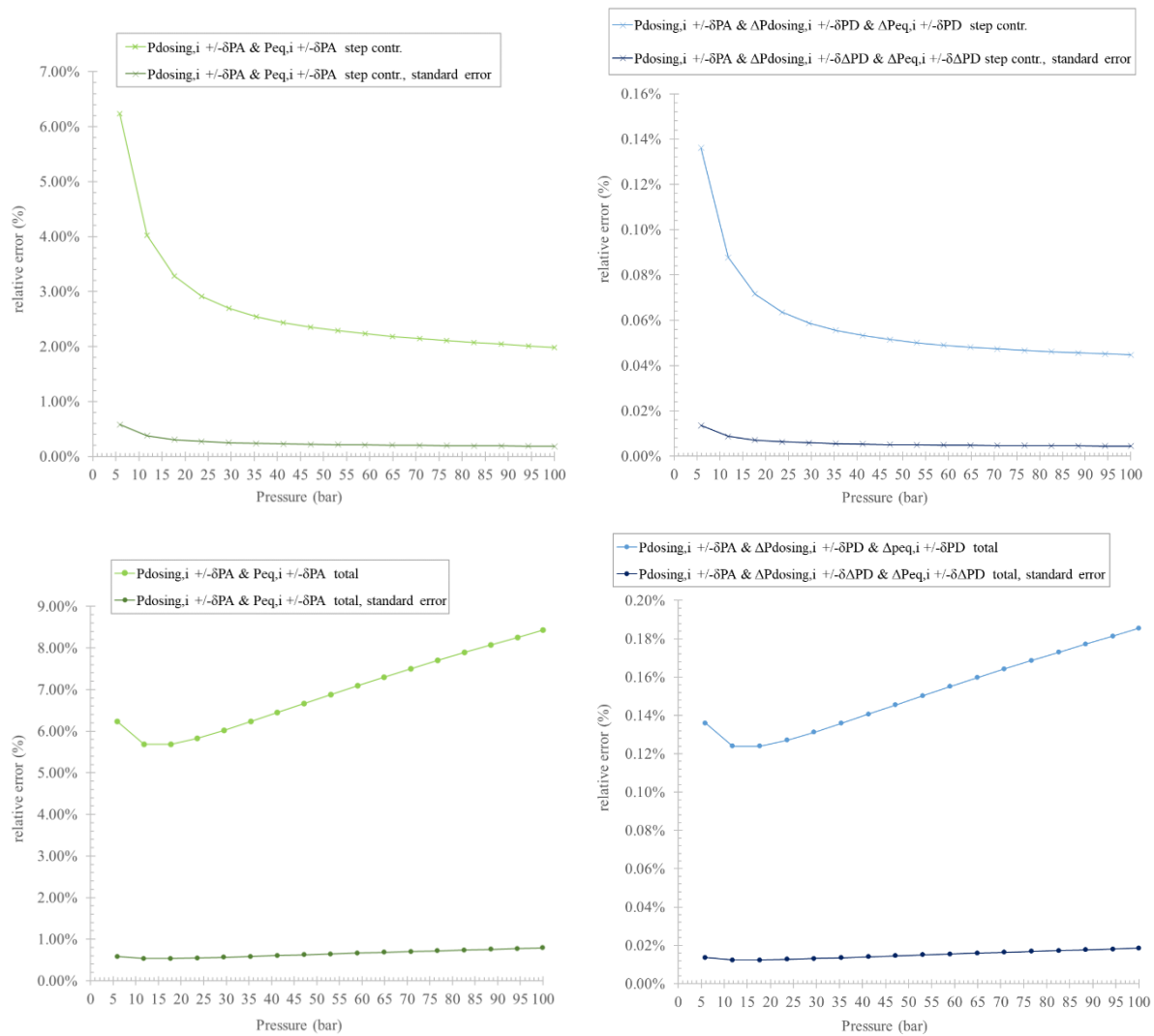
Figure 39 *– Relative errors(%) in gas uptake for N_2 adsorbed onto 100 mg 13X (Gibson et al., 2016) at 298 K, due to random errors in pressure readings measured by single-branch method (left) and differential method (right).*

It is quite evident the improvement in the system reliability when dealing with differential apparatus: the error decreases more than one order of magnitude among the two systems. Moreover, considering the inter-comparison among the two analytical approaches, the calculation of standard error leads to the reduction of the generated error of a factor of 10, which is effectively, the denominator selected in the equation (32). In conclusion, the way in which the accuracy of a sensor is considered is a key aspect to obtain results which are more realistic.

As mentioned before, randomization can in a way be neglected if a lot of measurements are considered, which is what effectively happens in a real system. So, the analysis of potential systematic error aims to see the effect of a wrongly calibrated transmitter in calculating the correct final isotherm.

In Fig. 40, the errors generated are illustrated over equilibrium pressure by comparing the effect of the whole pressure contribution for single-branch and differential apparatus. Focusing on the relative error(%) calculation (inset plot in Fig. 40), for the conventional system, a linear increasing trend is obtained over pressure while, for the double-branch system, the trend is increasing too but reaching a sort of asymptote at high-pressure. In both cases the values of error are quite low and negligible. The increasing trend is in line with the cumulative procedure performing multistep adsorption isotherm.
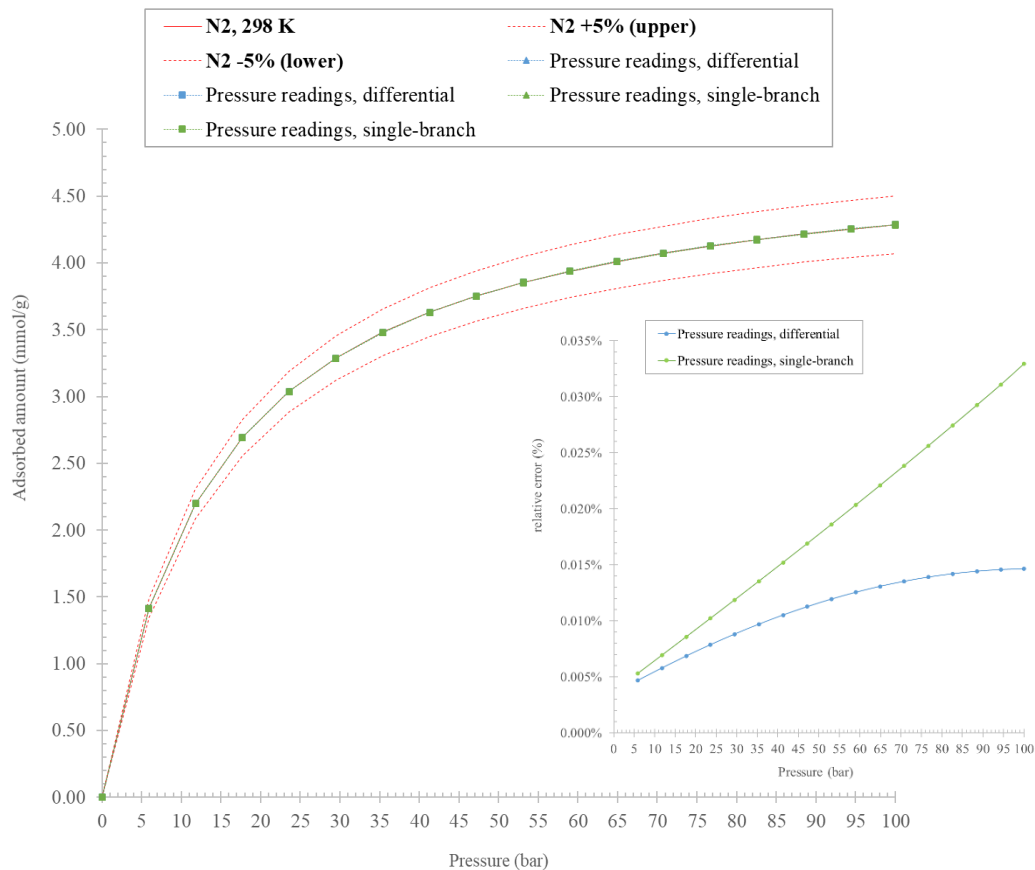

Figure 40 *– Comparison of the effect of errors in pressure readings for N₂ adsorbed onto 100 mg 13X (Gibson et al., 2016) at 298 K, measured by single-branch and differential method. Main plot: absolute errors trend, expected isotherm (red solid line), percentual error ±5% (red dashed lines); Inset plot: relative error (%) over pressure.*

85

These results are important for two main reasons: firstly, they suggest the improvement that can be obtained using a differential apparatus instead of a conventional one to obtain reliable results in the entire pressure range (low to high-pressure); then, they confirm the considerably high accuracy of the devices available in the system for pressure measurements. If a lower accuracy pressure transmitter is used, the errors raised due to pressure readings will be consistently higher affecting the final result.

Another consideration has been done to analyse the effect of pressure measurement which is the effect of systematic pressure error introduction in the procedure for volume calibration. In *Section 6.1*, the importance of a correctly calibrated instrument has been assessed; the calibration is mostly based on pressure measurements so how and to which extent a volume can be calibrated wrongly is strictly connected to the correctness of pressure readings.

By simulating real conditions for volume calibration and introducing the same systematic error on pressure readings (Table 12), an effect of cancellation is evident being the final result not affected by the error introduced. This is because the analytical procedure is based on pressures which are corrected with the baseline of the measurement: the baseline is loaded experimentally and it should hypothetically contain the systematic error. This leads to numerical cancellation of the error introduced.

6.5 Temperature readings

The last operating parameter studied is the temperature: K-type thermocouple are connected to the dosing and uptake cell to monitor, during the entire experiment, the exact value of temperature. The system set-up has been explained in detail in *Chapter 2* (*Section 2.1*), mentioning that the system is not provided with a temperature control system for the dosing volumes. The uptake cells, on the other hand, are immersed in a thermostatic bath to maintain the adsorbent sample at the desired temperature, but the dosing sections are exposed to room temperature.

In the analysis proposed, the only effect of thermocouple readings is considered: how much the accuracy of the thermocouples installed in the system affect the correctness of the final isotherm. As for the valve volume, the consideration of all temperature contributions, distinguishing among sample/reference branches, for example, is new because the majority of examples in literature approximate the temperature of the two branches as perfectly equal.

Additionally, also for the temperature measurements, the same reflection applied to pressure can be moved: distinction among the consideration of random or systematic error is done to see the discrepancies among the approaches. In this case the accuracy of the thermocouple used has been found in the product' datasheet.

δT	±1.5 K

Table 13 – Thermocouple manufacturer's accuracy.

Starting from the provided accuracy, the analysis has been performed considering an arbitrarily chosen number of measurements, performed each time by the transmitter, by which the random standard error is then calculated (Eq. (32)):

$$\text{selected number of temperature measurements (N) for each pressure point} = 100^4$$

In Fig. 41 the relative errors in gas uptake for each pressure step ("step contribution") and the accumulation over pressure ("total") are reported (for the procedure see *Chapter 5*, *Section 5.1*, Eq. (25)). In particular, the plots of the left refer to single-branch, while, on the right, to the differential apparatus. The comparison is made between the error originated considering the given accuracy of the thermocouple and the standard error accounting 100 measurements for each pressure point.

As for the pressure, the charts (Fig. 41) are obtained by considering the whole effect of temperature contributions, which are both measurements of dosing and uptake cell temperature. An intermediate analysis has been done to see the individual effect of each pressure contribution (see Fig. 52, *APPENDIX A5*).
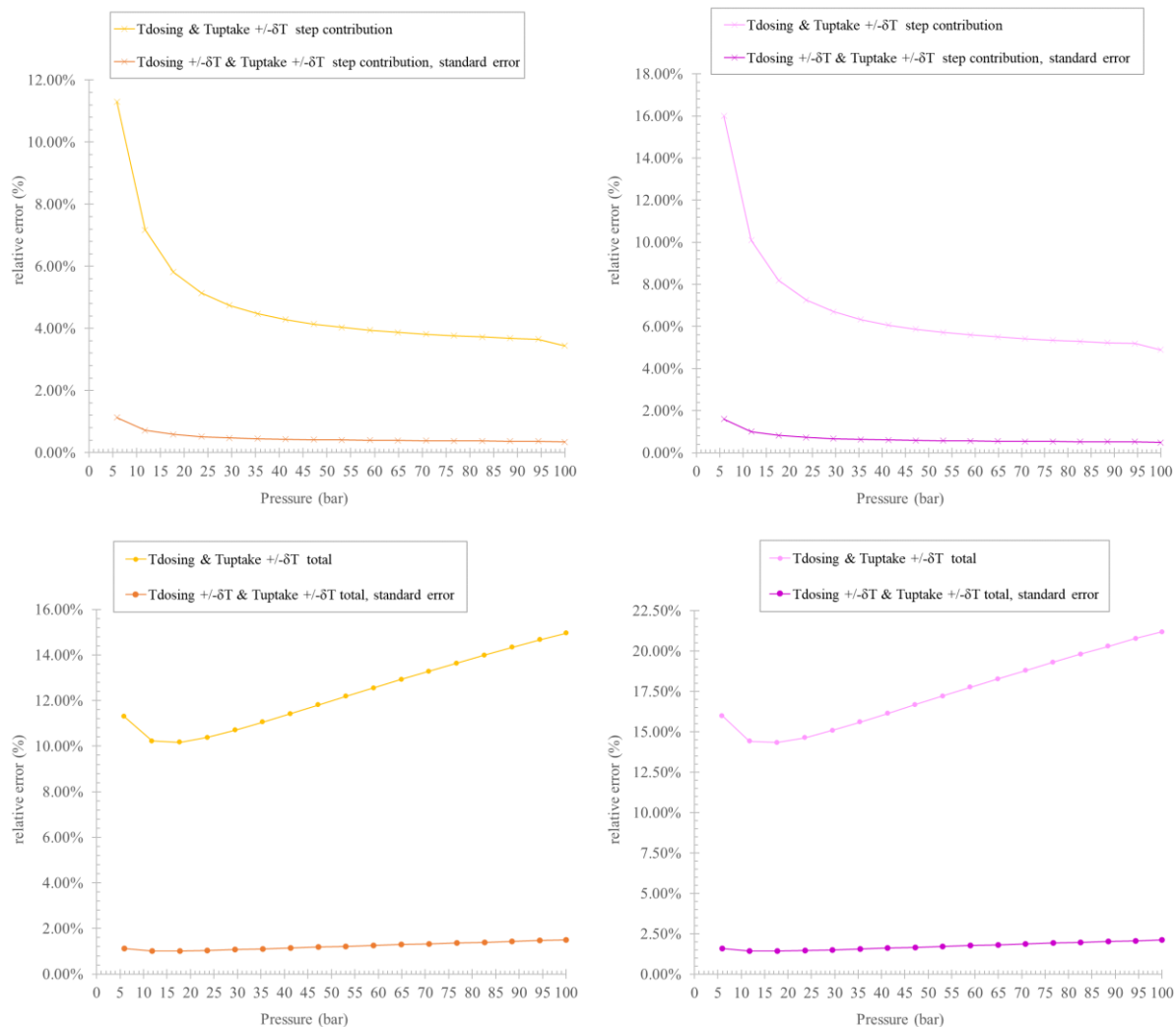
Figure 41 – Relative errors(%) in gas uptake for N_2 adsorbed onto 100 mg 13X (Gibson et al., 2016) at 298 K, due to random errors in temperature readings measured by single-branch method (left) and differential method (right).

In case of random errors, the thermocouples have a huge effect in the final isotherm: in the more realistic scenario, so considering the case of 100 temperature measurements for each pressure point, the error accumulated at P = 100 bar in gas uptake reaches the ±1.50% for single-branch and ±2.12% for double-branch apparatus. Applying blindly the error analysis one would consider the temperature measurement as random error, this would lead to an overestimation of the error. In reality, similarly to the case of the pressure measurement it is a systematic error. Moreover, the high error in the first adsorption point is due to the fact that in the first point a lot of moles are adsorbed.

Analysing the situation for wrongly calibrated thermocouples, the results are provided in Fig. 42.
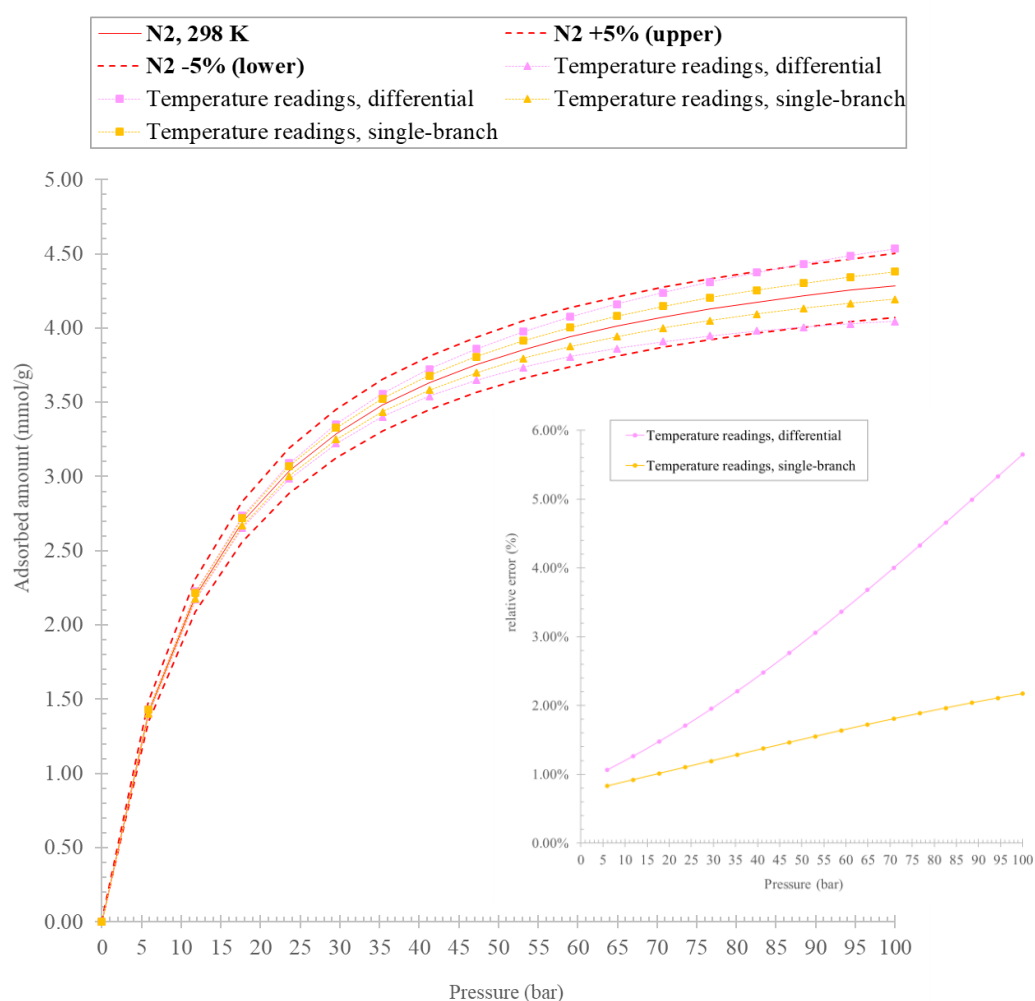

***Figure 42** – Comparison of the effect of errors in temperature readings for N₂ adsorbed onto 100 mg 13X (Gibson et al., 2016) at 298 K, measured by single-branch and differential method. Main plot: absolute errors trend, expected isotherm (red solid line), percentual error ±5% (red dashed lines); Inset plot: relative error (%) over pressure.*

The analysis pointed out an interesting peculiarity of the system: both configuration, single-branch and differential systems are highly sensitive to temperature discrepancies. In particular, the errors given by using differential apparatus seem higher than in conventional system. This is a starting point for the consideration of temperature control and measurement as a key aspect in adsorption measurements with volumetric systems. Following these findings, the possibility to enclose the dosing section of the apparatus inside a thermostatic apparatus where the temperature conditions can be better controlled avoiding system asymmetries creation. In

addition, the installation of more accurate thermocouples for temperature readings has been proposed too, to overall improve the system design.

The analysis of the effect of systematic error introduction of temperature values in volume calibration leads to similar results with respect to the pressure: very low errors are obtained having a maximum order of magnitude of ±0.03%. Numerically, this is due to the fact that the estimation of internal volume is done by calculating volume ratios. Introducing a ±1.5 K of error in a temperature ratio (Kelvin magnitudes) is a very low contribution. This is a further confirmation of the stability of the analytical method used for apparatus calibration.

By the results of the sensitivity analysis an hypothesis has been moved trying to explain the unexpected behaviour evidenced with the experimental campaign: some criticalities may be introduced by temperature readings. In Fig. 43, the trend over time of the thermocouple signal during a real experiment. As it is possible to notice, a gradient is formed among the dosing sections of the sample and reference branches, even if the two sides are exposed to the same room temperature. Moreover, the thermocouples seem to have different offset points to be considered. This needs to be accounted for in data analysis to avoid the introduction of errors in final results: as we have seen the effect of temperature readings is quite consistent so misleading results can be obtained. Normally, thermocouples are not calibrated, so to have more accurate measurements it is necessary to calibrate the thermocouples against a calibrated ones.
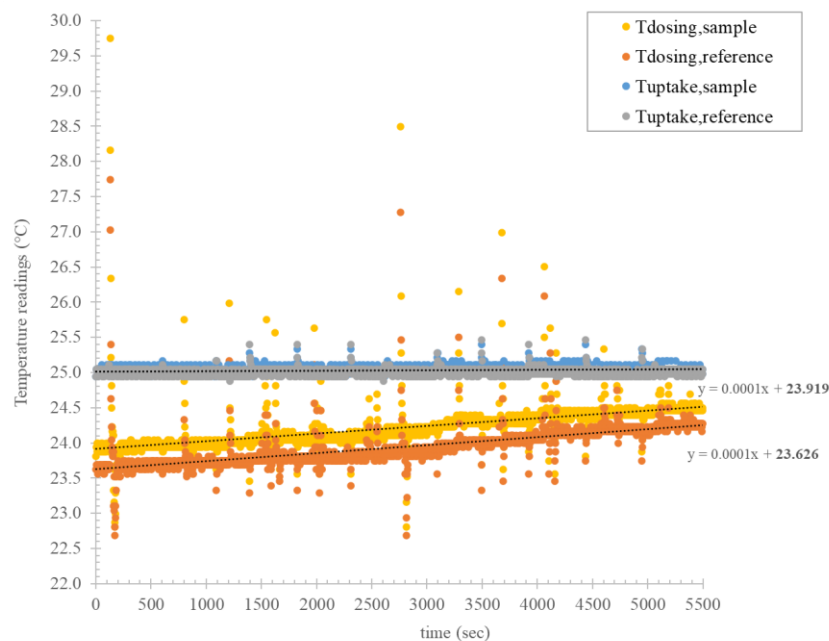

Figure 43 *– HP-ADVA thermocouples signal detected over time.*

90

6.6 Summary and cumulative error

The proposed tables summarize the error in the measurement of each parameter and the corresponding uncertainties in N_2 adsorption onto a hypothetical material (Gibson et al., 2016) at 298 K, at minimum and maximum gas uptake (P = 5 bar and P = 100 bar). The reported data refers to the relative error percentages (Eq. (28)). A rough estimation of cumulative error is given by using the error propagation law (Eq. (24)). Different error configurations are reported to provide an overall view of the results.

Tables 14 and 15 report the most realistic error configurations based on apparatus design and analytical methods used for data analysis.

Parameter	Parameter uncertainty	Adsorption by conventional system (%)	Adsorption by differential system (%)
Volume (cc)	$\pm 1\%$ (± 0.1) same sign[5]	2.120	1.014
V_{valve} (cc)	$\pm 1\%$ (± 0.002)	0.063	0.000
m_{sample} (mg)	± 0.02	0.019	0.019
m_{beads} (mg)	± 0.02	0.000	0.000
Pressure (bar/mbar)	$\pm 0.0085/\pm 0.185$	0.005	0.005
Temperature (K)	± 1.5	0.278	1.080
Cumulative	-	*2.139*	*1.482*

*Table 14 – Parameters uncertainty and error in the **minimum uptake** for N_2 adsorbed onto 13X (Gibson et al., 2016) at 298 K. Configuration 1*

---

[5] *Volume* stands for V_{dosing}, and V_{uptake}: "same sign" of systematic error introduced among dosing and uptake section, "opposite sign" of systematic error introduced among dosing and uptake section

Parameter	Parameter uncertainty	Adsorption by conventional system (%)	Adsorption by differential system (%)
Volume (cc)	$\pm1\%$ (±0.1) same sign[5]	14.767	0.630
V_{valve} (cc)	$\pm1\%$ (±0.002)	1.954	0.000
m_{sample} (mg)	±0.02	0.013	0.013
m_{beads} (mg)	±0.02	0.002	0.000
Pressure (bar/mbar)	$\pm0.0085/\pm0.185$	0.033	0.015
Temperature (K)	±1.5	3.358	5.804
Cumulative	-	*14.529*	*5.838*

*Table 15 – Parameters uncertainty and error in the **maximum uptake** for N_2 adsorbed onto 13X (Gibson et al., 2016) at 298 K. Configuration 1*

From the analysis a general feature is evident: less issues arise at low pressure conditions at which, single-branch and differential apparatus behave similarly. On the contrary, at high pressure, the differential method shows significantly better results than the single-branch, halving the error in the gas uptake. Moreover, at low-pressure conditions the cumulative error remains within the acceptance limit established while, at 100 bar it is exceeded by single-branch method and the differential is at limit of acceptability ($\pm$ 5% absolute error, see *Chapter 5, Section 5.2*), this is because at high pressure saturation is approached, i.e. $N_{ads} \sim 0$, so instrument accuracy is crucial for the measurements. The case of systematic error in volume calibration, having different signs among dosing and uptake cells (of the same branch) is reported too: indeed the results of the experimental campaign pointed out the possibility to face this situation, however, as previously said, this is a less common situation if the system is well set-up (Table 16 and 17).

Parameter	Parameter uncertainty	Adsorption by conventional system (%)	Adsorption by differential system (%)
Volume (cc)	±1% (±0.1) opposite sing[5]	34.89	0.080
V_{valve} (cc)	±1% (±0.002)	0.063	0.000
m_{sample} (mg)	±0.02	0.019	0.019
m_{beads} (mg)	±0.02	0.000	0.000
Pressure (bar/mbar)	±0.0085/±0.185	0.005	0.005
Temperature (K)	±1.5	0.278	1.080
Cumulative	-	*34.89*	*1.083*

Table 16 – *Parameters uncertainty and error in the **minimum uptake** for N_2 adsorbed onto 13X (Gibson et al., 2016) at 298 K. Configuration 2*

Parameter	Parameter uncertainty	Adsorption by conventional system (%)	Adsorption by differential system (%)
Volume (cc)	±1% (±0.1) opposite sign[5]	191.3	0.140
V_{valve} (cc)	±1% (±0.002)	1.954	0.000
m_{sample} (mg)	±0.02	0.013	0.013
m_{beads} (mg)	±0.02	0.002	0.000
Pressure (bar/mbar)	±0.0085/±0.185	0.033	0.015
Temperature (K)	±1.5	3.358	5.804
Cumulative	-	*191.3*	*5.806*

Table 17 – *Parameters uncertainty and error in the **maximum uptake** for N_2 adsorbed onto 13X (Gibson et al., 2016) at 298 K. Configuration 2*

In this case, the differences among conventional and differential methods are exacerbated: the single-branch system seems very sensitive giving rise to very high errors in gas uptake. Consider that, introducing a different systematic error for dosing/uptake cell volume, in a single-branch system, means changing completely the apparatus configuration: as mentioned in the *Section 6.1*, both volumes are multiplied by absolute pressure values which are generally big quantities generating big errors in the isotherm construction.

Lastly, the case of volume asymmetries for differential apparatus is reported (Table 18):

Pressure point	Parameter	Parameter uncertainty	Adsorption by differential system (%)
Minimum uptake	V_{ds} / V_{us} & V_{dr} / V_{ur} (cc)	$\pm 1\%$ (± 0.1) opposite sign among branches	5.254
Maximum uptake	V_{ds} / V_{us} & V_{dr} / V_{ur} (cc)	$\pm 1\%$ (± 0.1) opposite sign among branches	30.17

***Table 18** – Parameters uncertainty and error in the minimum and maximum uptake for N_2 adsorbed onto 13X (Gibson et al., 2016) at 298 K, measured by differential method. Configuration 3*

Asymmetries generate a consistent error in final gas uptake and this phenomenon is exacerbated at high pressure conditions. The importance in maintaining as much as possible symmetric conditions is then confirmed.

For completeness, the cumulative random errors generated considering the introduction of random errors due to pressure and temperature measurements have been estimated too, through the equations (24)-(26):
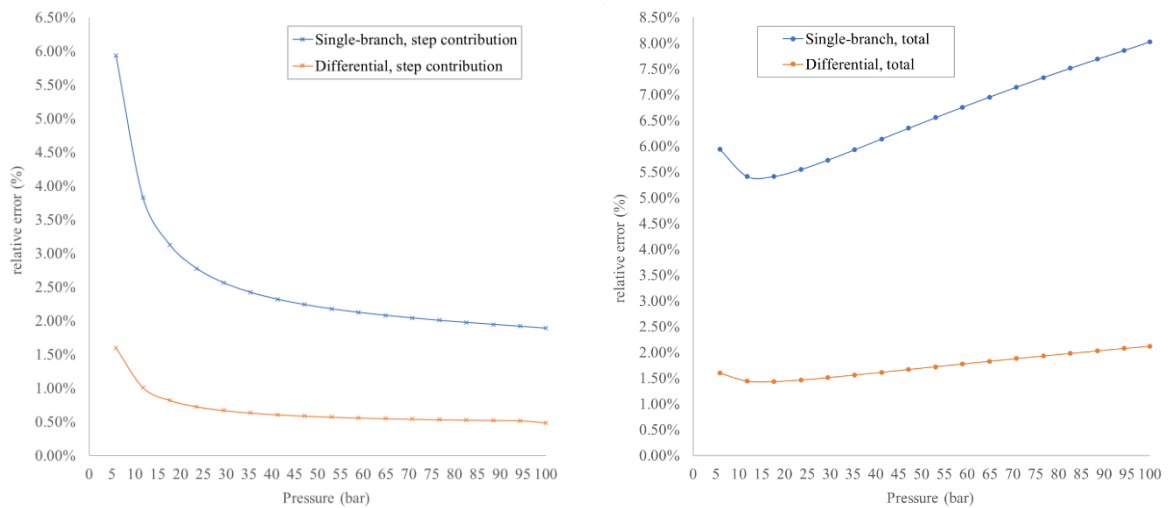

***Figure 44** – Comparison of the cumulative relative random errors(%) in gas uptake for N_2 adsorbed onto 100 mg 13X (Gibson et al., 2016) at 298 K, due to random errors in temperature and pressure readings measured by single-branch method and differential method. Cumulative error step contribution (left), total cumulative error (right).*

To be precise, the relative errors reported in Fig. 44 refers to the ones originated by considering N = 100 measurements (Eq. (32)), for pressure and temperature, at each pressure point. Also in this case a noticeable improvement in using a differential system for adsorption analysis con be noticed, indeed the double-branch seems to be 4-fold more accurate than the same apparatus but in single-branch configuration, regarding the only random errors accumulation.

Conclusion and future work

An integrated approach has been proposed to discover and assess the criticalities of the high-pressure differential volumetric apparatus (HP-ADVA) for adsorption analysis.

The experimental campaign evidenced the need for a deeper understanding of the system behaviour, particularly at high-pressure conditions. The discrepancies in results are, indeed, originated by the contribution of issues in the system set-up and in the analytical methods used for data analysis.

The interesting and new outcome of the analysis is that, if in the common practices the attention was mainly focused on pressure measurements, by installing devices which allow to have very high accuracy in pressure readings, now the attention needs to be shifted to other aspects which have not been accounted for deeply until now.

The sensitivity analysis confirmed in a way the hypothesis moved from the experimental results: first of all, the influence of valve volume cannot be neglected in the entire pressure range, being the apparatus specifically designed for high-pressure adsorption measurements. Moreover, how the valve volume needs to be accounted should be of interest for next studies on the system. Indeed, the experimental campaign pointed out characteristics of symmetricity of the valves, confirmed also by the sensitivity analysis by which, the results considering the configurations with $\alpha = 1$ and $\alpha = 0$, seems not much affecting the result.

Another consideration regards the temperature measurement and control: the introduction of discrepancies in temperature measurements affects consistently the result. It is possible to assume that the majority of inconsistencies raised up in the experimental campaign are effectively connected to temperature measurement. Indeed, Fig. 43 shows a behaviour of the installed thermocouples which cannot be ignored in data analysis and the sensitivity analysis confirmed that the introduction of systematic error in temperature measurements will lead to very high errors in the results. As previously said, this is because, at high pressure, saturation is approached ($N_{ads} \sim 0$).

In this regard, the need for a thermostatic chamber for dosing cells placing and the installation of more accurate thermocouples for temperature measurements is in the next ideas for improvement of the system design. Additionally, further studies at cryogenics seem to be interesting, firstly attempting to maintain as much as possible symmetry among branches. This is very attractive in the prospect of developing a system for high-pressure adsorption

measurements able to work in cryogenic conditions. Indeed, no systems are currently available giving the possibility in performing cryogenic experiments reaching that high pressure conditions, but it is a field in which the research could be profitably expanded.

Promising results have been obtained regarding the general reliability of the HP-ADVA apparatus: the analytical method developed for volume calibration seems to be quite stable avoiding the introduction of systematic pressure errors. Moreover, apart from temperature measurements, the system appears free from consistent errors if well calibrated and avoiding the formation of asymmetries in the system.

An interesting point to underline is the possibility to use this study as starting point for a change in the way the sensitivity and error analysis are performed and applied to volumetric systems: a general and more realistic method is needed with respect to the ones commonly proposed in literature. Indeed, from literature, the volumetric systems appeared being not so reliable, situation which clearly does not match the reality: a confirmation can be given by the paper (Nguyen et al., 2020), in which an inter-laboratory study is proposed for measuring CH_4 adsorption onto zeolite Y. The apparatus used for the measurement was the HP-ADVA volumetric system and the results seem perfectly in line with other laboratories and other systems used for the analysis.

The analysis gives the opportunity to thing about further studies of the system: for example, the sensitivity and error analysis could be performed for different adsorbate-adsorbent systems to evidence peculiarities at low and high adsorption conditions (e.g. H_2, CO_2). For instance, analysing the Hydrogen uptake with the method proposed could be worthwhile due to the possibility of a direct comparison with literature examples. Moreover, the hot/cold regions, mentioned when dealing with experiments at cryogenic conditions, could be accounted for in the analysis to see the effective relevance of the temperature gradient formation. In this regard, no literature has been written until now.

In view of the results obtained, two further recommendations can be moved to facilitate the correct understanding of the HP-ADVA type apparatus: an accurate characterisation of the differential pressure transducer is advised before installation to see the performances of the internal diaphragm exposed to different pressure and account for it in the mass balance, eventually. Likewise, a more accurate characterisation of the pneumatic-actuated high-pressure bellow sealed valves to better understand the behaviour.

References

Aforkoghene Aromada, S., & Øi, L. (2015). Simulation of improved absorption configurations for CO2 capture. *Proceedings of the 56th Conference on Simulation and Modelling (SIMS 56), October, 7-9, 2015, Linköping University, Sweden*, *119*, 21–29. https://doi.org/10.3384/ecp1511921

Ahn, C. C., Ye, Y., Ratnakumar, B. V., Witham, C., Bowman, R. C., & Fultz, B. (1998). Hydrogen desorption and adsorption measurements on graphite nanofibers. *Applied Physics Letters*, *73*(23), 3378–3380. https://doi.org/10.1063/1.122755

Belmabkhout, Y., Frère, M., & De Weireld, G. (2004). High-pressure adsorption measurements. A comparative study of the volumetric and gravimetric methods. *Measurement Science and Technology*, *15*(5), 848–858. https://doi.org/10.1088/0957-0233/15/5/010

Bereznitski, Y., Jaroniec, M., & Gadkaree, K. P. (1997). Influence of analysis conditions on low pressure adsorption measurements and its consequences in characterization of energetic and structural heterogeneity of microporous carbons. *Adsorption*, *3*(4), 277–282. https://doi.org/10.1007/BF01653630

Blach, T. P., & Gray, E. M. A. (2007). Sieverts apparatus and methodology for accurate determination of hydrogen uptake by light-atom hosts. *Journal of Alloys and Compounds*, *446–447*, 692–697. https://doi.org/10.1016/j.jallcom.2006.12.061

Blackburn, J. L., Parilla, P. A., Gennett, T., Hurst, K. E., Dillon, A. C., & Heben, M. J. (2008). Measurement of the reversible hydrogen storage capacity of milligram Ti-6Al-4V alloy samples with temperature programmed desorption and volumetric techniques. *Journal of Alloys and Compounds*, *454*(1–2), 483–490. https://doi.org/10.1016/j.jallcom.2007.01.006

Blackman, J. M., Patrick, J. W., & Snape, C. E. (2006). An accurate volumetric differential pressure method for the determination of hydrogen storage capacity at high pressures in carbon materials. *Carbon*, *44*(5), 918–927. https://doi.org/10.1016/j.carbon.2005.10.032

Bose, A. (2009). *Inorganic membranes for energy and environmental applications* (Chapter 2). Springer.

Brandani, S., Mangano, E., & Sarkisov, L. (2016). Net, excess and absolute adsorption and adsorption of helium. *Adsorption*, *22*(2), 261–276. https://doi.org/10.1007/s10450-016-9766-0

Broom, D. P., & Moretto, P. (2007). Accuracy in hydrogen sorption measurements. *Journal of Alloys and Compounds*, *446–447*(March), 687–691. https://doi.org/10.1016/j.jallcom.2007.03.022

Browning, D. J., Gerrard, M. L., Lakeman, J. B., Mellor, I. M., Mortimer, R. J., & Turpin, M. C. (2002). Studies into the Storage of Hydrogen in Carbon Nanofibers: Proposal of a Possible Reaction Mechanism. *Nano Letters*, *2*(3), 201–205. https://doi.org/10.1021/nl015576g

Checchetto, R., Trettel, G., & Miotello, A. (2004). Sievert-type apparatus for the study of hydrogen storage in solids. *Measurement Science and Technology*, *15*(1), 127–130. https://doi.org/10.1088/0957-0233/15/1/017

Cheng, H. H., Deng, X. X., Li, S. L., Chen, W., Chen, D. M., & Yang, K. (2007). Design of PC based high pressure hydrogen absorption/desorption apparatus. *International Journal of Hydrogen Energy*, *32*(14), 3046–3053. https://doi.org/10.1016/j.ijhydene.2007.01.010

Demirocak, D. E., Srinivasan, S. S., Ram, M. K., Goswami, D. Y., & Stefanakos, E. K. (2013). Volumetric hydrogen sorption measurements-Uncertainty error analysis and the importance of thermal equilibration time. *International Journal of Hydrogen Energy*, *38*(3), 1469–1477. https://doi.org/10.1016/j.ijhydene.2012.11.013

Do, D. D. (1998). Adsorption Analysis: Equilibria and Kinetics. In *Chemical Engineering* (Vol. 2, Issue Imperial College Press). Imperial College Press. https://doi.org/10.1142/9781860943829

Eic, M., & Ruthven, D. M. (1988). A new experimental technique for measurement of intracrystalline diffusivity. *Zeolites*, *8*(1), 40–45. https://doi.org/10.1016/S0144-

2449(88)80028-9

Emerson. (2019). *Product Data Sheet: Rosemount™ 3051 Pressure Transmitter* [File PDF] (p. 108). Retrieved from https://www.emerson.com/

Giacobbe, F. W. (1991). A high-pressure volumetric gas adsorption system. *Review of Scientific Instruments*, *62*(9), 2186–2192. https://doi.org/10.1063/1.1142336

Gibson, J. A. A., Mangano, E., Shiko, E., Greenaway, A. G., Gromov, A. V., Lozinska, M. M., Friedrich, D., Campbell, E. E. B., Wright, P. A., & Brandani, S. (2016). Adsorption Materials and Processes for Carbon Capture from Gas-Fired Power Plants: AMPGas. *Industrial and Engineering Chemistry Research*, *55*(13), 3840–3851. https://doi.org/10.1021/acs.iecr.5b05015

Keller, J. U., & Staudt, R. (2005). Gas adsorption equilibria: Experimental methods and adsorptive isotherms. In *Gas Adsorption Equilibria: Experimental Methods and Adsorptive Isotherms*. Springer Science + Buisness Media, Inc. https://doi.org/10.1007/b102056

King, C. J. (1980). Separation Processes. In *Ensemble*. McGraw-Hill Chemical Engineering Series. https://doi.org/10.11436/mssj.15.250

Kunz, O., & Wagner, W. (2012). The GERG-2008 wide-range equation of state for natural gases and other mixtures: An expansion of GERG-2004. In *Journal of Chemical and Engineering Data* (Vol. 57, Issue 11). https://doi.org/10.1021/je300655b

Lachawiec, A. J., DiRaimondo, T. R., & Yang, R. T. (2008). A robust volumetric apparatus and method for measuring high pressure hydrogen storage properties of nanostructured materials. *Review of Scientific Instruments*, *79*(6). https://doi.org/10.1063/1.2937820

Lee, Y. W., Clemens, B. M., & Gross, K. J. (2008). Novel Sieverts' type volumetric measurements of hydrogen storage properties for very small sample quantities. *Journal of Alloys and Compounds*, *452*(2), 410–413. https://doi.org/10.1016/j.jallcom.2006.11.014

Luo, S., Zhang, Q., Zhu, L., Lin, H., Kazanowska, B. A., Doherty, C. M., Hill, A. J., Gao, P.,

& Guo, R. (2018). Highly Selective and Permeable Microporous Polymer Membranes for Hydrogen Purification and CO2 Removal from Natural Gas [Research-article]. *Chemistry of Materials*, *30*(15), 5322–5332. https://doi.org/10.1021/acs.chemmater.8b02102

Malbrunot, P., Vidal, D., Vermesse, J., Chahine, R., & Bose, T. K. (1997). Adsorbent helium density measurement and its effect on adsorption isotherms at high pressure. *Langmuir*, *13*(3), 539–544. https://doi.org/10.1021/la950969e

Mangano, E., Wang , J., & Brandani, S. (2019). Use of a Novel Volumetric Differential Pressure Apparatus for Adsorption Equilibrium Measurements. *AIChE 2019 Annual Meeting*. Orlando.

Mason, G., Buffham, B. A., & Heslop, M. J. (1997). Gas adsorption isotherms from composition and flow-rate transient times in Chromatographic columns III. Effect of gas viscosity changes. *Proceedings of the Royal Society A: Mathematical, Physical and Engineering Sciences*, *453*(1963), 1569–1592. https://doi.org/10.1098/rspa.1997.0084

Mettler Toledo. *Product Data Sheet: Mettler Toledo XSR205 Dual Rage Analytical Balance* [File PDF] (p. 108). Retrieved from https: https://www.mt.com/

Mohammad, S., Fitzgerald, J., Robinson, R. L., & Gasem, K. A. M. (2009). Experimental uncertainties in volumetric methods for measuring equilibrium adsorption. *Energy and Fuels*, *23*(5), 2810–2820. https://doi.org/10.1021/ef8011257

Nakashima, M., Shimada, S., Inagaki, M., & Centeno, T. A. (1995). On the adsorption of CO2 by molecular sieve carbons-Volumetric and gravimetric studies. *Carbon*, *33*(9), 1301–1306. https://doi.org/10.1016/0008-6223(95)00077-Q

Nguyen, H. G. T., Espinal, L., van Zee, R. D., Thommes, M., Toman, B., Hudson, M. S. L., Mangano, E., Brandani, S., Broom, D. P., Benham, M. J., Cychosz, K., Bertier, P., Yang, F., Krooss, B. M., Siegelman, R. L., Hakuman, M., Nakai, K., Ebner, A. D., Erden, L., … De Weireld, G. (2018). A reference high-pressure CO2 adsorption isotherm for ammonium ZSM-5 zeolite: results of an interlaboratory study. *Adsorption*, *24*(6), 531–539. https://doi.org/10.1007/s10450-018-9958-x

Nguyen, H. G. T., Sims, C. M., Toman, B., Horn, J., van Zee, R. D., Thommes, M., Ahmad,

R., Denayer, J. F. M., Baron, G. V., Napolitano, E., Bielewski, M., Mangano, E., Brandani, S., Broom, D. P., Benham, M. J., Dailly, A., Dreisbach, F., Edubilli, S., Gumma, S., … De Weireld, G. (2020). A reference high-pressure CH4 adsorption isotherm for zeolite Y: results of an interlaboratory study. *Adsorption*, *0123456789*. https://doi.org/10.1007/s10450-020-00253-0

Park, Y., Ju, Y., Park, D., & Lee, C. H. (2016). Adsorption equilibria and kinetics of six pure gases on pelletized zeolite 13X up to 1.0 MPa: CO2, CO, N2, CH4, Ar and H2. *Chemical Engineering Journal*, *292*, 348–365. https://doi.org/10.1016/j.cej.2016.02.046

Qajar, A., Peer, M., Rajagopalan, R., & Foley, H. C. (2012). High pressure hydrogen adsorption apparatus: Design and error analysis. *International Journal of Hydrogen Energy*, *37*(11), 9123–9136. https://doi.org/10.1016/j.ijhydene.2012.03.002

Ramaprabhu, S., Rajalakshmi, N., & Weiss, A. (1998). Design and development of hydrogen absorption/desorption high pressure apparatus based on the pressure reduction method. *International Journal of Hydrogen Energy*, *23*(9), 797–801. https://doi.org/10.1016/s0360-3199(97)00131-6

Rouquerol, F. (2014). *Adsorption by powders and porous solids*. Amsterdam: Elsevier, Academic Press.

Ruthven, D. M. (1985). Principles of adsorption and adsorption processes. In *Chemical Engineering and Processing: Process Intensification* (Vol. 19, Issue 2). John Wiley & Sons, Inc. https://doi.org/10.1016/0255-2701(85)80013-1

Sing, K. S. W., Everett, D. H., Haul, R. A. W., Moscou, L., Pierotti, R. A., & Rouquerol, J. Siemieniewska, T. (1985). REPORTING PHYSISORPTION DATA FOR GAS/SOLID SYSTEMS with Special Reference to the Determination of Surface Area and Porosity. *Pure & Appl. Chem.*, *57*(4), 603–619. https://doi.org/10.1351/pac198557040603

Sircar, S., Wang, C. Y., & Lueking, A. D. (2013). Design of high pressure differential volumetric adsorption measurements with increased accuracy. *Adsorption*, *19*(6), 1211–1234. https://doi.org/10.1007/s10450-013-9558-8

Suzuki, I. (1982). Temperature-compensated, differential tensimeter for measuring gas adsorption by low surface area solids. *Review of Scientific Instruments*, *53*(7), 1061–1066. https://doi.org/10.1063/1.1137088

Suzuki, I., Kakimoto, K., & Oki, S. (1987). Volumetric determination of adsorption of helium over some zeolites with a temperature-compensated, differential tensimeter having symmetrical design. *Review of Scientific Instruments*, *58*(7), 1226–1230. https://doi.org/10.1063/1.1139659

Tibbetts, G. G., Meisner, G. P., & Olk, C. H. (2001). Hydrogen storage capacity of carbon nanotubes, filaments, and vapor-grown fibers. *Carbon*, *39*(15), 2291–2301. https://doi.org/10.1016/S0008-6223(01)00051-3

Wang, J. Y., Mangano, E., Brandani, S., & Ruthven, D. M. (2020). A review of common practices in gravimetric and volumetric adsorption kinetic experiments. *Adsorption*, *0123456789*. https://doi.org/10.1007/s10450-020-00276-7

Webb, C. J., & Gray, E. M. (2014a). Analysis of the uncertainties in gas uptake measurements using the Sieverts method. *International Journal of Hydrogen Energy*, *39*(1), 366–375. https://doi.org/10.1016/j.ijhydene.2013.09.155

Webb, C. J., & Gray, E. M. (2014b). The effect of inaccurate volume calibrations on hydrogen uptake measured by the Sieverts method. *International Journal of Hydrogen Energy*, *39*(5), 2168–2174. https://doi.org/10.1016/j.ijhydene.2013.11.121

Yang, R. T. (2003). Adsorbents: Funtamentals and Applications. In *Physics* (Vol. 677, Issue 1). John Wiley & Sons, Inc. https://doi.org/10.1016/j.aca.2010.06.020

Zhang, C., Lu, X. S., & Gu, A. Z. (2004). How to accurately determine the uptake of hydrogen in carbonaceous materials. *International Journal of Hydrogen Energy*, *29*(12), 1271–1276. https://doi.org/10.1016/j.ijhydene.2003.12.001

Zielinski, J. M., Coe, C. G., Nickel, R. J., Romeo, A. M., Cooper, A. C., & Pez, G. P. (2007). High pressure sorption isotherms via differential pressure measurements. *Adsorption*, *13*(1), 1–7. https://doi.org/10.1007/s10450-007-9005-9

APPENDIX

A1. Corrective factors for blank response

	Protocol 1	Protocol 2	Protocol 3	Protocol 4
Corrective factor	0.9770	1.0065	0.9930	1.0065
Deviation from unity	+0.023	-0.0065	+0.007	-0.0065

Table 19 - *Corrective factors used in blank response at cryogenics analysis; calculated deviation from unity.*

A2. Effect of differential pressure transducer offset
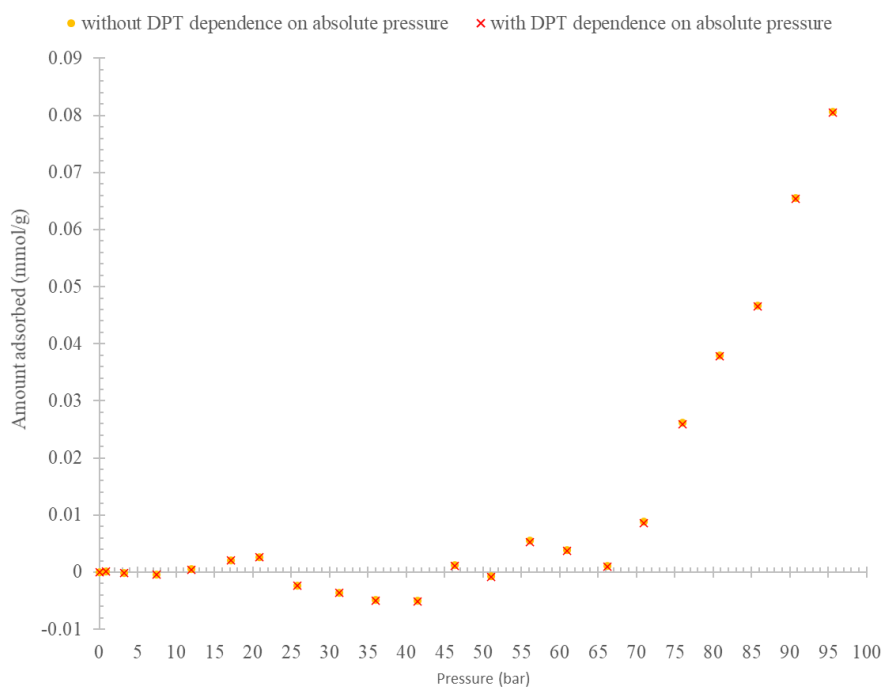
Figure 45 – Comparison of blank isotherms (Helium at Temperature = 25°C, Pressure = 0-100 bar$_a$)
considering the offset of the differential pressure transducer dependence on absolute pressure.

A3. Pneumatically-actuated valve compressed air

System pressure (bar)	Compressed air pressure (bar) (valve opening/closing)
100	6
55	6-6.5
30	7-7.5
5	8
2	8

Table 20 - Compressed air pressure set for opening/closing of the pneumatic activated valves depending on the operating pressure.

A4. Supplementary analytical methods

In the case of a single-branch system, the partial derivatives of n_i relatives to the parameters are calculated analytically, by referring to the governing equation (12) (see *Chapter 3*). Then the adsorbed amount q_i are considered by considering:

$$(33) \quad q_i = \frac{n_i}{M_A}$$

For the configuration with $\alpha = 1$ (see Eq. (13), *Chapter 3*), the partial derivatives have the following forms:

$$(34) \quad \frac{\partial q_i}{\partial P_{S_i}} = \frac{V_{DS}}{M_A R T_{DS_i}} \left(\frac{z_i(T_{DS_I}, P_{S_i}) - P_{S_i} \frac{\partial \left(z_i(T_{DS_I}, P_{S_i}) \right)}{\partial P_{S_i}}}{z_i \left(T_{DS_I}, P_{S_i} \right)^2} \right) + \frac{(V_{US} - V_{CS} - V_A)}{M_A R T_{US_i}} \left(\frac{z_i(T_{US_I}, P_{S_i}) - P_{S_i} \frac{\partial \left(z_{i+1}(T_{US_I}, P_{S_i}) \right)}{\partial P_{S_i}}}{z_i \left(T_{US_I}, P_{S_i} \right)^2} \right)$$

$$(35) \quad \frac{\partial q_i}{\partial T_{DS}} = \frac{P_{DS_{i-1}}(V_{DS} - \alpha V_{valve})}{M_A R} \left(-\frac{1}{T_{DS_{i-1}}^2} \right) - \frac{P_{S_i} V_{DS}}{M_A R} \left(-\frac{1}{T_{DS_i}^2} \right)$$

$$(36) \quad \frac{\partial q_i}{\partial T_{US}} = \frac{P_{US_{i-1}}(V_{US} - V_{CS} - V_A)}{M_A R} \left(-\frac{1}{T_{US_{i-1}}^2} \right) - \frac{P_{S_i}(V_{US} - V_{CS} - V_A)}{M_A R} \left(-\frac{1}{T_{US_i}^2} \right)$$

As approximation, $T_{Dsi-1} = T_{Dsi}$ as well as $T_{Usi-1} = T_{Usi}$, which is a plausible conditions, generally, the uptake cell is indeed maintained at constant temperature, the dosing cell is exposed to room temperature but very low temperature changes are appreciable during one single adsorption experiment.

For the configuration with $\alpha = 0$ (see Eq. (13), *Chapter 3*), the alternative expressions are listed below:

$$(37)\quad \frac{\partial q_i}{\partial P_{DS_{i-1}}} = \frac{(V_{DS}-(1-\alpha)V_{valve})}{M_A R T_{DS_{i-1}}}\left(\frac{z_{i-1}\left(T_{DS_{i-1}}.P_{DS_{i-1}}\right)-P_{DS_{i-1}}\frac{\partial\left(z_{i-1}\left(T_{DS_{i-1}}.P_{DS_{i-1}}\right)\right)}{\partial P_{DS_{i-1}}}}{z_{i-1}\left(T_{DS_{i-1}}.P_{DS_{i-1}}\right)^2}\right)$$

$$(38)\quad \frac{\partial q_i}{\partial P_{S_i}} = \frac{(V_{DS}-(1-\alpha)V_{valve})}{M_A R T_{DS_i}}\left(\frac{z_i(T_{DS_I},P_{S_i})-P_{S_i}\frac{\partial\left(z_i(T_{DS_I},P_{S_i})\right)}{\partial P_{S_i}}}{z_i\left(T_{DS_I},P_{S_i}\right)^2}\right)+$$

$$\frac{(V_{US}-V_{CS}-V_A)}{M_A R T_{US_i}}\left(\frac{z_i(T_{US_I},P_{S_i})-P_{S_i}\frac{\partial\left(z_{i+1}(T_{US_I},P_{S_i})\right)}{\partial P_{S_i}}}{z_i\left(T_{US_I},P_{S_i}\right)^2}\right)$$

$$(39)\quad \frac{\partial q_i}{\partial T_{DS}} = \frac{P_{DS_{i-1}}(V_{DS}-\alpha V_{valve})}{M_A R}\left(-\frac{1}{T_{DS_{i-1}}^2}\right) - \frac{P_{S_i}(V_{DS}-(1-\alpha)V_{valve})}{M_A R}\left(-\frac{1}{T_{DS_i}^2}\right)$$

$$(40)\quad \frac{\partial q_i}{\partial T_{US}} = \frac{P_{US_{i-1}}(V_{US}-V_{CS}-V_A-(1-\alpha)V_{valve})}{M_A R}\left(-\frac{1}{T_{US_{i-1}}^2}\right) - \frac{P_{S_i}(V_{US}-V_{CS}-V_A)}{M_A R}\left(-\frac{1}{T_{US_i}^2}\right)$$

In case of differential apparatus, the partial derivatives of the mole balance (Eq. (18)) are written as well to perform the error analysis; also in this case, the derivatives of the adsorbed amount q_i is considered, for the configuration $\alpha = 1$:

$$(41)\quad \frac{\partial q_i}{\partial P_{D_{i-1}}} = \left(\frac{(V_{DS}-\alpha V_{valve})}{M_A R T_{DS_{i-1}}}\left(\frac{z_{i-1}(T_{DS_{i-1}},P_{DS_{i-1}})-P_{DS_{i-1}}\frac{\partial\left(z_i(T_{DS_{i-1}},P_{DS_{i-1}})\right)}{\partial P_{DS_{i-1}}}}{z_{i-1}\left(T_{DS_{i-1}},P_{DS_{i-1}}\right)^2}\right)-\right.$$

$$\left.\frac{(V_{DR}-\alpha V_{valve})}{M_A R T_{DR_{i-1}}}\left(\frac{z_{i-1}(T_{DR_{i-1}},P_{DR_{i-1}})-P_{DR_{i-1}}\frac{\partial\left(z_{i-1}(T_{DR_{i-1}},P_{DR_{i-1}})\right)}{\partial P_{DR_i}}}{z_{i-1}\left(T_{DR_{i-1}},P_{DR_{i-1}}\right)^2}\right)\right)$$

$$(42)\quad \frac{\partial q_i}{\partial \Delta P_{D_{i-1}}} = \frac{(V_{DS}-\alpha V_{valve})}{M_A R T_{DS_{i-1}}}\left(\frac{1}{z_i(T_{DS_{i-1}},P_{DS_{i-1}})}\right)$$

$$(43)\quad \frac{\partial q_i}{\partial \Delta P_i} = \left(\frac{V_{DS}}{M_A R T_{DS_i}}\left(\frac{1}{z_i(T_{DS_I},P_{S_i})}\right)+\frac{(V_{US}-V_{CS}-V_A)}{M_A R T_{US_i}}\left(\frac{1}{z_i(T_{US_I},P_{S_i})}\right)\right)$$

$$(44)\quad \frac{\partial q_i}{\partial T_{DS}} = \left(\frac{(P_{DR_{i-1}}-\Delta P_{D_{i-1}})(V_{DS}-\alpha V_{valve})}{M_A R}\right)\left(-\frac{1}{T_{DS_{i-1}}^2}\right)+\frac{(-P_{R_i}+\Delta P_i)V_{DS}}{M_A R}\left(-\frac{1}{T_{DS_i}^2}\right)$$

$$(45) \quad \frac{\partial q_i}{\partial T_{DR}} = \left(\frac{P_{DR_{i-1}}(V_{DR}-\alpha V_{valve})}{M_A R}\right)\left(\frac{1}{T_{DR_{i-1}}^2}\right) + \frac{P_{R_i}V_{DR}}{M_A R}\left(-\frac{1}{T_{DR_i}^2}\right)$$

$$(46) \quad \frac{\partial q_i}{\partial T_{US}} = \left(\frac{(P_{UR_{i-1}}-\Delta P_{U_{i-1}})(V_{US}-V_{CS}-V_A)}{M_A R}\right)\left(-\frac{1}{T_{US_{i-1}}^2}\right) + \frac{(-P_{R_i}+\Delta P_i)(V_{US}-V_{CS}-V_A)}{M_A R}\left(-\frac{1}{T_{US_i}^2}\right)$$

$$(47) \quad \frac{\partial q_i}{\partial T_{UR}} = \left(-\frac{P_{UR_{i-1}}(V_{UR}-V_{CR})}{M_A R}\right)\left(-\frac{1}{T_{UR_{i-1}}^2}\right) + \frac{P_{R_i}(V_{UR}-V_{CR})}{M_A R}\left(-\frac{1}{T_{UR_i}^2}\right)$$

For the configuration with $\alpha = 0$ (see Eq. (13), *Chapter 3*), the alternative expressions are:

$$(48) \quad \frac{\partial q_i}{\partial P_{D_{i-1}}} = \left(\frac{(V_{DS}-(1-\alpha)V_{valve})}{M_A R T_{DS_{i-1}}}\left(\frac{z_{i-1}(T_{DS_{i-1}},P_{DS_{i-1}})-P_{DS_{i-1}}\frac{\partial\left(z_i(T_{DS_{i-1}},P_{DS_{i-1}})\right)}{\partial P_{DS_{i-1}}}}{z_{i-1}\left(T_{DS_{i-1}},P_{DS_{i-1}}\right)^2}\right) - \right.$$

$$\left.\frac{(V_{DR}-(1-\alpha)V_{valve})}{M_A R T_{DR_{i-1}}}\left(\frac{z_{i-1}(T_{DR_{i-1}},P_{DR_{i-1}})-P_{DR_{i-1}}\frac{\partial\left(z_{i-1}(T_{DR_{i-1}},P_{DR_{i-1}})\right)}{\partial P_{DR_i}}}{z_{i-1}\left(T_{DR_{i-1}},P_{DR_{i-1}}\right)^2}\right)\right)$$

$$(49) \quad \frac{\partial q_i}{\partial\Delta P_{D_{i-1}}} = \frac{(V_{DS}-(1-\alpha)V_{valve})}{M_A R T_{DS_{i-1}}}\left(\frac{1}{z_i(T_{DS_{i-1}},P_{DS_{i-1}})}\right)$$

$$(50) \quad \frac{\partial q_i}{\partial\Delta P_i} = \left(\frac{(V_{DS}-(1-\alpha)V_{valve})}{M_A R T_{DS_i}}\left(\frac{1}{z_i(T_{DS_I},P_{S_i})}\right) + \frac{(V_{US}-V_{CS}-V_A)}{M_A R T_{US_i}}\left(\frac{1}{z_i(T_{US_I},P_{S_i})}\right)\right)$$

$$(51) \quad \frac{\partial q_i}{\partial T_{DS}} = \left(\frac{(P_{DR_{i-1}}-\Delta P_{D_{i-1}})(V_{DS}-(1-\alpha)V_{valve})}{M_A R}\right)\left(-\frac{1}{T_{DS_{i-1}}^2}\right) + \frac{(-P_{R_i}+\Delta P_i)(V_{DS}-(1-\alpha)V_{valve})}{M_A R}\left(-\frac{1}{T_{DS_i}^2}\right)$$

$$(52) \quad \frac{\partial q_i}{\partial T_{DR}} = \left(\frac{P_{DR_{i-1}}(V_{DR}-(1-\alpha)V_{valve})}{M_A R}\right)\left(\frac{1}{T_{DR_{i-1}}^2}\right) + \frac{P_{R_i}(V_{DR}-(1-\alpha)V_{valve})}{M_A R}\left(-\frac{1}{T_{DR_i}^2}\right)$$

$$(53) \quad \frac{\partial q_i}{\partial T_{US}} = \left(\frac{(P_{UR_{i-1}}-\Delta P_{U_{i-1}})(V_{US}-V_{CS}-V_A-(1-\alpha)V_{valve}))}{M_A R}\right)\left(-\frac{1}{T_{US_{i-1}}^2}\right) + $$

$$\frac{(-P_{R_i}+\Delta P_i)(V_{US}-V_{CS}-V_A)}{M_A R}\left(-\frac{1}{T_{US_i}^2}\right)$$

$$(54) \quad \frac{\partial q_i}{\partial T_{UR}} = \left(-\frac{P_{UR_{i-1}}(V_{UR}-V_{CR}-(1-\alpha)V_{valve})}{M_A R}\right)\left(-\frac{1}{T_{UR_{i-1}}^2}\right) + \frac{P_{R_i}(V_{UR}-V_{CR})}{M_A R}\left(-\frac{1}{T_{UR_i}^2}\right)$$

where the partial derivative of the compressibility factor *z(T,P)* with respect to the pressure has been estimated, at constant temperature (25 °C), approximating with second order fitting polynomial. While, for the partial derivative of *z(T,P)* with respect to the temperature, ideal behaviour has been considered.

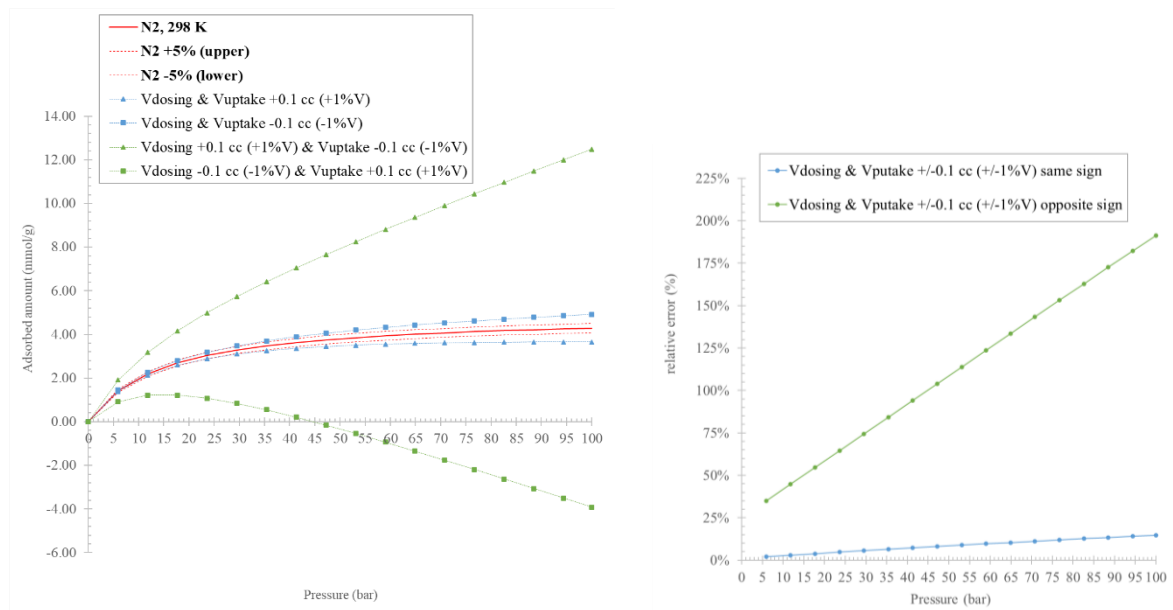# A5. Supplementary results of sensitivity analysis

Figure 46 *– Effect of errors in volume calibration for N₂ adsorbed onto 100 mg 13X (Gibson et al., 2016) at 298 K, measured by single-branch method. Plot (left): absolute errors trend, expected isotherm (red solid line), percentual error ±5% (red dashed lines); plot (right): relative error (%) over pressure. Configuration 2*
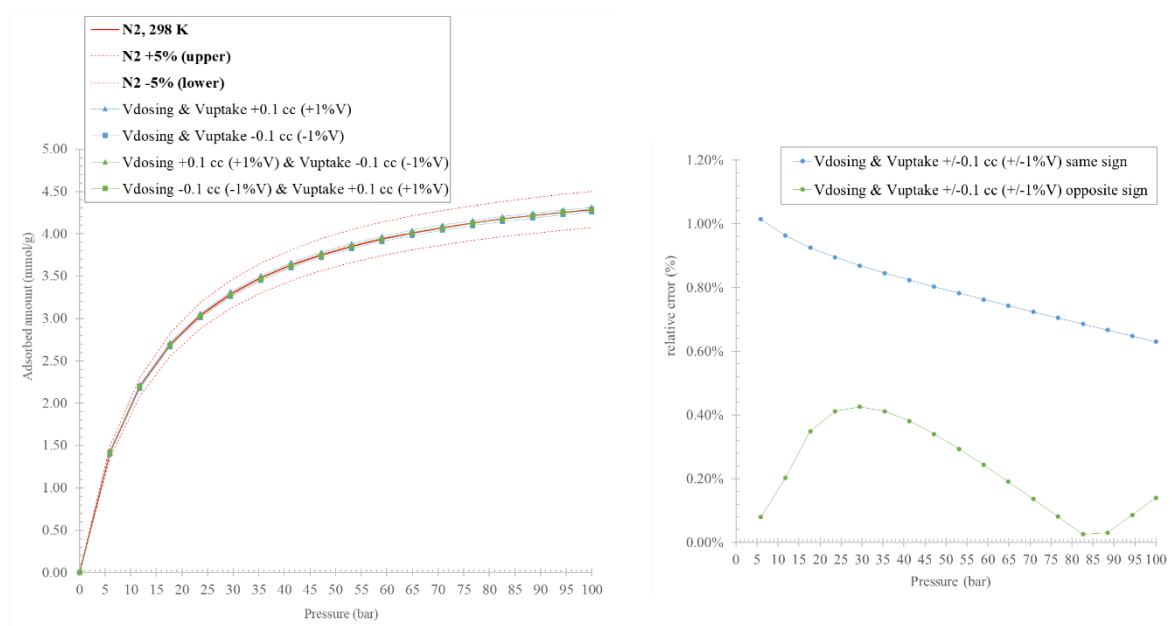

Figure 47 *– Effect of errors in volume calibration for N₂ adsorbed onto 100 mg 13X (Gibson et al., 2016) at 298 K, measured by differential method. Plot (left): absolute errors trend, expected isotherm (red solid line), percentual error ±5% (red dashed lines); plot (right): relative error (%) over pressure. Configuration 2*
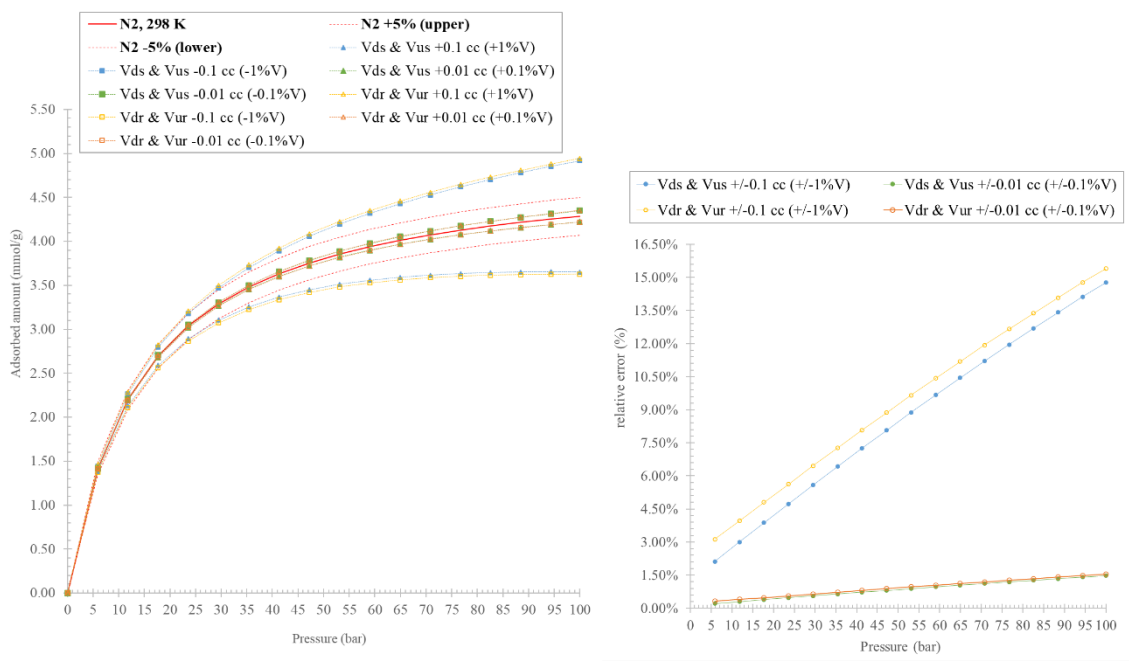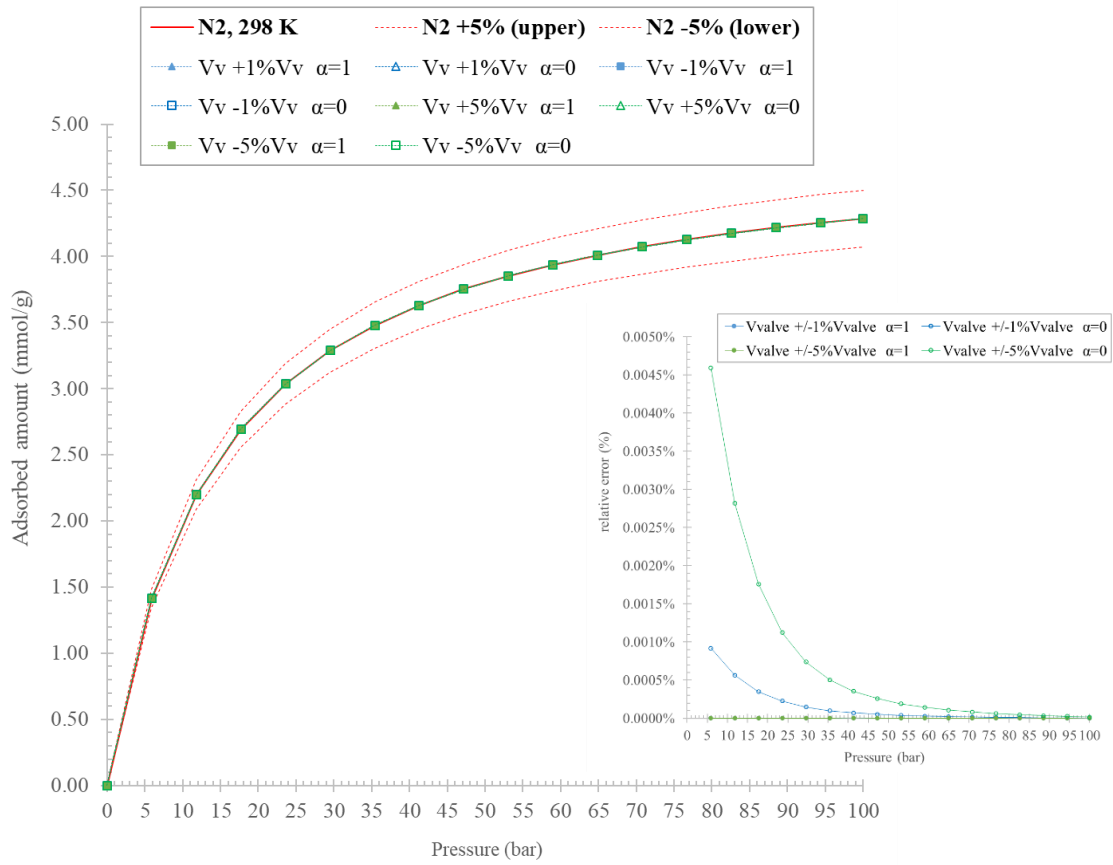
Figure 48 – *Effect of asymmetric errors in volume calibration for N_2 adsorbed onto 100 mg 13X (Gibson et al., 2016) at 298 K, measured by differential method. Plot (left): absolute errors trend, expected isotherm (red solid line), percentual error ±5% (red dashed lines); plot (right): relative error (%) over pressure. Configuration 2*

Figure 49 *- Effect of the errors in valve volume calibration for N_2 adsorbed onto 100 mg 13X (Gibson et al., 2016) at 298 K, measured by differential method. Main plot: absolute errors trend, expected isotherm (red solid line), percentual error ±5% (red dashed lines); Inset plot: relative error (%) over pressure. Configuration 2*
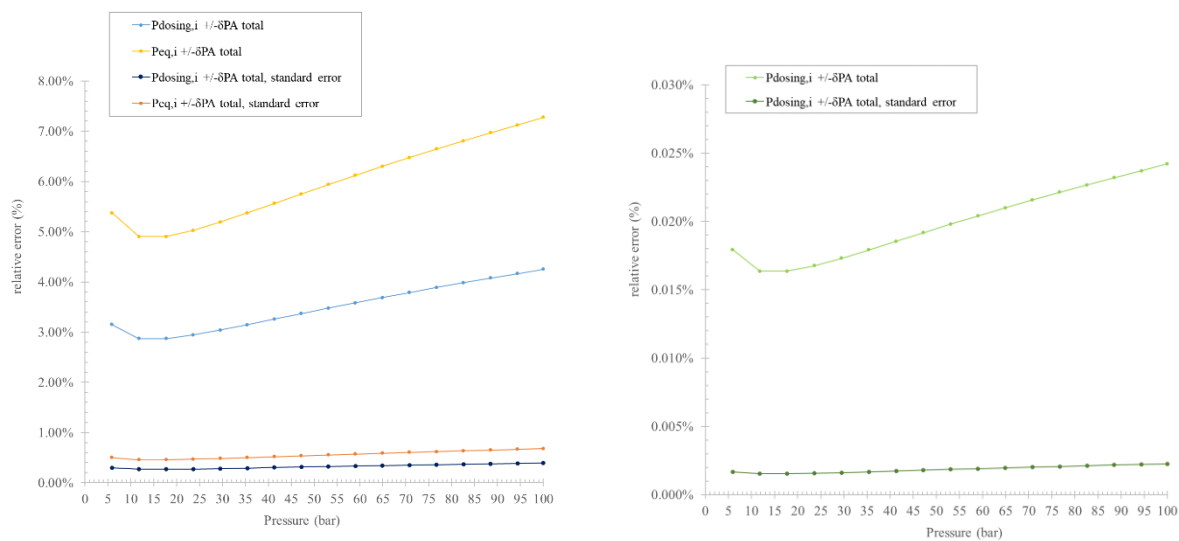
Figure 50 *– Comparison of the total relative errors in gas uptake for N$_2$ adsorbed onto 100 mg 13X (Gibson et al., 2016) at 298 K, due to random errors in absolute pressure readings measured by single-branch method (left) and differential method (right).*
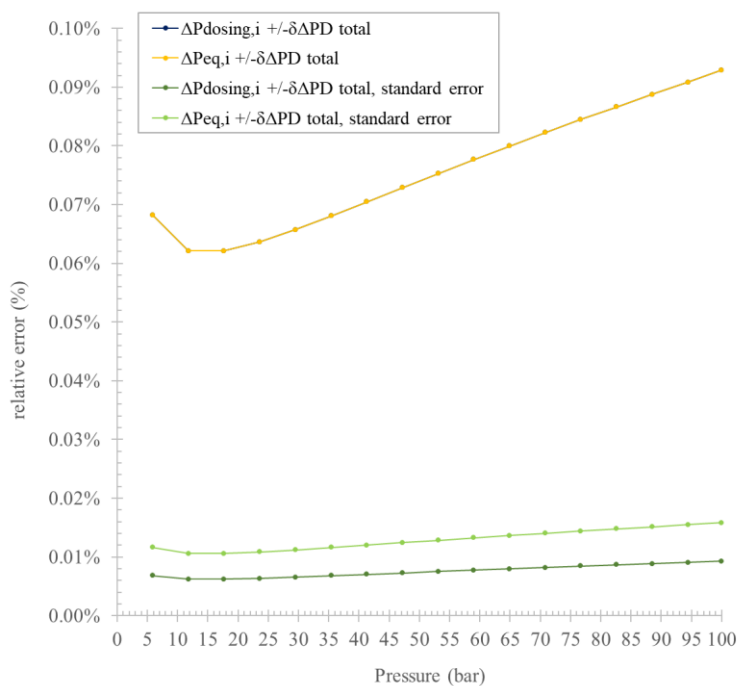

Figure 51 *– Comparison of the total relative errors in gas uptake for N$_2$ adsorbed onto 100 mg 13X (Gibson et al., 2016) at 298 K, due to random errors in differential pressure readings measured by differential method.*
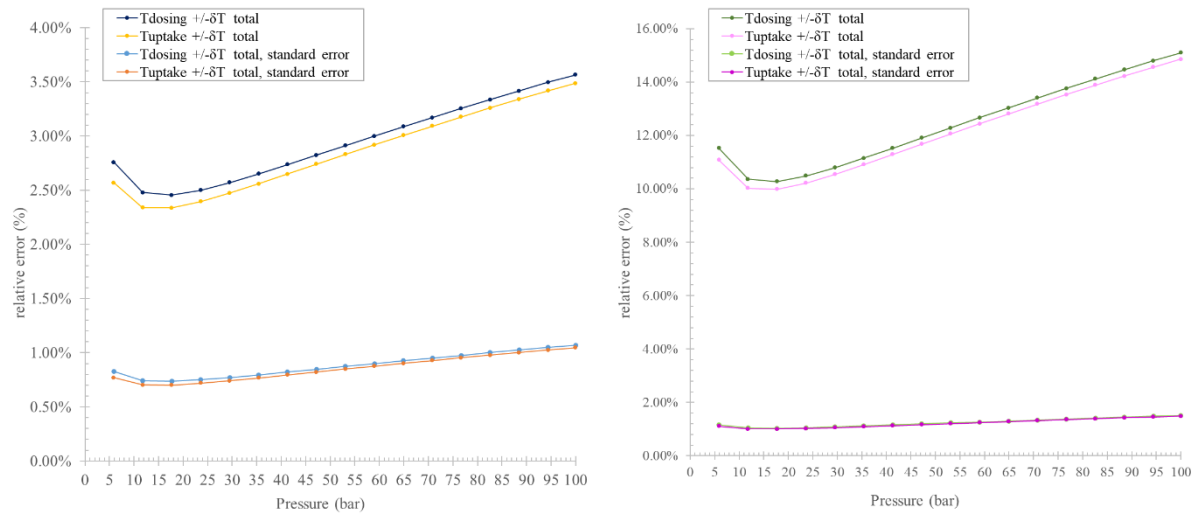
Figure 52 *– Comparison of the total relative errors in gas uptake for N₂ adsorbed onto 100 mg 13X (Gibson et al., 2016) at 298 K, due to random errors in temperature readings measured by single-branch method (left) and differential method (right).*